The Dissertation Committee for Erich D. Gust certifies that this is the approved version of the following dissertation:

Characteristic Relaxation Rates of a Bose Gas in the Classical, Quantum and Condensed Regimes

Committee:

Linda E. Reichl, Supervisor

Mark G. Raizen

Irene M. Gamba

Arno Bohm

Austin Gleeson

Qian Niu

Characteristic Relaxation Rates of a Bose Gas in the Classical, Quantum and Condensed Regimes

by

Erich D. Gust, B. S.

Dissertation

Presented to the Faculty of the Graduate School of

The University of Texas at Austin

in Partial Fulfillment

of the Requirements

for the Degree of

Doctor of Philosophy

The University of Texas at Austin

August 2011

Acknowledgements

I must first thank my parents, who continuously loved and supported me, and never failed in encouraging me to be whatever I wanted to be. Secondly, I thank my adviser, Dr. Linda E. Reichl, for introducing me to the topic of my research. She has been extraordinary in helping me find direction in the midst of monstrous calculations, and in helping me to focus my efforts towards obtaining the most physically interesting and relevant results. I cannot hope to recall and enumerate the contributions of numerous friends, professors and mentors that I have had throughout the years, and so I thank them all equally for the discussions, entertainment and advice that they have provided. I thank the members of my dissertation committee for serving, especially Dr. Austin Gleeson for doing so on short notice, and Dr. Qian Niu for his patience in dealing with scheduling issues. I also thank the Physics department for the providing the opportunity for me to teach in a substantial and meaningful way, and I estimate that I have learned as much from this experience as I have from my formal research. Finally, I wish to thank the Robert A. Welch Foundation (Grant No. F-1051) for financial support of my work during the summer semesters.

Characteristic Relaxation Rates of a Bose Gas in the Classical, Quantum and Condensed Regimes

Erich D. Gust, Ph. D.

The University of Texas at Austin, 2011

Supervisor: Linda E. Reichl

We obtain the characteristic relaxation rates and relaxation modes of a Bose gas in three regimes. The classical regime corresponds to a classical gas of hard spheres and the quantum regime corresponds to an interacting quantum Bose gas with no Bose-Einstein condensate present. In the condensed regime a Bose-Einstein condensate is present and modifies the behavior of the gas. In each regime there is a different kinetic equation that describes the evolution of the relevant distribution function. The classical kinetic equation is the Boltzmann equation and the quantum kinetic equation with no condensate present is the Uehling-Uhlenbeck equation. When a condensate is present, we derive a new kinetic equation that describes the evolution of the momentum distribution of Bogoliubov excitations or bogolons. For each of the three kinetic equations, we linearize the collision integral and use it to generate the elements of a collision matrix. The eigenvalues of this matrix give us the characteristic relaxation rates and the eigenvectors give us the relaxation modes. We report numerical results for the eigenvalues in each regime as the particle species, density and temperature of the gas are varied.

Table of Contents

List of Figures

List of Tables

1 Introduction

1.1 Gases and Eigenvalues

Gases are one of the most familiar forms of matter that we encounter in our universe. Though they are often invisible to the naked eye, their influence on our experiences is great. The large-scale behavior of gases is responsible for the weather, our ability to hear sound, technologies such as refrigeration, engines and much more. Less familiar is the small-scale behavior of gases. Our microscopic picture of gases is one of innumerable particles whizzing about, colliding with each other and colliding with other objects. Almost miraculously, this microscopic picture can explain the macroscopic behavior that we observe with our senses. The derivation of the large-scale (hydrodynamic) equations of gases from the small-scale interactions of particles is truly one of the great triumphs of classical statistical mechanics.

In this report, we will not concern ourselves with the large-scale equations of hydrodynamics, nor their derivation from the small-scale interactions. Instead we shall focus intently on the small-scale behavior of gases, as the particles collide with each other to exchange momentum and energy. In this microscopic picture, each particle possesses some momentum and energy. If each particle's momentum and energy were known, we could in principle determine the trajectory of every particle, the instant of every collision and know all there is to know about the gas. Since the total number of particles in a macroscopic quantity of gas is very large, this is clearly a futile task.

The methods of statistical mechanics offer hope in this situation. Instead of tracking every individual particle, we can instead discuss the average number of particles that possess a momentum or energy within a certain range. Such a quantity is known as a distribution function. It is common that the distribution function of a given gas will not remain constant over time, since collisions between particles cause some particles to change their momentum or energy. During a collision, a particle will change its previous momentum to a new momentum and the average number of particles with the previous momentum will decrease, and the average number of particles with the new momentum will

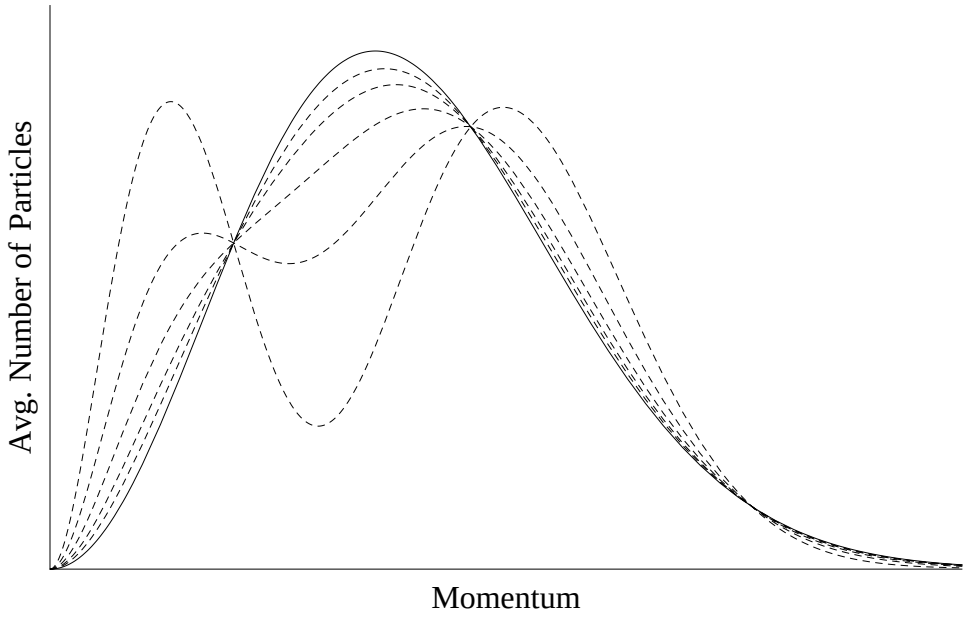

Figure 1.1: A schematic depiction of a momentum distribution function evolving towards the equilibrium momentum distribution function. The dashed curves indicate the momentum distribution as time progresses. The solid curve is a Maxwell-Boltzmann equilibrium distribution.

increase. The collective effect of all these collisions in a gas is to cause the distribution function to approach a certain form, which is the same for all classical monatomic gases, regardless of their identity or interaction properties. This special form of the distribution function is known as the equilibrium distribution function and for classical monatomic gases is known specifically as a "Maxwell-Boltzmann" distribution. A schematic depiction of this process can be seen in figure 1.1. When the gas eventually reaches this equilibrium distribution, collisions between particles still occur, but the transfer of momentum from one collision is precisely balanced by that of other collisions in such a way as to cause no change in the distribution function.

It is our main objective in this report to answer questions about the evolution of such "non-equilibrium" distribution functions towards the equilibrium distribution function. The evolution of distribution functions for classical gases is given by the Boltzmann equation, which we discuss in Chapter 2. The Boltzmann equation is only one of three such evolution equations which we will discuss. The second will be the Uehling-Uhlenbeck equation (Chapter 5) and the third will be a new evolution equation which we derive in Chapters 4 and 6. All of these equations are differential equations for the time rate of change of a distribution function, but the terms which include the

effects of collisions involve certain integrals containing products of the distribution functions in the integrand. Thus the Boltzmann equation and others are non-linear integro-differential equations for the distribution function.

Non-linear integro-differential equations cannot be solved in the traditional sense without some level of approximation, and are often intractable even when using numerical methods. In this report, we choose to only analyze systems which are very close to equilibrium in a certain sense, which could be considered infinitesimally close to equilibrium. For these systems, the products of distribution functions in the collision integral can be written in terms of the equilibrium distributions and functions representing the *difference* of the actual distribution from equilibrium. Since we assume the actual distribution is infinitesimally close to the equilibrium distribution we can neglect all terms that are second order or higher in the difference functions. This process, called "linearization" produces a *linear* integro-differential equation from a non-linear integro-differential equation. These linearized equations can be solved numerically to any desired accuracy.

A linearized integro-differential equation is closely related to the linear matrix evolution equation

$$\frac{d\phi}{dt} = -\mathbf{C} \cdot \phi, \tag{1.1}$$

where ϕ is a vector and $\mathbf{C}$ is a matrix. The quantities ϕ and $\mathbf{C}$ are of infinite dimension and some sort of truncation is required to begin analysis. Equations such as (1.1) are commonplace and can be solved numerically by the powerful algorithms of linear algebra. The result of such algorithms is generally a set of values known as the eigenvalues, denoted by λ_n, and a set of vectors known as the eigenvectors, denoted by ϕ_n. If $\mathbf{C}$ is a symmetric matrix, the eigenvalues are real and the eigenvectors have the special property that

$$\mathbf{C} \cdot \phi_n = \lambda_n \phi_n \qquad \text{and} \qquad \phi_m \cdot \phi_n = \begin{cases} 1, & n = m \\ 0, & n \neq m \end{cases} \tag{1.2}$$

This special property allows us to solve Eq. (1.1),

$$\phi(t) = \sum_n (\phi_n \cdot \phi(0)) e^{-\lambda_n t} \phi_n, \tag{1.3}$$

assuming that the initial vector $\phi(0)$, all of the eigenvalues λ_n and eigenvectors ϕ_n are known.

The type of solution given in Eq. (1.3) gives us a great deal of information not only about the evolution, but also about the matrix itself. The eigenvectors and eigenvalues mentioned above are inherent properties of the matrix. If the matrix results from analysis of some physical system, the eigenvalues and eigenvectors often have great physical significance and contain valuable information about the system. Our analysis of linearized evolution equations for distribution functions will indeed generate matrices, and determining the eigenvalues and eigenvectors of these matrices is our goal. These matrices represent the collective effects of inter-particle collisions on the distribution functions of the gas. Because of this, we shall henceforth refer to them as collision matrices or collision operators.

The collision matrix depends upon the microscopic properties of the interactions between particles. The form of the interaction is specified as a force acting between a pair of particles and the two-body scattering problem of this force is then solved, to the extent where one can provide the differential scattering cross section for the two-particle collision. This scattering cross section enters into the collision matrix and determines the values of its elements. In this report, we discuss two types of particle interactions, and one of them only briefly. The main type of interaction we are concerned with are hard sphere interactions, where the particles are considered as indestructible perfect spheres with no internal structure that undergo completely elastic collisions. The second type of interaction that we discuss is a force proportional to the inverse fifth power of the separation distance. Such a gas is historically known as a gas of "Maxwell Molecules" or a "Maxwell gas" even though the particles do not necessarily have internal structure.

The eigenvalues that we find for collision matrices are directly related to the rate at which the gas approaches equilibrium. As seen by the example solution of Eq. (1.3), the approach to equilibrium is that of exponential relaxation. The eigenvalues set the timescale of this relaxation. The link between the microscopic viewpoint and the macroscopic hydrodynamic viewpoint can be bridged by the eigenvalues and eigenvectors of the collision matrix to obtain the macroscopic transport coefficients from knowledge of the microscopic interactions.

1.2 Previous Work

The Maxwell gas is of historical significance because the eigenvalue problem of the Maxwell gas collision operator was solved by Wang Chant and Uhlenbeck in 1952 [1]. They obtain an explicit integral formula for the eigenvalues as well as the exact forms of the eigenvectors. The eigenvectors of the Maxwell gas can be used as an expansion basis to compute the collision matrix elements for a hard sphere gas. Alterman, Frankowski and Pekeris [2] used this fact in 1962 to numerically compute the eigenvalues for one portion of the hard sphere collision matrix. Jenssen [3] followed this up in 1972 for the entire collision matrix, but encountered convergence issues as his computational resources were limited. In 1984, Shizgal [4] applied a more modern method to compute the elements of the collision matrix without using the eigenvectors of the Maxwell gas. As a historical note, reading these papers one can reflect on the paradigm shift from arcane and elegant analytical methods to brute force numerical algorithms.

The collision matrices have also been used to model relaxation processes in more complex situations such as the relaxation of light-induced changes of the velocity distribution tracer atoms immersed in a light insensitive buffer gas [5, 6, 7, 8, 9], and the effect of collisions on spectral line shapes [10].

The accurate calculation of all of the eigenvalues for the hard sphere collision operator is hampered by a simple fact: In general, the eigenvalue spectrum may contain continuous regions as well as discrete values [11, 12, 13, 14] and For hard spheres, the discrete eigenvalues accumulate at a limit point [15]. This makes the higher order discrete eigenvalues difficult to calculate because they are very close to one another. However, the value of this limit point can be calculated, so the first few eigenvalues and the value of the limit point contain the important information about the system.

The central equation which describes the evolution of the classical gas is the Boltzmann equation. There is a large body of work in the Mathematics community concerned with the properties of solutions to the Boltzmann equation under a variety of circumstances. For representative examples of this aspect of the Boltzmann equation, consult Bobylev [16, 17], Cercignani [11] and others [18, 19, 20]. The amount and diversity of these works serves to illustrate the richness of the Boltzmann equation and the difficulty of constructing mathematically rigorous arguments concerning it. Even so, the majority of mathematics literature deals only with the classical Boltzmann equation.

To extend the Boltzmann equation to quantum systems, we must start from scratch with a quantum description instead of a classical one and derive an analogue of the Boltzmann equation, which we do in Chapter 4. We will obtain our kinetic equation following a procedure introduced by Peletminskii, et al [21, 22]. This procedure has been applied to Fermi superfluids [23, 24, 25] and Bose-Einstein condensates [26, 27] by other authors. The basic idea behind the work of these authors was first formulated by Bogoliubov [28]. For a system that is out of equilibrium, the relaxation to equilibrium can occur in several stages when the timescales of the stages are very different from each other. During each relaxation stage, the number of parameters necessary to describe the system accurately is reduced. This reduction allows us to focus on the evolution of a few parameters rather than solve the full N-body problem.

The first application of the results of Chapter 4 will yield an evolution equation (or kinetic equation) known as the Uehling-Uhlenbeck equation. The Uehling-Uhlenbeck (U-U) equation [29], also known as the Boltzmann-Nordheim equation [30], is a semiclassical extension of the Boltzmann equation that accounts for the identity of the particles.

The second application of the results of Chapter 4 will be to a ultracold system of bosonic particles that contains a Bose-Einstein condensate. It is well known that in many-particle quantum systems, interaction between particles often lead to a description in terms of non-interacting or weakly-interacting excitations. Two classic examples are phonons in a solid or Cooper pairs in a superconductor. In the case of the interacting Bose gas, a Bogoliubov transformation leads to a description in terms of Bogoliubov excitations or bogolons. At zero temperature there are, on average, zero bogolons present and bogolons are viewed as the elementary excitations of the system to which the normal methods of quantum field theory can be applied [31, 32]. At finite temperature, there are a large number of interacting bogolons in the system, and the theoretical approach must change. The proper course is to derive a kinetic equation, analogous to the Boltzmann equation, for the average number of bogolons in each state. In doing this we assume that the number of bogolons in each state gives a complete description of the system, and fluctuations in the bogolon number operators are neglected.

Kinetic equations have been used to describe evolution properties of BECs, but they have mostly focused on the relaxation properties of particle distributions at very low temperatures [26, 27, 33, 34, 35], prediction of observed collective mode frequencies [36] or growth of the condensate from thermal vapor [37, 38, 39]. These works find at most two types of collisions that appear in the collision integral:

$2 \leftrightarrow 2$ collisions, and $2 \leftrightarrow 1$ collisions where one of the particles enters or is ejected from the condensate. A familiar result from these approaches is the Uehling-Uhlenbeck equation [29, 30] which only includes the effects of $2 \leftrightarrow 2$ collisions. These types of derivations, when merged with hydrodynamics have been successful in describing the dynamics of Bose-Einstein condensation. However, the relaxation rates of the momentum distribution and related quantities such as transport coefficients are rarely discussed or accurately calculated.

1.3 Outline of this Report

We begin in Chapter 2 by introducing the phase space distribution function and its evolution equation, the Boltzmann equation. Working with the hard sphere Boltzmann equation, we derive its equilibrium distribution and show how to linearize it for small perturbations about this equilibrium. We review method of expansion in terms of the eigenfunctions of the Maxwell gas and repeat the results of Wang Chang and Jenssen. The resulting eigenvalues are reported. We then discuss the method of Shizgal in detail and demonstrate its application to find the eigenvalues and eigenvectors of the hard sphere collision matrix. This section is important since it forms the foundation for our analysis of the U-U equation and bogolon kinetic equation. We end Chapter 2 by discussing one method of relating the collision matrix to the macroscopic transport coefficients.

In Chapter 3 we discuss the construction and results of a hard spheres simulation intended to verify the predictions of Chapter 2. The results of the simulation are evolution curves for the amplitudes of various perturbation modes. Analysis of these curves provides us with "measured" eigenvalues for a small hard sphere system. These "measured" eigenvalues agree well with the predictions of Chapter 2.

In Chapter 4 we begin from a quantum description of an interacting Bose field and derive very general kinetic equations. These general kinetic equations, when applied, will yield both the U-U equation and the bogolon kinetic equation.

Chapter 5 provides an application of the formulas of Chapter 4 to produce the Uehling-Uhlenbeck equation. As the U-U equation is also a nonlinear integro-differential equation, we will linearize it about its equilibrium distributions to obtain its collision matrix. To make it analogous to the Boltzmann equation, we concern ourselves with its behavior when applied to systems which are spatially uniform.

We then apply the methods developed in Chapter 2 to obtain the eigenvalues and eigenvectors of the U-U collision matrix. We find that the eigenvalues and eigenvectors are significantly modified from their Boltzmann versions as the temperature becomes low. However, this modification is not drastic, as the U-U equation assumes the absence of a condensate. To our knowledge, this type of analysis has not been performed on the U-U equation.

The full power of the general kinetic equation derived in Chapter 4 is finally applied in Chapter 6 to derive the kinetic equations for the bogolon momentum distribution. The mechanism for relaxation of the momentum distribution is collisions between bogolons and the effects of collisions appear in the kinetic equation as collision operators. We derive the bogolon kinetic equation for a spatially homogeneous low density Bose gas containing a Bose-Einstein condensate (BEC). Our bosons are in a rectangular box with periodic boundary conditions and not a harmonic trap. We then use these kinetic equations to obtain numerical values of the relaxation rates for dilute gases of sodium and rubidium atoms at temperatures from roughly 0.01 to 0.99 of the critical temperature for BEC and densities from roughly 7.0×10^{19} m^{-3} to 1.5×10^{23} m^{-3}. We find that the structure of the collision operators for the bogolon gas is similar to that obtained from the Boltzmann equation [40], which describes a classical dilute gas, and the Uehling-Uhlenbeck equation [41], which describes a degenerate but non-condensed Bose gas. Near equilibrium we expand the bogolon momentum distribution in terms of the eigenmodes of the collision operator.

For bogolons we find three types of collisions that appear in the kinetic equation with two of them similar to those mentioned in the literature. The new third type of collision involves the synthesis of three bogolons into one and the inverse process of one bogolon decaying into three. Additionally, we give the precise forms of the weighting functions that depend on the parameters of the Bogoliubov transformation for each collision type. As expected, we recover the Uehling-Uhlenbeck equation for the limit of vanishing condensate. The eigenvalues and eigenvectors show an interesting dependence on temperature and density that is not present in the classical and non-condensed cases.

Finally, we conclude in Chapter 7 by briefly summarizing the work that we have done and some of its implications. Two appendices give the details of several derivations mentioned in the text and the details of the symbolic algebra code that is used to help process terms during the derivation of the kinetic equations.

2 Characteristic Relaxation Rates of the Boltzmann Equation

2.1 The Boltzmann Equation

In classical statistical mechanics, a central concept in the theoretical description of gases is the phase space distribution function $f(\mathbf{r}, \mathbf{v}, t)$. The phase space distribution function represents the average number of particles with position $\mathbf{r}$ and velocity $\mathbf{v}$ at time t. Many quantities of interest can be found from the phase space distribution function such as total particle number

$$N = \int d\mathbf{r} \int d\mathbf{v} f(\mathbf{r}, \mathbf{v}, t), \tag{2.1}$$

total momentum

$$\mathbf{p} = m \int d\mathbf{r} \int d\mathbf{v}\mathbf{v} f(\mathbf{r}, \mathbf{v}, t), \tag{2.2}$$

and the total kinetic energy

$$E = \frac{m}{2} \int d\mathbf{r} \int d\mathbf{v} v^2 f(\mathbf{r}, \mathbf{v}, t). \tag{2.3}$$

In these expressions, m is the mass of each particle. Thermodynamic quantities such as temperature T and the components of the pressure tensor P_{ij} can also be derived from the phase space distribution function.

The Boltzmann equation describes the evolution of the phase space distribution function. It is

$$\frac{\partial f}{\partial t} + \mathbf{v} \cdot \nabla_{\mathbf{r}} f + \frac{\mathbf{F}(\mathbf{r})}{m} \cdot \nabla_{\mathbf{v}} f = \mathcal{C}[f], \tag{2.4}$$

where $\mathbf{F}(\mathbf{r})$ is the external force acting on a particle at the point $\mathbf{r}$ and $\mathcal{C}[f]$ is a functional of f that represents the effects of collisions between the particles. Since $\mathcal{C}[f]$ is a *functional* and not a function it is also known as the collision integral. The terms involving gradients of the distribution function

are known as the "streaming" terms. When the particles are non-interacting, or collisions between particles are neglected, the streaming terms simply describe the Newtonian dynamics of the particles under the effects of the external force.

The more interesting case is when interactions or collisions between particles become important, and $\mathcal{C}[f]$ becomes a significant contribution to the evolution of the phase space density function. To explicitly give the collision integral, we must use information about the microscopic nature of the interactions between the particles. Because of this, the Boltzmann equation can provide a way to relate the macroscopic behavior of the phase space distribution function to the microscopic interactions between particles.

A derivation of the collision integral for particles interacting through a spherically symmetric potential can be found in most standard textbooks on statistical mechanics [42, 43]. These derivations rely on several key assumptions. Firstly the timescale of a collision must be much shorter than the average time between collisions. This can be satisfied by requiring the gas to be dilute compared to the effective size of the particles, which is determined by their interactions. Quantitatively we require that the density of the gas times the effective length cubed must be much less than unity. Secondly, the effects of three or more particles participating in one collision are neglected. This can also be satisfied if the gas is dilute. In order to obtain the collision integral in its simplest form, we also assume that collision are elastic and do not change the internal state of the particles. Thirdly, $f(\mathbf{r}, \mathbf{v}, t)$ and $\mathbf{F}(\mathbf{r})$ must be slowly varying in space compared to the length scale of a collision event, so that we may treat the collision as an interaction between two free particles. Lastly we must make the famous assumption of *molecular chaos*, meaning that particles with different velocities are uncorrelated. This assumption can also be interpreted as declaring that the single particle phase space distribution function $f(\mathbf{r}, \mathbf{v}, t)$ contains all relevant information and that higher order distributions such as the two-particle phase space distribution function can be written in terms of $f(\mathbf{r}, \mathbf{v}, t)$.

These assumptions, taken together, allow one to derive the classical result for the Boltzmann collision integral, which is given by

$$\mathcal{C}[f_1] = \int d\mathbf{v}_2 \int d\Omega u I(u, \theta)(f_3 f_4 - f_2 f_1), \tag{2.5}$$

where f_i is shorthand for $f(\mathbf{r}, \mathbf{v}_i, t)$. The other quantities appearing in this equation are related to the

two-body collision: u is the relative velocity

$$u = |\mathbf{v}_1 - \mathbf{v}_2| \tag{2.6}$$

and θ is the angle between the relative velocities

$$u^2 \cos\theta = (\mathbf{v}_1 - \mathbf{v}_2) \cdot (\mathbf{v}_3 - \mathbf{v}_4). \tag{2.7}$$

The quantity $I(u, \theta)$ is the microscopic two-body differential scattering cross section at relative velocity u through an angle θ. The velocities $\mathbf{v}_3$ and $\mathbf{v}_4$ are determined by conservation of energy and momentum and the relations (2.6) and (2.7). Though the expression for the collision integral (2.5) is compact, the algebra involved in the calculation of $\mathbf{v}_3$ and $\mathbf{v}_4$ makes it unwieldy for theoretical use.

We can write the collision integral in a much more symmetric form by imposing momentum and energy conservation with Dirac delta functions.

$$\mathcal{C}[f_1] = \int d\mathbf{v}_2 d\mathbf{v}_3 d\mathbf{v}_4 I(u,\theta) \delta^3 \left(\frac{\mathbf{v}_1 + \mathbf{v}_2}{2} - \frac{\mathbf{v}_3 + \mathbf{v}_4}{2} \right) \delta \left(v_1^2 + v_2^2 - v_3^2 - v_4^2 \right) (f_3 f_4 - f_1 f_2) \tag{2.8}$$

In this form, the relative velocity u and angle θ are determined by $\mathbf{v}_3$ and $\mathbf{v}_4$ instead of the other way around. This is advantageous from a theoretical point of view since, depending on the form of $I(u, \theta)$, we can postpone or skip evaluation of u and θ. There may also exist parameterizations of $I(u, \theta)$ in terms of different quantities which are more convenient than u and θ.

2.2 Equilibrium

Experience shows that an isolated quantity of gas will eventually evolve to a state which no longer has any time dependence. This final state, which is known as the equilibrium state, is denoted by $f^0(\mathbf{r}, \mathbf{v})$. The equilibrium state must satisfy

$$\mathbf{v} \cdot \nabla_{\mathbf{r}} f^0 + \frac{\mathbf{F}(\mathbf{r})}{m} \cdot \nabla_{\mathbf{v}} f^0 = \mathcal{C}[f^0]. \tag{2.9}$$

Ignoring the possibility of a special balance between nonzero gradient terms and a nonzero collision integral, we begin by first finding the solutions that satisfy

$$\mathcal{C}[f^0] = 0. \tag{2.10}$$

The most general form of the distribution function that produces zero when inserted into the collision integral is

$$f^0(\mathbf{r}, \mathbf{v}) = A \exp\left[\mathbf{B} \cdot \mathbf{v} - Cv^2\right]. \tag{2.11}$$

One can see that this gives zero when inserted into the collision integral by observing that $\mathbf{v}_3 + \mathbf{v}_4 = \mathbf{v}_1 + \mathbf{v}_1$ and $v_4^2 + v_3^2 = v_1^2 + v_2^2$. The quantities A, $\mathbf{B}$ and C are undetermined parameters which in general may be functions of $\mathbf{r}$ if $\mathbf{F}(\mathbf{r})$ is nonzero. The quantities A and C must be positive. Using the form 2.11 in Eq. 2.9, it can be shown that $\mathbf{B}$ must take the form $\mathbf{B}(\mathbf{r}) = \mathbf{B}_0 + \mathbf{\Omega} \times \mathbf{r}$ and must also satisfy $\mathbf{B} \cdot \mathbf{F} = 0$. Furthermore, if the force $\mathbf{F}$ derives from a potential function $U(\mathbf{r})$, then C must be constant and A must be proportional to $e^{-2CU(\mathbf{r})/m}$. The vectors $\mathbf{B}_0$ and $\mathbf{\Omega}$ are related to uniform translation and rotation, respectively. The quantity C is related to the temperature T and is conventionally written as $\frac{m}{2k_BT}$ where k_B is Boltzmann's constant, $1.3806488 \times 10^{-23}$J/K. The quantity A is related to the density of particles at the point $\mathbf{r}$. The condition $\mathbf{B} \cdot \mathbf{F} = 0$ means that all but the most symmetric of confining potentials must have $\mathbf{B}_0 = 0$ and $\mathbf{\Omega} = 0$.

From here on, we will be mainly interested in the properties of the collision integral and not the effects of the Newtonian dynamics in an external force, and so we set $\mathbf{F}$ to zero. From the discussion in the previous paragraph, this means that A must become constant. Also the vector $\mathbf{\Omega}$ must be zero, or the distribution function would approach infinity for large distances from the rotation axis. We then obtain the familiar Maxwell-Boltzmann equilibrium distribution,

$$f^0(\mathbf{r}, \mathbf{v}) = n\left(\frac{m}{2\pi k_B T}\right)^{\frac{3}{2}} \exp\left[-\frac{m(\mathbf{v} - \bar{\mathbf{v}})^2}{2k_BT}\right], \tag{2.12}$$

where we have now written the parameters A, $\mathbf{B}$ and C in terms of the more conventional physical quantities of density (n), temperature (T) and average velocity ($\bar{\mathbf{v}}$). Notice that the equilibrium phase space distribution function is specified by five parameters. Each parameter corresponds to one of the conserved quantities in a two-body collision. If a quantity is conserved in a collision, then its value does

not change over time as the system approaches equilibrium. Thus each conserved quantity should have a role in determining the final equilibrium distribution. The parameter n corresponds to conservation of particle number, the three components of $\bar{\mathbf{v}}$ correspond to the three components of momentum and the parameter T corresponds to conservation of energy. Equations of the form (2.1 - 2.3) can be used to relate the five parameters n, $\bar{\mathbf{v}}$ and T to other properties of the gas. Throughout the rest of this Chapter, we set the mean velocity $\bar{\mathbf{v}}$ to zero. This is permissable since one can always perform a coordinate transformation such that $\bar{\mathbf{v}} = 0$.

2.3 Linearized Boltzmann Equation

If the momentum distribution of the gas is driven out of equilibrium, its relaxation back to equilibrium will be governed by the evolution of the phase space distribution function. The timescale of this relaxation in the momentum distribution is much faster that the timescale of hydrodynamics caused by the streaming terms in the Boltzmann equation [1, 42, 43, 44, 45]. Thus for small amplitude deviations from equilibrium, the streaming terms in the Boltzmann equation (2.4) can be neglected. The Boltzmann equation can then be linearized and becomes an eigenvalue equation for the characteristic relaxation rates which determine the evolution of the gas to its equilibrium distribution. Let us first write Boltzmann equation (2.4) in terms of the dimensionless velocity vector

$$\mathbf{c} = \sqrt{\frac{m}{2k_B T}}\mathbf{v} \tag{2.13}$$

as

$$\begin{aligned}\frac{\partial f_1}{\partial t} = &\left(\frac{2k_B T}{m}\right)^2 \int d\mathbf{c}_2 d\mathbf{c}_3 d\mathbf{c}_4 I(u,\theta) \\ &\times \delta^3\left(\frac{\mathbf{c}_1+\mathbf{c}_2}{2} - \frac{\mathbf{c}_3+\mathbf{c}_4}{2}\right)\delta\left(c_1^2+c_2^2-c_3^2-c_4^2\right)(f_3 f_4 - f_1 f_2).\end{aligned} \tag{2.14}$$

We then linearize this equation by using the linearization scheme

$$f(\mathbf{v},t) = f^0(\mathbf{v}) + f^0(\mathbf{v})\phi(\mathbf{c},t) \tag{2.15}$$

where the dimensionless deviation function $\phi(\mathbf{c},t)$ represents perturbations about equilibrium and we have dropped the $\mathbf{r}$ dependence of the distribution functions since we are neglecting streaming terms. We shall assume that $\phi(\mathbf{c},t) \ll 1$ and, as the system relaxes, $\phi(\mathbf{c},t) \to 0$.

If we keep terms linear in $\phi(\mathbf{c},t)$, the Boltzmann equation can be written as a linear evolution equation for $\phi(\mathbf{c},t)$, namely

$$\begin{aligned}\frac{\partial \phi_1}{\partial t} =& 8n\sqrt{\frac{2k_BT}{m}}\frac{1}{\pi^{3/2}}\int d\mathbf{c}_2 d\mathbf{c}_3 d\mathbf{c}_4 I(u,\theta) \\ &\times \delta^3\left(\mathbf{c}_1+\mathbf{c}_2-\mathbf{c}_3-\mathbf{c}_4\right)\delta\left(c_1^2+c_2^2-c_3^2-c_4^2\right)e^{-c_2^2}(\phi_4+\phi_3-\phi_2-\phi_1),\end{aligned} \tag{2.16}$$

where the fact that $f_3^0 f_4^0 = f_1^0 f_2^0$ has been used to simplify this result.

At this point it is convenient to specify the form of the interaction between the particles and thus the form of $I(u,\theta)$ so that only dimensionless quantities remain in the calculations. Different types of interactions can be accounted for by different forms of $I(u,\theta)$. For continuity with the following Chapters, we focus on Hard sphere interactions where

$$V(r) = \begin{cases} 0, & r > a \\ \infty, & r \le a \end{cases} \qquad \text{and} \qquad I(u,\theta) = \frac{a^2}{4}. \tag{2.17}$$

The only other interaction we will mention is of "Maxwell molecules" where

$$V(r) = V_4\left(\frac{a}{r}\right)^4 \qquad \text{and} \qquad I(u,\theta) = \frac{a^2}{8}\sqrt{\frac{2V_4}{m}}\frac{1}{u}F(\theta). \tag{2.18}$$

The significance of the r^{-4} potential is that the cross section has a $1/u$ dependence allowing an analytic diagonalization of the linearized collision operator. The explicit expression for the angular function $F(\theta)$ will be given in appendix A.3 where we discuss the solution of the linearized collision operator for Maxwell molecules.

Regardless of the form of the interaction, the differential cross section will have dimensions of area. When this is combined with the existing coefficient, the resulting dimension of the right hand side of Eq. (2.16) is time^{-1}. For hard spheres, this timescale is given by

$$\frac{1}{\tau_{\text{HS}}} = n\pi a^2\sqrt{\frac{8k_BT}{\pi m}}. \tag{2.19}$$

The evolution equation (2.16) can now be written in a dimensionless standard form as

$$\frac{\partial\phi(\mathbf{c}_1,t)}{\partial t} = -\frac{1}{\tau_{\rm HS}}\left(M_{\rm HS}(\mathbf{c}_1)\phi(\mathbf{c}_1) + \frac{1}{\pi^2}\int d\mathbf{c}_2 e^{-c_2^2}\left[Q_{\rm HS}(\mathbf{c}_1,\mathbf{c}_2) - 2R_{\rm HS}(\mathbf{c}_1,\mathbf{c}_2)\right]\phi(\mathbf{c}_2,t)\right), \quad (2.20)$$

where

$$Q_{\rm HS}(\mathbf{c}_1,\mathbf{c}_2) = \int d\mathbf{c}_3 d\mathbf{c}_4 \delta^3\left(\mathbf{c}_1+\mathbf{c}_2-\mathbf{c}_3-\mathbf{c}_4\right)\delta\left(c_1^2+c_2^2-c_3^2-c_4^2\right), \quad (2.21)$$

$$R_{\rm HS}(\mathbf{c}_1,\mathbf{c}_2) = \int d\mathbf{c}_3 d\mathbf{c}_4 \delta^3\left(\mathbf{c}_1-\mathbf{c}_2+\mathbf{c}_3-\mathbf{c}_4\right)\delta\left(c_1^2-c_2^2+c_3^2-c_4^2\right)e^{c_2^2-c_3^2} \quad (2.22)$$

and

$$M_{\rm HS}(\mathbf{c}_1) = \frac{1}{\pi^2}\int d\mathbf{c}_2 e^{-c_2^2} Q_{\rm HS}(\mathbf{c}_1,\mathbf{c}_2), \quad (2.23)$$

The functions $Q_{\rm HS}(\mathbf{c}_1,\mathbf{c}_2)$ and $R_{\rm HS}(\mathbf{c}_1,\mathbf{c}_2)$ are called the collision kernels while the function $M_{\rm HS}(\mathbf{c}_1)$ is known as the dynamic scattering rate. Both of the kernels are symmetric under interchange of $\mathbf{c}_1$ and $\mathbf{c}_2$.

The linearized Boltzmann equation given in Eq. (2.20) can be converted into a matrix equation where the evolution is governed by a "collision matrix". The eigenvalues of the collision matrix give the characteristic relaxation rates of perturbations in the gas, and the eigenvectors of the collision matrix give the relaxation modes. The inverse of the collision matrix can also be linked to the transport coefficients. In order to obtain the collision matrix, we must discretize Eq. (2.20). In the following two sections, we discuss two acceptable methods of discretization.

2.4 Relaxation Rates: Polynomial Expansion

One of the methods of discretization is to expand the function $\phi(\mathbf{c}_1)$ in a set of orthogonal polynomials [40] and truncate this expansion at some high order. The standard set of orthogonal polynomials for this problem are the Burnett functions [1, 44, 45]

$$\chi_{n,l,m}(\mathbf{c}) = \sqrt{\frac{2n!}{\Gamma(n+l+\frac{3}{2})}} L_n^{l+\frac{1}{2}}(c^2) c^l Y_l^m(\hat{\mathbf{c}}), \quad (2.24)$$

which can be shown to be the exact eigenvectors of the linearized Boltzmann equation for Maxwell molecules. Here, $L_n^l(c^2)$ is a Laguerre polynomial and $Y_l^m(\hat{\mathbf{c}})$ is a spherical harmonic. The radial part

of a Burnett function is related to a Sonine polynomial. The Burnett functions have the orthogonality relationship

$$\int d\mathbf{c} e^{-c^2} \chi^*_{n,l,m}(\mathbf{c}) \chi_{n',l',m'}(\mathbf{c}) = \delta_{n,n'} \delta_{l,l'} \delta_{m,m'}. \tag{2.25}$$

We can expand the function $\phi(\mathbf{c}, t)$ in terms of the Burnett functions,

$$\phi(\mathbf{c}, t) = \sum_{n=0}^{\infty} \sum_{l=0}^{\infty} \sum_{m=-l}^{l} g_{n,l,m}(t) \chi_{n,l,m}(\mathbf{c}) \tag{2.26}$$

where $g_{n,l,m}(t) = \int d\mathbf{c} e^{-c^2} \phi(\mathbf{c}, t) \chi^*_{n,l,m}(\mathbf{c})$. The linearized Boltzmann equation then takes the discretized form

$$\frac{dg_{n,l,m}(t)}{dt} = -\frac{1}{\tau_{\mathrm{HS}}} \sum_{n',l',m'} C^{n,l,m}_{n',l',m'} g_{n',l',m'}(t) \tag{2.27}$$

where

$$\begin{aligned} C^{n,l,m}_{n',l',m'} = & \int d\mathbf{c}_1 d\mathbf{c}_2 e^{-c_1^2 - c_2^2} \chi^*_{n,l,m}(\mathbf{c}_1) \chi_{n',l',m'}(\mathbf{c}_2) \\ & \times \left(e^{c_2^2} M_{\mathrm{HS}}(\mathbf{c}_1) \delta^3(\mathbf{c}_1 - \mathbf{c}_2) + \frac{1}{\pi^2} Q_{\mathrm{HS}}(\mathbf{c}_1, \mathbf{c}_2) - \frac{2}{\pi^2} R_{\mathrm{HS}}(\mathbf{c}_1, \mathbf{c}_2) \right) \end{aligned} \tag{2.28}$$

The functions $Q_{\mathrm{HS}}(\mathbf{c}_1, \mathbf{c}_2)$ and $R_{\mathrm{HS}}(\mathbf{c}_1, \mathbf{c}_2)$ are pure scalar functions of the vectors $\mathbf{c}_1$ and $\mathbf{c}_2$ only. Therefore they can only depend on the magnitudes $|\mathbf{c}_1|$, $|\mathbf{c}_2|$ and the angle between these two vectors. Also, the function $M_{\mathrm{HS}}(\mathbf{c}_1)$ is a pure scalar function of the single vector $\mathbf{c}_1$ and therefore can only depend on the magnitude of $\mathbf{c}_1$. These fact results in $C^{n,l,m}_{n',l',m'}$ being diagonal in l and m and independent of m so that

$$C^{n,l,m}_{n',l',m'} = C^l_{n,n'} \delta_{l,l'} \delta_{m,m'}. \tag{2.29}$$

For each value of l and m, we have a independent system and we are left with a simple matrix equation of the form

$$\frac{dg_{n,l,m}}{dt} = -\frac{1}{\tau_{\mathrm{HS}}} \sum_{n'=0}^{\infty} C^l_{n,n'} g_{n',l,m}. \tag{2.30}$$

where

$$\begin{aligned} C^l_{n,n'} = & \frac{1}{4\pi} \sqrt{\frac{4n!n'!}{\Gamma(n + l + \frac{3}{2}) \Gamma(n' + l + \frac{3}{2})}} \int d\mathbf{c}_1 d\mathbf{c}_2 e^{-c_1^2 - c_2^2} c_1^l c_2^l L_n^{l+\frac{1}{2}}(c_1^2) L_{n'}^{l+\frac{1}{2}}(c_2^2) P_l(\hat{\mathbf{c}}_1 \cdot \hat{\mathbf{c}}_2) \\ & \times \left(e^{c_2^2} M_{\mathrm{HS}}(\mathbf{c}_1) \delta^3(\mathbf{c}_1 - \mathbf{c}_2) + \frac{1}{\pi^2} Q_{\mathrm{HS}}(\mathbf{c}_1, \mathbf{c}_2) - \frac{2}{\pi^2} R_{\mathrm{HS}}(\mathbf{c}_1, \mathbf{c}_2) \right). \end{aligned} \tag{2.31}$$

In this expression, the spherical harmonic addition theorem (appendix A.1) has been used to eliminate explicit dependence on m. The method of expansion in terms of Burnett functions is worthwhile because the matrix elements $C^l_{n,n'}$ can be calculated. This calculation makes use of the method of generating functions and is discussed in appendix A.2. The result is that

$$C^l_{n,n'} = \sqrt{\frac{n!n'!}{8\Gamma(n+l+\frac{3}{2})\Gamma(n'+l+\frac{3}{2})}} \sum_{j=0}^{n,n'} \sum_{k=0}^{l} \frac{\Gamma\left(-\frac{1}{2}+n+n'+l-2j-k\right) l!}{(n-j)!(n'-j)!(l-k)!2^{n+n'+l-2j-k}} B^k_j, \tag{2.32}$$

where $B^k_j = -\frac{(j+k+1)!}{j!k!} - \delta_{j0}\delta_{k0} + 2\frac{(2j+k+1)!}{(2j+1)!k!2^k}$.

The evolution equation (2.30) is the desired discretization of the linearized Boltzmann equation. Since Eq. (2.30) does not couple expansion coefficients $g_{n,l,m}(t)$ of different l and m, it can be treated as a separate matrix equation for each value of l and m. The matrix, however, does not depend on m so we have $2l+1$ identical systems for each value of l. Let us introduce the collision matrix or order l as $\mathbf{C}^l$, where the elements are given by $[\mathbf{C}^l]_{n,n'} = C^l_{n,n'}$. Since the Boltzmann equation describes relaxation to an equilibrium state while conserving the five quantities of particle number, three components of momentum and energy, we expect the collision matrices collectively will have five zero eigenvalues, and that all other eigenvalues will be positive.

We can refine these expectations by noting that relaxation modes with $l = 0$ depend only on the magnitude of $\mathbf{v}$, a property that is shared by the conserved quantities of particle number and energy. Relaxation modes with $l = 1$ are proportional to single components of $\mathbf{v}$, a property that is shared by the conserved quantity of momentum. Therefore, we should expect $\mathbf{C}^0$ to have two zero eigenvalues and $\mathbf{C}^1$ to have one zero eigenvalue. The single zero eigenvalue of $\mathbf{C}^1$ will actually correspond to three degenerate zero eigenvalues, due to the three values of m (-1, 0, +1) that can be chosen for $l = 1$. It is in this manner that conservation of all three components of momentum is described by one zero eigenvalue.

Performing explicit computation with Eq. (2.32), the matrix $\mathbf{C}^0$ is given by

$$\mathbf{C}^0 = \begin{pmatrix} 0 & 0 & 0 & 0 & 0 & \cdots \\ 0 & 0 & 0 & 0 & 0 & \cdots \\ 0 & 0 & 0.754247 & -0.174574 & -0.0205738 & \cdots \\ 0 & 0 & -0.174574 & 1.25259 & -0.319048 & \cdots \\ 0 & 0 & -0.0205738 & -0.319048 & 1.64374 & \cdots \\ \vdots & \vdots & \vdots & \vdots & \vdots & \ddots \\ . & & & & & \end{pmatrix}, \tag{2.33}$$

We find eigenvalues of $\mathbf{C}^0$ numerically using the first 200 rows and columns. They are

$$\lambda^0_{\mathrm{HS}} = \Big(0, \quad 0, \quad 0.67123, \quad 0.91157, \quad 0.98206, \quad \cdots, \quad 1\Big). \tag{2.34}$$

For $l = 1$, the collision matrix is

$$\mathbf{C}^1 = \begin{pmatrix} 0 & 0 & 0 & 0 & \cdots \\ 0 & 0.754247 & -0.142539 & -0.0145479 & \cdots \\ 0 & -0.142539 & 1.21218 & -0.283177 & \cdots \\ 0 & -0.0145479 & -0.283177 & 1.58734 & \cdots \\ \vdots & \vdots & \vdots & \vdots & \ddots \end{pmatrix}, \tag{2.35}$$

and its eigenvalues computed from the first 200 rows and columns are

$$\lambda^1_{\mathrm{HS}} = \Big(0, \quad 0.69503, \quad 0.92114, \quad 0.98581, \quad \cdots, \quad 1\Big). \tag{2.36}$$

Perturbations that contain combinations such as $c_x c_y$ are represented by the $l = 2$ matrix. The eigenvalues of $\mathbf{C}^2$ are given by

$$\lambda^2_{\mathrm{HS}} = \Big(0.95840, \quad 0.99505, \quad \cdots, \quad 1\Big). \tag{2.37}$$

In contrast to the eigenvalues, the diagonal elements of the matrix $\mathbf{C}^2$ are

$$\text{diag}[\mathbf{C}^2] = \Big(1.13137, \quad 1.38054, \quad 1.66801, \quad 1.94575, \quad 2.20563, \cdots\Big) \tag{2.38}$$

showing that the off-diagonal elements have substantial influence in slowing the relaxation rates. For $l \geq 3$ it appears that no discrete eigenvalues exist [3, 4] or they are all equal to 1. We have not performed full investigation into this area.

The zero eigenvalues of the collision matrices appear exactly where we expect them. The matrices $\mathbf{C}^2$ and $\mathbf{C}^3$ have no zero eigenvalues, $\mathbf{C}^1$ has exactly one, and $\mathbf{C}^0$ has exactly two. This confirms our picture of conserved quantities and shows that additional conserved quantities do not exist.

Note that all of the eigenvalues appear to asymptotically approach unity from below. It is well known that for hard spheres, all discrete relaxation rates are greater than $-\frac{\lambda_M}{\tau_{\text{HS}}}$ and all discrete eigenvalues are less than λ_M [3, 4] where λ_M is the minimum value of the function $M_{\text{HS}}(c)$. The proof of this fact by Kuščer and Williams [15] relies in a certain way on the continuity and integrability of Q_{HS} and R_{HS}. It shows that all of the discrete eigenvalues must accumulate below the value λ_M. Beyond the value λ_M there is a continuous spectrum of eigenvalues and the eigenvectors are expected to be singular or unphysical [12, 13, 14].

Since the minimum of the function $M_{\text{HS}}(c)$ occurs at $c = 0$, we can easily calculate that for hard spheres, $\lambda_M = M_{HS}(0) = 1$. Thus our dimensionless eigenvalues will accumulate at the value 1. Our results are consistent with that observation. In the more complicated collision operators that appear later, the function M_{HS} changes in form. In general, we call the function $M(c)$. The proof that λ_M exists and is equal to the minimum of $M(c)$ is not easy to generalize to these collision kernels. However, we will continue to assert that the minimum of $M(c)$ represents the maximum possible discrete eigenvalue λ_M, and see if our numerically computed eigenvalues agree. The accumulation of eigenvalues may seem strange at first glance, but consideration of some other physical systems shows that it is not. Indeed, the spectrum of eigenvalues of the Schrödinger equation often has this form.

2.5 Finite Ordinate Method

For the hard sphere gas and the gas of Maxwell molecules we are actually quite lucky that we can find closed form expressions for the elements of the collision matrix. For most other interaction potentials

the integrals similar to Eqs. (2.21), (2.22) and (2.23) must be done by numerical quadrature. This will certainly be the case in the following Chapters. However, there are other methods of discretizing Eq. (2.20) besides expanding in a set of orthogonal polynomials.

Here we outline a method of computing the relaxation rates and modes that embraces numerical calculations. We demonstrate this method in a general form which can be applied to the other eigenvalues equations that occur later. The idea is to begin with Eq. (2.20) and use it to directly generate a collision matrix. The general form of Eq. (2.20), which will appear again, is

$$\frac{d\phi(\mathbf{c}_1,t)}{dt} = \mathcal{M}(\mathbf{c}_1)\phi(\mathbf{c}_1,t) + \int d\mathbf{c}_2 \frac{\mathcal{W}(c_2)}{\mathcal{V}(c_1)}\mathcal{K}(\mathbf{c}_1,\mathbf{c}_2)\phi(\mathbf{c}_2,t) \tag{2.39}$$

The functions $\mathcal{W}(c)$ and $\mathcal{V}(c)$ have been inserted for generality that will be needed later. For the linearized Boltzmann equation, $\mathcal{W}(c) = e^{-c^2}$ and $\mathcal{V}(c) = 1$.

Our first task is to turn this into a one-dimensional equation using the properties of the functions $\mathcal{M}(\mathbf{c}_1)$ and $\mathcal{K}(\mathbf{c}_1,\mathbf{c}_2)$. As mentioned above, the function $\mathcal{M}$ only depends on the magnitude of its argument and $\mathcal{K}$ only depends on the magnitude of each argument and the angle between them. This allows us to write them as

$$\mathcal{M}(\mathbf{c}_1) = \mathcal{M}(c_1) \qquad \text{and} \qquad \mathcal{K}(\mathbf{c}_1,\mathbf{c}_2) = \sum_{l=0}^{\infty} \frac{2l+1}{2}\mathcal{K}^l(c_1,c_2)P_l(\hat{\mathbf{c}}_1\cdot\hat{\mathbf{c}}_2). \tag{2.40}$$

If we then do a partial expansion of the angular dependence of the function $\phi(\mathbf{c},t)$ as

$$\phi(\mathbf{c},t) = \sum_{l=0}^{\infty}\sum_{m=-l}^{l} \phi_{l,m}(c,t)Y_l^m(\hat{\mathbf{c}}), \tag{2.41}$$

we obtain

$$\frac{d\phi_{l,m}(c_1,t)}{dt} = \mathcal{M}(c_1)\phi_{l,m}(c_1,t) + 2\pi\int_0^{\infty} dc_2 c_2^2 \frac{\mathcal{W}(c_2)}{\mathcal{V}(c_1)}\mathcal{K}^l(c_1,c_2)\phi_{l,m}(c_2,t), \tag{2.42}$$

where

$$\mathcal{K}^l(c_1,c_2) = \int_{-1}^{1} d(\hat{\mathbf{c}}_1\cdot\hat{\mathbf{c}}_2)\mathcal{K}(\mathbf{c}_1,\mathbf{c}_2)P_l(\hat{\mathbf{c}}_1\cdot\hat{\mathbf{c}}_2). \tag{2.43}$$

The spherical harmonic addition theorem (Eq. (A.1)) has been used to eliminate the angular integrations.

Equation (2.42) is the sought one dimensional kinetic equation. The properties of the kernel function allow the different angular modes to decouple, similarly to how the angular modes decoupled in Eq. (2.29). We define the eigenvalues λ_n^l and eigenvectors $\phi_n^l(c_1)$ (which again do not depend on m) as the set which satisfies

$$\lambda_n^l \phi_n^l(c_1) = \mathcal{M}(c_1)\phi_n^l(c_1) + 2\pi \int_0^\infty dc_2 c_2^2 \frac{\mathcal{W}(c_2)}{\mathcal{V}(c_1)} \mathcal{K}^l(c_1, c_2)\phi_n^l(c_2). \tag{2.44}$$

The presence of the factor $c_2^2 \frac{\mathcal{W}(c_2)}{\mathcal{V}(c_1)}$ makes the overall kernel of the convolution asymmetric and makes the orthogonality relationship of $\phi_n^l(c)$ much more complicated. We define the "symmetrized eigenfunction"

$$\psi_n^l(c) \equiv c\sqrt{\mathcal{W}(c)\mathcal{V}(c)}\phi_n^l(c), \tag{2.45}$$

which converts Eq. (2.44) to

$$\lambda_n^l \psi_n^l(c_1) = \mathcal{M}(c_1)\psi_n^l(c_1) + \int_0^\infty dc_2 \left[2\pi c_1 c_2 \sqrt{\frac{\mathcal{W}(c_1)\mathcal{W}(c_2)}{\mathcal{V}(c_1)\mathcal{V}(c_2)}} \mathcal{K}^l(c_1, c_2) \right] \psi_n^l(c_2). \tag{2.46}$$

The eigenvectors ψ_n^l obey the orthogonality relation

$$\int_0^\infty dc \psi_n^l(c)\psi_{n'}^l(c) = \delta_{n,n'} \tag{2.47}$$

Equation (2.46) is known as a symmetric Fredholm integral equation of the second kind for the function $\psi_n^l(c_1)$. Several results on the spectrum of eigenvalues for such an equation are discussed in Kondo [46] and for hard spheres in ref. [15]. For our purposes, we only require one of these results. If the kernel function $\mathcal{K}^l(c_1, c_2)$ is completely continuous then this equation is guaranteed to have a countable set of real eigenvalues. This means we are "safe" to compute eigenvalues of a discretized equation numerically and interpret them as the "true" eigenvalues that have physical meaning.

We now generate a matrix representation of Eq. (2.46) by first choosing a quadrature scheme for evaluating integrals on the interval $(0, \infty)$:

$$\int_0^\infty dx f(x) \approx \sum_{i=1}^{N_Q} w_i f(x_i), \tag{2.48}$$

where x_i are the quadrature points and w_i are the quadrature weights. Different quadrature schemes may be better suited to capture the details of the kernel $\mathcal{K}^l(c_1, c_2)$, but any choice will increase in accuracy as the total number of quadrature points, N_Q, increases. We then use this quadrature scheme to directly evaluate the integral in Eq. (2.46) and demand that the equation be satisfied when c_1 is equal to any of the quadrature points. This results in the matrix equation

$$\lambda_n^l \psi_n^l(x_i) = \sum_{j=1}^{N_Q} \left[\mathcal{M}(x_i)\delta_{i,j} + 2\pi w_j x_i x_j \sqrt{\frac{\mathcal{W}(x_i)\mathcal{W}(x_j)}{\mathcal{V}(x_i)\mathcal{V}(x_j)}} \mathcal{K}^l(x_i, x_j) \right] \psi_n^l(x_j). \tag{2.49}$$

This matrix equation can be analyzed by standard methods to find its eigenvalues and eigenvectors. Matrices generated in this way for the hard-spheres collision operator give the same eigenvalues as the polynomial expansion method. For more complicated collision operators, this method has a significant advantage in that it is impartial and robust when the details of the eigenvectors are not well known. As knowledge about the eigenvectors improves, one can change quadrature schemes to better capture behavior such as rapid oscillations of the eigenvectors.

Of course these numerically computed eigenvalues will always differ from the true eigenvalues due to truncation error in the discretization. There are several ways to determine whether an eigenvalue is good or not. The simplest way is to generate matrices of increasing size and see if the eigenvalues converge as $N_Q \to \infty$. A reliable method is to plot each eigenvalue versus $\frac{1}{N_Q}$ and perform some kind of fit on this plot. The vertical intercept of this fit offers a best estimate of the true eigenvalue. We shall illustrate this fitting procedure for actual data in Chapter 5, Fig. 5.3.

Another method to check the quality of the eigenvalues is to look at a plot of the associated eigenvector. If it appears to be continuous and smooth, with nodes in reasonable locations, then the eigenvalue is probably acceptable or at least on the right track. If the eigenvector is discontinuous or has extremely rapid variations, the associated eigenvalue should not be trusted.

In the following sections, we will use this finite ordinate method exclusively, pointing out any differences from this discussion when they occur. The only modifications of this method will be the form of the functions $\mathcal{M}$, $\mathcal{W}$, $\mathcal{V}$ and $\mathcal{K}$. Determining the kernel values $\mathcal{K}^l(x_i, x_j)$ constitutes the bulk of the calculation. Using the quadrature scheme (2.48), the values $\mathcal{M}(x_i)$ can usually be written as simple sums over the already calculated components of $\mathcal{K}^l(x_i, x_j)$.

2.6 Relaxation Rates: Finite Ordinate

In this section, we apply the finite ordinate method to the linearized Boltzmann collision operator and give explicit expressions that are involved in the calculation. Our first task is to find simpler forms of Eqs. (2.21) and (2.22) by doing as many integrations as possible. These manipulations are straightforward but do require some intuition concerning the symmetries of the integrand. The derivations are not particularly illuminating, so we only quote the results, which are

$$Q_{\mathrm{HS}}(\mathbf{c}_1, \mathbf{c}_2) = \frac{\pi}{2}|\mathbf{c}_1 - \mathbf{c}_2| \tag{2.50}$$

and

$$R_{\mathrm{HS}}(\mathbf{c}_1, \mathbf{c}_2) = \frac{\pi}{2|\mathbf{c}_1 - \mathbf{c}_2|} \exp\left[\frac{(\mathbf{c}_1 \times \mathbf{c}_2)^2}{(\mathbf{c}_1 - \mathbf{c}_2)^2}\right]. \tag{2.51}$$

This form of the collision kernels is known as Hilbert's form [47].

Next, we must compare Eqs. (2.20) and (2.39) to see that

$$\mathcal{M}(\mathbf{c}) = M_{\mathrm{HS}}(\mathbf{c}), \qquad \mathcal{W}(c_2) = e^{-c_2^2}, \qquad \mathcal{V}(c_1) = 1 \tag{2.52}$$

and

$$\mathcal{K}(\mathbf{c}_1, \mathbf{c}_2) = \frac{1}{\pi^2}\left(Q_{\mathrm{HS}}(\mathbf{c}_1, \mathbf{c}_2) - 2R_{\mathrm{HS}}(\mathbf{c}_1, \mathbf{c}_2)\right). \tag{2.53}$$

The overall factor of $1/\tau_{\mathrm{HS}}$ in Eq. (2.20) sets the timescale of the relaxation, meaning that in the solution, the elapsed time t will always appear in the form t/τ_{HS}. This form of $\mathcal{W}$ and $\mathcal{V}$ gives

$$\psi_n^l(c) = ce^{-\frac{1}{2}c^2}\phi_n^l(c), \tag{2.54}$$

according to Eq. (2.45).

The third step is to choose l and obtain the l^{th} order collision matrix by using Eq. (2.43) to obtain the angular reduced values $\mathcal{K}^l(c_1, c_2)$. Given the form of $\mathcal{K}^l(\mathbf{c}_1, \mathbf{c}_2)$, we define two functions analogous to $\mathcal{K}^l(c_1, c_2)$,

$$Q_{\mathrm{HS}}^l(c_1, c_2) = \int_{-1}^{1} d(\hat{\mathbf{c}}_1 \cdot \hat{\mathbf{c}}_2) Q_{\mathrm{HS}}(\mathbf{c}_1, \mathbf{c}_2) P_l(\hat{\mathbf{c}}_1 \cdot \hat{\mathbf{c}}_2), \tag{2.55}$$

and

$$R^l_{\mathrm{HS}}(c_1, c_2) = \int_{-1}^{1} d(\hat{\mathbf{c}}_1 \cdot \hat{\mathbf{c}}_2) R_{\mathrm{HS}}(\mathbf{c}_1, \mathbf{c}_2) P_l(\hat{\mathbf{c}}_1 \cdot \hat{\mathbf{c}}_2). \tag{2.56}$$

These two simpler functions can be used to write the final matrix equation. After choosing an appropriate quadrature scheme (2.48), we can use Eq. (2.49) to find the matrix elements of the matrix that will be sent to the computational eigenvalue/eigenvector routines. These are given by

$$H^l_{i,j} = M_{\mathrm{HS}}(x_i)\delta_{i,j} + \frac{2}{\pi} w_j x_i x_j e^{-\frac{1}{2}(x_i^2 + x_j^2)} \left(Q^l_{\mathrm{HS}}(x_i, x_j) - 2R^l_{\mathrm{HS}}(x_i, x_j) \right) \tag{2.57}$$

We also note that we can use the angular reduction and the quadrature scheme as a method of calculating $M_{\mathrm{HS}}(c)$. Doing this, we obtain

$$M_{\mathrm{HS}}(x_i) = \frac{2}{\pi} \sum_{j=1}^{N_Q} w_j x_j^2 e^{-x_j^2} Q^0_{\mathrm{HS}}(x_i, x_j). \tag{2.58}$$

Note that only the $l = 0$ kernel is necessary to compute $M_{\mathrm{HS}}(x_i)$.

The computation of the function values $Q_{\mathrm{HS}}(x_i, x_j)$ and $R_{\mathrm{HS}}(x_i, x_j)$ from Eqs. (2.55) and (2.56) constitute the bulk of the calculation for obtaining the matrix elements. While these functions can be written explicitly in closed form for the hard spheres Boltzmann equation, the derivation is rather long and the result is not very illuminating. The result is useful for rapid calculation of matrix elements. However, for the hard spheres Boltzmann equation, there is only ever one matrix for each value of l and the integrals in Eqs. (2.55) and (2.56) converge rapidly with most quadrature schemes. To avoid confusion later, note that the quadrature scheme that we just mentioned for evaluating Eqs. (2.55) and (2.56) is completely separate from the quadrature scheme (2.48) used to evaluate the convolution (2.46).

2.7 Mode Expansion

In this section, we also give a formal solution to the linearized Boltzmann equation (2.16) in terms of a mode expansion over the numerically computed eigenmodes. This expansion arises from a combination

of Eqs. (2.15), (2.41) and (2.54). This results in the expression

$$f(\mathbf{v},t) = f^0(\mathbf{v}) + \sqrt{\frac{4}{\sqrt{\pi}}}\frac{1}{ce^{-\frac{1}{2}c^2}}f^0(\mathbf{v})\sum_{n=0}^{\infty}\sum_{l=0}^{\infty}\sum_{m=-l}^{l}\mathcal{A}_{n,l,m}e^{-\lambda_l^n t/\tau_{\text{HS}}}\psi_n^l(c)Y_l^m(\hat{\mathbf{c}}), \tag{2.59}$$

where $\mathcal{A}_{n,l,m}$ is an expansion coefficient.

Before giving the expression for $\mathcal{A}_{n,l,m}$ and explaining the coefficient $\sqrt{\frac{4}{\sqrt{\pi}}}$, let us note that we can simplify the mode expansion by using the form of the first eigenfunction $\psi_0^0(c)$. From our knowledge of the conserved quantities, we know that

$$\phi_0^0(c) \propto 1, \qquad \phi_1^0(c) \propto c \qquad \textit{and} \qquad \phi_0^1(c) \propto c^2 + B. \tag{2.60}$$

The proportionality constants and the constant B will be determined from the orthogonality condition (2.47). Using the general forms (2.60) along with the relation (2.54) and the orthogonality condition (2.47) we can find that

$$\psi_0^0(c) = \sqrt{\frac{4}{\sqrt{\pi}}}ce^{-\frac{1}{2}c^2}, \tag{2.61}$$

$$\psi_1^0(c) = \sqrt{\frac{8}{3\sqrt{\pi}}}c^2e^{-\frac{1}{2}c^2} \tag{2.62}$$

and

$$\psi_0^1(c) = \sqrt{\frac{8}{3\sqrt{\pi}}}c\left(c^2 - \frac{3}{2}\right)e^{-\frac{1}{2}c^2}. \tag{2.63}$$

Equation (2.61) can be used to write the mode expansion in the form

$$f(\mathbf{v},t) = f^0(\mathbf{v}) + n\left(\frac{m}{2\pi k_B T}\right)^{\frac{3}{2}}\frac{1}{c^2}\sum_{n=0}^{\infty}\sum_{l=0}^{\infty}\sum_{m=-l}^{l}\mathcal{A}_{n,l,m}e^{-\lambda_l^n t/\tau_{\text{HS}}}\psi_0^0(c)\psi_n^l(c)Y_l^m(\hat{\mathbf{c}}), \tag{2.64}$$

where now

$$\mathcal{A}_{n,l,m} = \int d\mathbf{r}\int d\mathbf{v}[f(\mathbf{r},\mathbf{v},0) - f^0(\mathbf{r},\mathbf{v})]\frac{\psi_n^l(c)}{\psi_0^0(c)}Y_l^{m*}(\hat{\mathbf{c}}). \tag{2.65}$$

The introduction of the coefficient $\sqrt{\frac{4}{\sqrt{\pi}}}$ in Eq. (2.59) was simply so that we could make the replacement (2.61) in Eq. (2.64) resulted in no extra coefficients. In this mode expansion, we only sum over the discrete eigenmodes of the collision operator and exclude the eigenmodes from the continuous spectrum. This restricts the space of perturbation functions to a subspace of all functions, and this

restriction may cause disagreements with experiment in certain extreme situations.

Note that Eq. (2.64) describes exponential relaxation to the equilibrium distribution $f^0(\mathbf{v})$ for all eigenmodes with $\lambda_l^n > 0$. One may be concerned that for conserved quantities this eigenvalue is zero, so Eq. (2.64) seems to predict relaxation to some other state. However, consider Eq. (2.65) when applied to one of the eigenmodes for which $\lambda_l^n = 0$. This will result in that $\mathcal{A}_{n,l,m}$ being zero, since for any conserved quantity $q(\mathbf{c})$, $\int d\mathbf{r} \int d\mathbf{v} q(\mathbf{c}) f(\mathbf{r}, \mathbf{v}, t) = \int d\mathbf{r} \int d\mathbf{v} q(\mathbf{c}) f^0(\mathbf{r}, \mathbf{v})$ by definition. We note that a BGK type approximation [48] can be obtained by assuming that non-zero eigenvalues are identical.

2.8 Transport Coefficients

In this section, we show one way in which the transport coefficients of the classical hard sphere gas can be related to the collision matrix. To do this, we will use the method of expansion in terms of Burnett functions (c.f. sec. 2.4). We will not develop a general method for obtaining transport coefficients using the finite ordinate method, nor will we generalize this method to the other collision operators encountered later. We do note however, that such extension are possible in principle. Instead we outline one possible method to show that such relationships do exist.

The coefficients of shear viscosity η and thermal conductivity κ, in terms of dimensionless velocity coordinates, are given by [43, 44]

$$\eta = -\frac{4nk_BT}{\pi^{\frac{3}{2}}} \int d\mathbf{c} e^{-c^2} c_x c_y \mathbf{C}^{-1} c_y c_x \tag{2.66}$$

and

$$\kappa = -\frac{2nk_B^2T}{m\pi^{\frac{3}{2}}} \int d\mathbf{c} e^{-c^2} \left(c^2 - \frac{5}{2}\right) c_x \mathbf{C}^{-1} c_x \left(c^2 - \frac{5}{2}\right) \tag{2.67}$$

where the operation $\mathbf{C}\phi(\mathbf{c})$ is defined as the action of the right hand side of Eq. (2.20)

In general, transport coefficients contain an integral of the type

$$I = \int d\mathbf{c} e^{-c^2} A^*(\mathbf{c}) \mathbf{C}^{-1} A(\mathbf{c}), \tag{2.68}$$

where $\mathbf{C}^{-1}A(\mathbf{c})$ denotes the inverse of the operator $\mathbf{C}$ acting on the function $A(\mathbf{c})$.

By expanding the function $A(\mathbf{c})$ in terms of the polynomials $\chi_{n,l,m}$ we can express this as

$$I = \sum_{n,l,m} \sum_{n'} A^*_{n,l,m} \left[\mathbf{C}^l\right]^{-1}_{n,n'} A_{n',l,m} \tag{2.69}$$

where $A_{n,l,m}$ are the expansion coefficients of the function $A(\mathbf{c})$. We show how to obtain the result (2.68) in the following discussion. In order to resolve the inverse $\mathbf{C}^{-1}A(\mathbf{c})$, define $B(\mathbf{c})$ as the function for which

$$A(\mathbf{c}) = \mathbf{C}B(\mathbf{c}). \tag{2.70}$$

If we expand both $A(\mathbf{c})$ and $B(\mathbf{c})$ in terms of the polynomials $\chi_{n,l,m}(\mathbf{c})$, this becomes

$$\sum_{n",l",m"} A_{n",l",m"} \chi_{n",l",m"}(\mathbf{c}) = \sum_{n',l',m'} B_{n',l',m'} \mathbf{C}^{-1} \chi_{n',l',m'}(\mathbf{c}) \tag{2.71}$$

Multiplying by $e^{-c^2}\chi^*_{n,l,m}(\mathbf{c})$ and integrating over $\mathbf{c}$, we obtain

$$A_{n,l,m} = \sum_{n',l',m'} B_{n',l',m'} \int d\mathbf{c} e^{-c^2} \chi^*_{n,l,m}(\mathbf{c}) \mathbf{C}^{-1} \chi_{n',l',m'}(\mathbf{c}) \tag{2.72}$$

Comparing this to Eqs. (2.28) and (2.29) we see that

$$\int d\mathbf{c} e^{-c^2} \chi^*_{n,l,m}(\mathbf{c}) \mathbf{C}^{-1} \chi_{n',l',m'}(\mathbf{c}) = C^l_{n,n'} \delta_{l,l'} \delta_{m,m'} \tag{2.73}$$

and thus if the expansion coefficients $A_{n,l,m}$ are known, we determine $B_{n,l,m}$ as the values which satisfy

$$A_{n,l,m} = \sum_{n'} C^l_{n,n'} B_{n',l,m} \tag{2.74}$$

This is easily solved if we treat $C^l_{n,n'}$ as a matrix $\mathbf{C}^l$, but we know that $\mathbf{C}^0$ and $\mathbf{C}^1$ are non-invertible because they have zero eigenvalues. However, we can still find a solution to Eq. (2.74) provided that we use a function $A(\mathbf{c})$ for which $A_{0,0,m} = 0$, $A_{1,0,m} = 0$ and $A_{1,0,m} = 0$. In these cases, we trivially solve the zero rows and remove them from the matrix. The remaining matrix is then invertible and

can be used to find the remaining $B_{n,l,m}$. We therefore write

$$B_{n,l,m} = \sum_{n'} [\mathbf{C}^l]^{-1}_{n,n'} A_{n',l,m} \tag{2.75}$$

where the above process and condition on $A_{n,l,m}$ are implied. We now turn back to the integral expression I in Eq. (2.68) and substitute $B(\mathbf{c})$ for $\mathbf{C}^{-1}A(\mathbf{c})$. Then expand the function $A(\mathbf{c})$ and $B(\mathbf{c})$ in terms of $\chi_{n,l,m}(\mathbf{c})$,

$$I = \int d\mathbf{c} e^{-c^2} \sum_{n,l,m} A^*_{n,l,m} \chi^*_{n,l,m}(\mathbf{c}) \sum_{n',l',m'} B_{n',l',m'} \chi_{n',l',m'}(\mathbf{c}) \tag{2.76}$$

We quickly see that

$$I = \sum_{n,l,m} A^*_{n,l,m} B_{n,l,m} \tag{2.77}$$

and using the above expression for $B_{n,l,m}$ we obtain Eq. (2.69).

For the shear viscosity, the function is $A(\mathbf{c}) = c_x c_y$ and the expansion coefficients are given by

$$A_{n,l,m} = \frac{i\pi^{\frac{3}{4}}}{2\sqrt{2}} \delta_{n,0} \delta_{l,2} (\delta_{m,2} - \delta_{m,-2}) \tag{2.78}$$

The integral is equal to

$$I = \frac{\pi^{\frac{3}{2}}}{4} \left[\mathbf{C}^2\right]^{-1}_{0,0} \tag{2.79}$$

and so the transport coefficient is equal to

$$\eta = -n_0 k_B T \left[\mathbf{C}^2\right]^{-1}_{0,0} \tag{2.80}$$

Employing a similar procedure for κ results in

$$\kappa = -\frac{5 n_0 k_B^2 T}{2m} \left[\mathbf{C}^1\right]^{-1}_{1,1} \tag{2.81}$$

For hard spheres, we can compute the inverse matrix elements numerically, and obtain $[\mathbf{C}^2]^{-1}_{0,0} = -0.898056 \tau_{\mathrm{HS}}$ and $[\mathbf{C}^1]^{-1}_{1,1} = -1.35926 \tau_{\mathrm{HS}}$. The transport coefficients for a hard sphere gas are then

given by

$$\eta = (0.898056)\frac{1}{a^2}\sqrt{\frac{mk_BT}{8\pi}} \tag{2.82}$$

$$\kappa = (1.35926)\frac{5k_B}{2a^2}\sqrt{\frac{k_BT}{8\pi m}} \tag{2.83}$$

It is interesting to note that if we neglect the off-diagonal elements of the collision matrix, we obtain the same numerical coefficients given in standard texts [42, 43] of $\frac{5\sqrt{2}}{8} = 0.8838835$ for η and $\frac{15\sqrt{2}}{16} = 1.325825$ for κ.

The numerical coefficients computed from the inverse of the full matrix agree with the expected increase in the transport coefficients for hard spheres when off-diagonal contributions are included [44]. The power of this method is that once the elements of the collision matrix are known, transport coefficients can be computed quickly and accurately. This can be especially useful for collision matrices which are computed numerically from a scattering cross section and collision matrices resulting from phenomenological collision kernels.

The derivation of expressions for transport coefficients could certainly be an area of future work, as it provides a direct route to comparison with experiment. In this report however, we continue to focus on the computation of eigenvalues and eigenvectors of extensions of the Boltzmann equation into quantum regimes.

2.9 Summary

In this Chapter, we have discussed the origin of the Boltzmann equation and how it describes the evolution of a classical gas. We have discussed the equilibrium distribution, which is a steady-state solution of the Boltzmann equation and found that it depends on the five conserved quantities of a two-body collision: particle number, momentum and energy. We have linearized the Boltzmann equation for small perturbations about this equilibrium distribution and found the resulting characteristic relaxation rates. The relaxation rates are given by the eigenvalues of the linearized collision operator.

We have discussed several important techniques for analyzing the linearized collision operator. Expansion in a set of orthogonal polynomials is the classical approach to this problem, but the finite ordinate method of section 2.5 can be more readily applied to a wider variety of collision operators. We have shown how to approach the problem of the hard sphere collision operator by using the finite

ordinate method. This is an important discussion as it will be used again the Chapters 5 and 6 to analyze the collision operators appearing there. The discussion of mode expansions gives a formal solution to the linearized Boltzmann equation in terms of the eigenmodes and eigenvalues of the linearized collision operator. In the final section, we have offered a brief discussion of how one can relate the transport coefficients of the hard sphere gas to the collision operator. While we will not discuss the transport coefficients for any other collision operators, section 2.8 offers a starting point for such investigations.

3 Hard Sphere Simulation

The information presented in the preceding Chapter has been well-known for quite a long time. In order to add to this knowledge, we created a hard sphere simulation to verify the following points:

1. That a gas of hard spheres does in fact relax to an equilibrium distribution that is a Maxwell-Boltzmann distribution.

2. That evolution towards equilibrium takes place by an exponential relaxation of eigenmodes, with each eigenmode relaxing at a different rate.

3. That the eigenmodes of the hard sphere relaxation are different from the Burnett functions.

4. That the overall rate constant $1/\tau_{\mathrm{HS}}$ calculated from simulation parameters agrees with the observed overall rate of the simulation.

5. That the eigenvalues of specific modes agree with the theoretical predictions.

6. That the above points can be shown using a manageable number of particles.

Though some of these points may seem trivial upon the first reading. They are actually quite profound, given that the hard spheres simulation uses essentially only the interaction between particles (2.17) as its input. Note that the truth of the first two points depends on several of the assumptions that were made during the derivation of the Boltzmann collision integral. In particular, these statements should fail if we simulate a gas that is very dense. But a finite system of hard spheres affords us some leeway here, since collisions are pairwise in all but the most contrived of circumstances. The main method by which the first two points can fail is breaking of the *molecular chaos* assumption for dense gases. Here the particles develop velocity correlations that lead to long time tails of the form t^{-p} instead of exponential relaxation [49]. It is our belief that our simulations have a low enough density that such effects are not noticeable.

3.1 Simulation Method

For a hard spheres simulation, we begin by uniformly distributing N spheres of diameter a within a cubic cell of volume L^3, with periodic boundary conditions, in such a way that no sphere overlaps with any other sphere. Specifically, if $\mathbf{r}_i$ is the position of the i^{th} sphere then for all $j \neq i$ we must have $|\mathbf{r}_i - \mathbf{r}_j| > a$. We then assign each sphere a velocity $\mathbf{v}_i$ in such a way as to approximate a distribution function $f(\mathbf{v}) = f^0(\mathbf{v})(1 + \phi_0(\mathbf{c}))$ where $\phi_0(\mathbf{c})$ is our desired initial perturbation. Choice of the initial perturbation will be discussed below.

Schematically, the simulation is carried out as follows: (a) For each pair of spheres, we compute the contact time t_{ij}, which is the time at which the spheres i and j will collide, should they follow straight line paths. This is found by the contact condition $|\mathbf{r}_i + \mathbf{v}_i(t_{ij} - t) - \mathbf{r}_j - \mathbf{v}_j(t_{ij} - t)| = a$, where t is the current time. We solve the contact condition for t_{ij} and choose the smallest positive value for $t_{ij} - t$. (b) We then perform a search to find the smallest t_{ij} value, t^*, which represents the time of the next collision. (c) All spheres are advanced to t^* following straight-line paths according to their locations and velocities at t. (d) The colliding spheres have their velocities altered according to the kinematics of a purely elastic collision. (e) Then we update all values of t_{ij} that involve the colliding particles and return to step (b).

We implement periodic boundary conditions by adding two parts to the above algorithm: (1) In step (a), we calculate not 1, but 27 values for t_{ij}, each representing sphere j offset by $-L$, 0 or L in the x, y or z direction. Elastic collision kinematics are also adjusted accordingly. (2) We calculate the time at which each particle will strike each wall and add this list of times to our search in step (b). If a wall collision occurs as the next soonest collision, that sphere is simply moved to the opposite side of the simulation cell.

3.2 Data Measurement

As the simulation progresses, we have access to each $\mathbf{r}_i$ and each $\mathbf{v}_i$ at any iteration. With a typical particle number of $N = 1000$, this is clearly a vast amount of information. Since our goal is observation of relaxation rates, the expansion coefficients $g_{n,l,m}$ are of particular interest. Let us see how we go about extracting these values from each $\mathbf{r}_i$ and $\mathbf{v}_i$.

Assume that we are given an arbitrary continuous distribution function $f(\mathbf{r},\mathbf{v},t)$ that exists in a volume V. We must first determine the number of particles present and their most probably velocity v_p in equilibrium. These are given by $N=\int d\mathbf{r}d\mathbf{v}f(\mathbf{r},\mathbf{v},t)$ and $v_p^2=\frac{2}{3N}\int d\mathbf{r}d\mathbf{v}v^2f(\mathbf{r},\mathbf{v},t)$. In order to determine $g_{n,l,m}(t)$, we use the equations which define the perturbations, Eq. (2.15) and (2.26) to get

$$f(\mathbf{r},\mathbf{v},t)=\frac{N}{L^3\pi^{3/2}v_p^3}e^{-c^2}\left[1+\sum_{n,l,m}\chi_{n,l,m}(\mathbf{c})g_{n,l,m}(t)\right] \tag{3.1}$$

where $f^0(\mathbf{v})$ has be written in terms of v_p and $\mathbf{c}$. Using the orthogonality of the polynomials $\chi_{n,l,m}$, we can invert Eq. (3.1) to get an explicit formula for $g_{n,l,m}(t)$.

$$g_{n,l,m}(t)=-\pi^{\frac{3}{4}}\delta_{n,0}\delta_{l,0}\delta_{m,0}+\frac{\pi^{\frac{3}{2}}v_p^3}{N}\int d\mathbf{r}d\mathbf{c}\chi^*_{n,l,m}(\mathbf{c})f(\mathbf{r},\mathbf{v},t) \tag{3.2}$$

We now construct an artificial phase space density function $\nu(\mathbf{r},\mathbf{v},t)$ from $\mathbf{r}_i(t)$ and $\mathbf{v}_i(t)$ by writing

$$\nu(\mathbf{v},t)=\sum_{i=1}^{N}\delta^3(\mathbf{r}-\mathbf{r}_i(t))\delta^3(\mathbf{v}-\mathbf{v}_i(t)). \tag{3.3}$$

This phase space density function is used in place of $f(\mathbf{r},\mathbf{v},t)$ in Eq. (3.2). Explicitly, this is

$$g_{n,l,m}(t)=-\pi^{\frac{3}{4}}\delta_{n,0}\delta_{l,0}\delta_{m,0}+\frac{\pi^{\frac{3}{2}}}{N}\sum_{i=1}^{N}\chi^*_{n,l,m}\left(\frac{\mathbf{v}_i(t)}{v_p}\right) \tag{3.4}$$

With Eq. (3.4) we can measure the relaxation of perturbations as the system evolves. It is of interest to note that by construction, $g_{0,0,0}(t)=0$, $g_{0,1,0}(t)\propto\langle c_z\rangle=0$, $g_{0,1,1}(t)\propto\langle c_x\rangle-i\langle c_y\rangle=0$, $g_{0,1,-1}(t)\propto\langle c_x\rangle+i\langle c_y\rangle=0$, and $g_{1,0,0}(t)\propto v_p^2-\frac{2}{3}\langle v^2\rangle=0$. This enforces the idea that the quantities N, $\langle\mathbf{c}\rangle$ and $\langle c^2\rangle$ are not expressed as perturbations, and therefore are conserved.

3.3 Relaxation of Perturbations

For the physical hard spheres problem the time scale is set by $\frac{1}{\tau_{\text{HS}}}=n_0a^2\sqrt{4\pi v_p^2}$ when written in terms of v_p. Measuring our eigenvalues in units of $\frac{1}{\tau_{\text{HS}}}$ yields dimensionless eigenvalues that are universal to

any classical hard sphere system. We can compute the time scale for our simulations using the formula

$$\frac{1}{\tau_{\mathrm{HS}}} = \frac{Na^2}{L^3}\sqrt{4\pi\frac{2}{3N}\sum_{i=0}^{N} v_i^2}. \tag{3.5}$$

Note that events always occur at the same rate provided that time is measured in units of τ_{HS}. Because of this, and for convenience, we choose to normalize all velocities before the simulation begins such that $\frac{2}{3N}\sum_{i=0}^{N} v_i^2 = 1$. Once this is done, the timescale can be found from $\frac{1}{\tau_{\mathrm{HS}}} = \frac{Na^2}{L^3}\sqrt{4\pi}$.

We can characterize the density by the dimensionless ratio $\eta = \frac{Na^3}{L^3}$, where a is the diameter of the particle. This number can be used to compare a given choice of N, a and L to a real-world situation. Room temperature ideal gases have $\eta \approx 10^{-3}$. Simulations we have run up to this point have had $\eta \sim 10^{-4}$. Simulations with lower densities take considerably longer to complete, due to the dominance of wall collisions.

In order to observe relaxation to equilibrium, we must begin with a distribution that is not in equilibrium. This is accomplished by choosing the initial velocities of the spheres such that $\phi_0(\mathbf{c}) \neq 0$. We do not expect the specific distribution of initial velocities to have much effect on the evolution of the system, so we choose a form of $\phi_0(\mathbf{c})$ that gives large values for the lowest order perturbation amplitudes. The initial condition used was

$$\phi_0(\mathbf{c}) = \alpha\chi_{2,0,0}(\mathbf{c}) \tag{3.6}$$

where α is a parameter used to set the magnitude of the perturbation. In order to observe the exponential relaxation over the noise, α has to be chosen as large as 0.5 or 0.75. While this does not satisfy $\phi(\mathbf{c}) \ll 1$, we observed pure exponential relaxation with negligible nonlinear effects. However, some care must be taken, since too large a value for α will create regions where the distribution function f becomes negative.

Consider the relaxation of a given perturbation amplitude $g_{n,l,m}(t)$. In practice, the perturbation amplitudes $g_{n,l,m}(t)$ from a single run are far too noisy to give any useful estimation of the eigenvalues. To compensate for this, we run up to 100 trials for a single set of parameters and store the data from

each trial in a separate file. Later, we parse these files and merge them according to

$$\bar{g}_{n,l,m} = \frac{1}{M}\sum_{k=1}^{M} g^k_{n,l,m} \tag{3.7}$$

where M is the total number of trials included in the merge and $g^k_{n,l,m}$ indicates the data from the kth trial. Examples of results obtained for $\bar{g}_{2,0,0}(t)$ and $\bar{g}_{3,0,0}(t)$ are shown in Fig. 3.1.

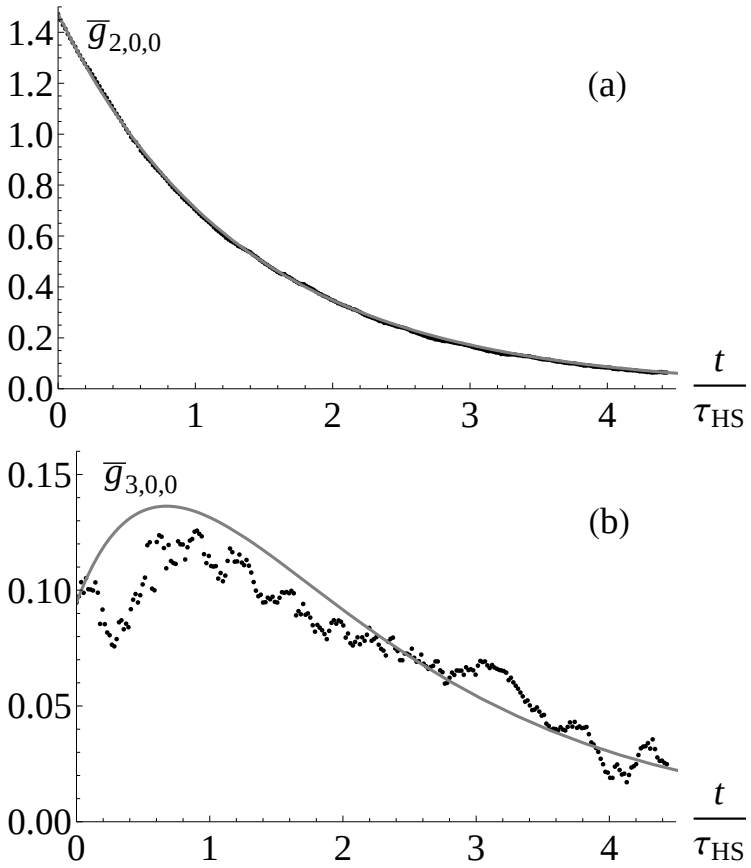

Figure 3.1: Plots of (a) $\bar{g}_{2,0,0}(t)$ and (b) $\bar{g}_{3,0,0}(t)$ obtained from numerical simulation (dots) compared to calculated values (solid curve) obtained from Eq. (2.30) using the same initial distribution.

3.4 Extraction of Eigenvalues

Note how, especially for $\bar{g}_{3,0,0}$ in Fig. 3.1, the evolution of the expansion coefficients $g_{n,l,m}(t)$ is not that of exponential relaxation. This shows clearly that the Burnett functions $\chi_{n,l,m}$ are not the eigenfunctions of the hard sphere collision operators. Performing an exponential fit to the expansion coefficients $g_{n,l,m}(t)$ will not yield the hard-spheres eigenvalues because the quantities $\bar{g}_{n,l,m}(t)$ do not exhibit independent exponential relaxation. The true eigenfunctions for hard spheres are given by a linear combination of $\chi_{n,l,m}$ that is determined by the eigenvectors of the collision operator matrices $\mathbf{C}^l$. We perform a linear transformation on the $\bar{g}_{n,l,m}(t)$ to obtain the correct coefficients of expansion terms of the eigenfunctions of the hard sphere collision operator,

$$h_{n,l,m}(t) = \sum_{n'=0}^{\infty} \Phi^l_{n,n'} \bar{g}_{n',l,m},(t) \tag{3.8}$$

where $\mathbf{\Phi}^l$ is the matrix of eigenvectors of the collision matrix $\mathbf{C}^l$. The quantities $h_{n,l,m}(t)$ do exhibit exponential relaxation. A plot of $h_{2,0,0}$ vs. $\frac{t}{\tau_{\mathrm{HS}}}$ is shown in Fig. (3.2) for $N = 1000$, $a = 0.010$ and $L = 2$.

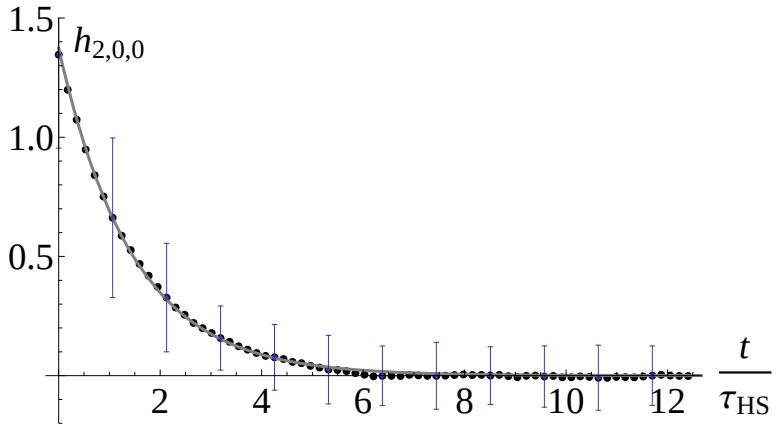

Figure 3.2: A plot of $h_{2,0,0}(t)$ as it evolves in the hard spheres simulation. Error bars show the extent of the statistical error. Dots show values obtained from numerical simulation. The solid line is an exponential regression. Here $N = 1000$, $a = 0.010$ and $L = 2$. These data points come from the same data set used to obtain Fig. (3.1).

To obtain the eigenvalues from these curves, we must perform a non-linear exponential regression on the data. Since, due to statistical errors, some of the $h_{n,l,m}(t)$ values may be negative, we cannot use transformations to do a standard linear regression. A comparison of values of the first and second largest non-zero eigenvalues for the hard sphere gas, obtained from theory and from the molecular dynamics simulation, are shown in Table 3.1 and are in good agreement. The uncertainties of higher order eigenvalues obtained from the simulation rapidly increases. This occurs because the chosen initial perturbation in Eq. (3.6) results in a very small amplitude for these eigenmodes.

N	a	η	λ_2^0	λ_3^0
600	0.005	9.37×10^{-6}	0.68 ± 0.10	0.92 ± 0.10
700	0.0075	3.69×10^{-5}	0.649 ± 0.048	0.775 ± 0.081
800	0.005	1.25×10^{-5}	0.682 ± 0.072	0.92 ± 0.21
1000	0.010	1.25×10^{-4}	0.686 ± 0.027	0.95 ± 0.12
1200	0.005	1.88×10^{-5}	0.670 ± 0.045	1.12 ± 0.33
1200	0.010	1.50×10^{-4}	0.669 ± 0.017	0.99 ± 0.12
Theory	-	-	0.671227	0.911572

Table 3.1: Simulated dimensionless eigenvalues for differing numbers of particles and particle radii. Each case results in similar eigenvalues, which are close to the theoretical eigenvalues. In all cases, $L_x = L_y = L_z = 2$.

3.5 Summary

In this Chapter we have discussed our method for performing a hard sphere simulation to verify the predictions of Chapter 2. The hard sphere simulation uses only the information about the microscopic interaction between the particles as its input. Analyzing the results of the hard sphere simulation requires computing the various moments of the velocity distribution and observing their evolution. Using the moments of the velocity distribution to compute the amplitude of each predicted hard sphere eigenmode, we observe independent exponential relaxation. The relaxation timescales match those predicted for each eigenmode. These results give us confidence that the methods outlined in Chapter 2 are fundamentally sound and should give correct results when applied to the systems we will study in Chapters 5 and 6.

4 Derivation of Kinetic Equations

4.1 Introduction

Our ultimate goal in this report is to extend the Boltzmann equation to describe degenerate quantum gases, in particular Bose-Einstein condensates. Unfortunately, the Boltzmann equation does not offer many hints about how to extend its range of applicability. We certainly can not expect the Boltzmann equation to correctly describe the behavior of quantum particles, since its derivation is explicitly based upon the dynamics of classical two-body collisions. To discuss quantum corrections to the Boltzmann equation, we must begin with a quantum-mechanical description of our system and try to derive from it an evolution equation that shares some of the characteristics of the Boltzmann equation. In considering what type of characteristics a quantum evolution equation could share with the Boltzmann equation, we are immediately faced with two important issues.

Firstly, the uncertainty principle prevents a description in terms of a phase space distribution. We cannot hope to specify the average amount of particles at position $\mathbf{r}$ and velocity $\mathbf{v}$, in fact we cannot even specify the position and velocity of a single particle simultaneously. What we can describe however, is the average number of particles in a particular quantum state. In fact, we have already made a choice that makes these quantum states correspond very closely to what we did with the Boltzmann equation. By considering particles in a rectangular box with periodic boundary conditions, we have made the single particle states produce a uniform spatial distribution of particles. We can then consider the average number of quantum particles in the quantum state with wave vector $\mathbf{k}$ to be the analogy of the average number of classical particles with velocity $\mathbf{v}$.

The second difficulty is that the primary evolution equation of non-relativistic quantum mechanics, the Schrödinger equation, describes only reversible (unitary) evolution. This means that we need to find a quantum analogue for the assumption of *molecular chaos*. This comes from an idea first put forth by Bogoliubov, known as the Bogoliubov assumption. It states that for a system that is out of equilibrium, the relaxation to equilibrium can occur in several stages when the timescales of the stages are very different from each other. During each relaxation stage, the number of parameters necessary

to describe the system accurately is reduced. This reduction allows us to focus on the evolution of a few parameters rather than solve the full N-body problem. The content of this assumption is similar to that of the *molecular chaos* assumption, in that we can describe the system by a reduced set of parameters (such as the single particle phase space distribution function) without needing additional information (such as two particle distribution functions). The application of this assumption is a bit more tedious than it may seem, but it does lead to an evolution equation which shares the relaxation behavior exhibited by the Boltzmann equation.

4.2 Hamiltonian in terms of particle operators

To begin our quantum description, we must first realize that we are dealing with an interacting many-body quantum system. In such systems, dealing with the wavefunction for each individual particle becomes incredibly cumbersome, and the methods of quantum field theory are employed to simplify the theoretical description. Since we wish to describe a system containing many interacting bosons, we begin by introducing the boson field $\hat{\psi}(\mathbf{r})$ and its conjugate $\hat{\psi}^\dagger(\mathbf{r})$ which obeys the commutation relation

$$[\hat{\psi}(\mathbf{r}), \hat{\psi}^\dagger(\mathbf{r}')] = \delta^3(\mathbf{r} - \mathbf{r}'). \tag{4.1}$$

The general Hamiltonian for this system can be written in terms of the field operators as

$$\hat{H} = \int d\mathbf{r} \hat{\psi}^\dagger(\mathbf{r}) \left[-\frac{\hbar^2}{2m}\nabla^2 + U(\mathbf{r}) + \frac{1}{2}\int d\mathbf{r}' \hat{\psi}^\dagger(\mathbf{r}') V(\mathbf{r}, \mathbf{r}') \hat{\psi}(\mathbf{r}') \right] \hat{\psi}(\mathbf{r}), \tag{4.2}$$

where $U(\mathbf{r})$ is a externally applied potential and $V(\mathbf{r}, \mathbf{r}')$ is the interaction potential between two particles at locations $\mathbf{r}$ and $\mathbf{r}'$. Since we will not discuss particles in an external trapping potential, and we want our single particle quantum states to be states of definite momentum, we immediately set $U(\mathbf{r}) = 0$. In order to duplicate the concept of hard sphere scattering, we take the interaction potential to have the form $V(\mathbf{r}, \mathbf{r}') = g\delta^3(\mathbf{r} - \mathbf{r}')$. This interaction is known as a contact interaction and is a low energy effective interaction.

Inserting these two forms for the external and interaction potentials, we obtain

$$\hat{H} = \int d\mathbf{r} \left[-\frac{\hbar^2}{2m}\hat{\psi}^\dagger(\mathbf{r})\nabla^2\hat{\psi}(\mathbf{r}) + \frac{g}{2}\hat{\psi}^\dagger(\mathbf{r})\hat{\psi}^\dagger(\mathbf{r})\hat{\psi}(\mathbf{r})\hat{\psi}(\mathbf{r}) \right]. \tag{4.3}$$

We want to write this Hamiltonian in a way that will lead to a description in terms of the average number of particles in a given momentum state. To do this, we introduced the operators $\hat{a}^\dagger_{\mathbf{k}}$ and $\hat{a}_{\mathbf{k}}$ and write the field operators as

$$\hat{\psi}(\mathbf{r}) = \sum_{\mathbf{k}} \hat{a}_{\mathbf{k}} f_{\mathbf{k}}(\mathbf{r}) \qquad \text{and} \qquad \hat{\psi}^\dagger(\mathbf{r}) = \sum_{\mathbf{k}} \hat{a}^\dagger_{\mathbf{k}} f^*_{\mathbf{k}}(\mathbf{r}). \tag{4.4}$$

The function $f_{\mathbf{k}}(\mathbf{r})$ is in general, the wavefunction of a single particle quantum state in the external potential. In order to implement our rectangular box with periodic boundary conditions, we take

$$f_{\mathbf{k}}(\mathbf{r}) = \frac{1}{\sqrt{L_x L_y L_z}} e^{i\mathbf{k}\cdot\mathbf{r}}. \tag{4.5}$$

The wave vector $\mathbf{k}$ takes the allowed values $\mathbf{k} = \left(\frac{2\pi n_x}{L_x}, \frac{2\pi n_y}{L_y}, \frac{2\pi n_z}{L_z}\right)$ where n_x, n_y and n_z is any integer, positive or negative. Integrals over $d\mathbf{r}$ likewise run over $0 \le x \le L_x$, $0 \le y \le L_y$ and $0 \le z \le L_z$.

The relations (4.4) can be inverted to obtain

$$\hat{a}_{\mathbf{k}} = \int d\mathbf{r} \hat{\psi}(\mathbf{r}) f^*_{\mathbf{k}}(\mathbf{r}) \qquad \text{and} \qquad \hat{a}^\dagger_{\mathbf{k}} = \int d\mathbf{r} \hat{\psi}^\dagger(\mathbf{r}) f_{\mathbf{k}}(\mathbf{r}). \tag{4.6}$$

These can be used along with Eq. (4.1) to show that

$$[\hat{a}_{\mathbf{k}}, \hat{a}^\dagger_{\mathbf{k}'}] = \delta_{\mathbf{k},\mathbf{k}'}, \tag{4.7}$$

where $\delta_{\mathbf{k}_1,\mathbf{k}_2}$ is the product of three Kronecker delta functions, one for each component of $\mathbf{k}$. Because of this relation, we can think of the operator $\hat{a}^\dagger_{\mathbf{k}}$ as creating a particle with wave vector $\mathbf{k}$ and the operator $\hat{a}_{\mathbf{k}}$ as annihilating a particle with wave vector $\mathbf{k}$.

Writing the Hamiltonian (4.3) in terms of the operators $\hat{a}_{\mathbf{k}}$ and $\hat{a}^\dagger_{\mathbf{k}}$, we obtain

$$\hat{H} = \sum_{\mathbf{k}_1} \epsilon_{\mathbf{k}_1} \hat{a}^\dagger_{\mathbf{k}_1} \hat{a}_{\mathbf{k}_1} + \frac{g}{2V} \sum_{\mathbf{k}_1} \sum_{\mathbf{k}_2} \sum_{\mathbf{k}_3} \sum_{\mathbf{k}_4} \delta_{\mathbf{k}_1+\mathbf{k}_2,\mathbf{k}_3+\mathbf{k}_4} \hat{a}^\dagger_{\mathbf{k}_1} \hat{a}^\dagger_{\mathbf{k}_2} \hat{a}_{\mathbf{k}_3} \hat{a}_{\mathbf{k}_4}, \tag{4.8}$$

where $\epsilon_{\mathbf{k}} = \frac{\hbar^2 k^2}{2m}$ and $V = L_x L_y L_z$. The first term of this Hamiltonian corresponds to the kinetic energy of a particle with wave vector $\mathbf{k}$ while the second term corresponds to a two-body collision between two particles. This collision automatically conserves particle number because it annihilates

two particles while creating two. It also automatically conserves momentum because of the Kronecker delta function. Conservation of energy emerges later as a consequence of the dynamics.

4.3 Perturbative Solution of the Quantum Liouville Equation

From a quantum mechanical standpoint, the Boltzmann equation arises essentially from the quantum Liouville equation, which describes the evolution of the density matrix. However, the path from the Liouville equation to an evolution equation that is an extension of the Boltzmann equation is not straightforward. We will obtain our evolution equation by using the Bogoliubov assumption and following a procedure introduced by Peletminskii, et al [21, 22]. This procedure has been applied to Fermi superfluids [23, 24, 25] and Bose-Einstein condensates [26, 27] by other authors.

Let us begin by introducing a shorthand notation that will be used throughout the rest of this report. We will let $\sum_{\mathbf{k}_1} \rightarrow \sum_1$, $\hat{a}^\dagger_{\mathbf{k}_1} \rightarrow \hat{a}^\dagger_1$, and $\hat{a}_{\mathbf{k}_1} \rightarrow \hat{a}_1$. We will keep this subscript convention for all quantities which are functions of the wave vector $\mathbf{k}_i$, such as $\epsilon_1 = \epsilon_{\mathbf{k}_1}$ and $\delta_{1,2} = \delta_{\mathbf{k}_1,\mathbf{k}_2}$. The Hamiltonian (4.8) is then

$$\hat{H} = \sum_1 \epsilon_1 \hat{a}^\dagger_1 \hat{a}_1 + \frac{g}{2V} \sum_{1,2,3,4} \delta_{1+2,3+4} \hat{a}^\dagger_1 \hat{a}^\dagger_2 \hat{a}_3 \hat{a}_4. \tag{4.9}$$

We must keep in mind that the summations run over all single particle states for both positive and negative components of $\mathbf{k}$.

The full state of the system is described by the full density matrix $\hat{\rho}(t)$ which obeys the Liouville equation

$$i\hbar \frac{\partial \hat{\rho}}{\partial t} = [\hat{H}, \hat{\rho}]. \tag{4.10}$$

We now implement the Bogoliubov assumption that, after a short time, the system evolution will relax to one governed by the behavior of the single particle reduced density function and the density matrix $\hat{\rho}(t)$ will be a functional of the single particle reduced density function

$$\Gamma_{i,j}(t) = \mathrm{Tr}[\hat{\rho}(t)\hat{\gamma}_{i,j}]. \tag{4.11}$$

where

$$\hat{\gamma}_{i,j} = \begin{pmatrix} \hat{a}_i^\dagger \hat{a}_j & \hat{a}_i^\dagger \hat{a}_{-j}^\dagger \\ \hat{a}_{-i} \hat{a}_j & \hat{a}_{-i} \hat{a}_{-j}^\dagger \end{pmatrix}. \tag{4.12}$$

Because we consider a spatially homogeneous system, we only need to consider diagonal elements $\hat{\gamma}_{i,i}$ of the more general operator $\hat{\gamma}_{i,j}$. After sufficiently long time, the density operator can be written

$$\hat{\rho}(t) = \hat{\rho}(\mathbf{\Gamma}(t)), \tag{4.13}$$

where $\mathbf{\Gamma}(t)$ denotes a vector containing $\Gamma_{i,i}(t)$ for all values of i. The components $\Gamma_{i,i}(t)$ are defined self-consistently such that

$$\Gamma_{i,i}(t) = \mathrm{Tr}[\hat{\rho}(\mathbf{\Gamma}(t))\hat{\gamma}_{i,i}] = \begin{pmatrix} \langle \hat{a}_i^\dagger \hat{a}_i \rangle & \langle \hat{a}_i^\dagger \hat{a}_{-i}^\dagger \rangle \\ \langle \hat{a}_{-i} \hat{a}_i \rangle & \langle \hat{a}_{-i} \hat{a}_{-i}^\dagger \rangle \end{pmatrix} \tag{4.14}$$

The Liouville equation (4.10) then takes the form

$$i\hbar \frac{\partial \hat{\rho}(\mathbf{\Gamma}(t))}{\partial t} = i\hbar \sum_i \frac{\partial \hat{\rho}(\mathbf{\Gamma}(t))}{\partial \Gamma_{i,i}^{\mu\nu}(t)} \frac{\partial \Gamma_{i,i}^{\mu\nu}(t)}{\partial t} = [\hat{H}, \hat{\rho}(\mathbf{\Gamma}(t))], \tag{4.15}$$

where $\Gamma_{i,i}^{\mu\nu}(t)$ denotes the $(\mu,\nu)^{\text{th}}$ matrix element of the 2×2 matrix $\Gamma_{i,i}(t)$ and the expression is summed over μ and ν. The equation for the single particle reduced probability density takes the form

$$i\hbar \frac{\partial \Gamma_{i,i}(t)}{\partial t} = \mathrm{Tr}\left(\hat{\rho}(\mathbf{\Gamma}(t))[\hat{\gamma}_{i,i}, \hat{H}] \right). \tag{4.16}$$

Let us now combine Eqs. (4.15) and (4.16) to obtain a self-consistent equation for $\hat{\rho}(\mathbf{\Gamma}(t))$,

$$\sum_i \frac{\partial \hat{\rho}(\mathbf{\Gamma}(t))}{\partial \Gamma_{i,i}^{\mu\nu}(t)} \mathrm{Tr}\left(\hat{\rho}(\mathbf{\Gamma}(t))[\hat{\gamma}_{i,i}, \hat{H}] \right)^{\mu\nu} = [\hat{H}, \hat{\rho}(\mathbf{\Gamma}(t))]. \tag{4.17}$$

Eq. (4.17) is the starting point of the derivation of the particle kinetic equation. In order to simplify notation for the remainder of this section, we will suppress the dependence of $\Gamma_{i,i}(t)$ on time t.

The first step in solving Eq. (4.17) is the decomposition of the Hamiltonian $\hat{H}$ into a mean field Hamiltonian $\hat{H}^0(\mathbf{\Gamma})$ and an interaction term $\hat{H}^1(\mathbf{\Gamma})$ so that $\hat{H} = \hat{H}^0(\mathbf{\Gamma}) + \hat{H}^1(\mathbf{\Gamma})$. The form of the mean field Hamiltonian $\hat{H}^0(\mathbf{\Gamma})$ is determined by the microscopic conservation laws and broken symmetries.

The resulting kinetic equation will depend on the form of $\hat{H}^0(\mathbf{\Gamma})$ that is chosen. In this report, we consider two forms, one leading to the Uehling-Uhlenbeck equation (Chapter 5) and the other leading to a kinetic equation appropriate for BEC's. The Hamiltonian $\hat{H}^0$ phase mixes components $\hat{\gamma}_{i,i}$ of the single particle reduced density function such that

$$[\hat{\gamma}_{i,i}, \hat{H}^0(\mathbf{\Gamma})] = \sum_j c_{i,j}(\mathbf{\Gamma})\hat{\gamma}_{j,j}. \tag{4.18}$$

We can now rewrite Eq. (4.17) in terms of $\hat{H}^0(\mathbf{\Gamma})$ and $\hat{H}^1(\mathbf{\Gamma})$. It takes the form

$$\sum_i \frac{\partial \hat{\rho}(\mathbf{\Gamma})}{\partial \Gamma_{i,i}^{\mu\nu}} \mathrm{Tr}\left(\hat{\rho}(\mathbf{\Gamma})[\hat{\gamma}_{i,i}, \hat{H}^0(\mathbf{\Gamma})]\right)^{\mu\nu} - [\hat{H}^0(\mathbf{\Gamma}), \hat{\rho}(\mathbf{\Gamma})] = \hat{\mathfrak{F}}(\mathbf{\Gamma}) \tag{4.19}$$

where

$$\hat{\mathfrak{F}}(\mathbf{\Gamma}) = -\sum_i \frac{\partial \hat{\rho}(\mathbf{\Gamma})}{\partial \Gamma_{i,i}^{\mu\nu}} \mathrm{Tr}\left(\hat{\rho}(\mathbf{\Gamma})[\hat{\gamma}_{i,i}, \hat{H}^1(\mathbf{\Gamma})]\right)^{\mu\nu} + [\hat{H}^1(\mathbf{\Gamma}), \hat{\rho}(\mathbf{\Gamma})]. \tag{4.20}$$

To solve Eq. (4.19) perturbatively as an expansion in powers of interaction $\hat{H}^1(\mathbf{\Gamma})$, let us introduce an evolution in fictitious "time" s governed by the mean field Hamiltonian $\hat{H}^0(\mathbf{\Gamma})$. First we shall introduce the density matrix $\hat{\rho}(\mathbf{\Gamma}, s)$ given by

$$\hat{\rho}(\mathbf{\Gamma}, s) \equiv \hat{U}^0(s, 0)\hat{\rho}(\mathbf{\Gamma})\hat{U}^{0\dagger}(s, 0), \tag{4.21}$$

where $\hat{U}^0(s_2, s_1) = e^{-i\hat{H}^0(\mathbf{\Gamma}(t))(s_2 - s_1)/\hbar}$. Note that $\hat{\rho}(\mathbf{\Gamma}, s)$ is simply the s-evolution of the density matrix $\hat{\rho}(\mathbf{\Gamma})$ with the initial condition $\hat{\rho}(\mathbf{\Gamma}, 0) = \hat{\rho}(\mathbf{\Gamma})$. From this definition, we can see that

$$i\hbar \frac{\partial \hat{\rho}(\mathbf{\Gamma}, s)}{\partial s} = [\hat{H}^0(\mathbf{\Gamma}), \hat{\rho}(\mathbf{\Gamma}, s)] \tag{4.22}$$

Next we shall introduce the quantity $\Gamma_{i,i}(s)$ which is given by

$$\Gamma_{i,i}(s) = \mathrm{Tr}\left(\hat{\rho}(\mathbf{\Gamma}, s)\hat{\gamma}_{i,i}\right), \tag{4.23}$$

from which we can see that

$$i\hbar\frac{\partial\Gamma_{i,i}(s)}{\partial s} = \mathrm{Tr}\left(\hat{\rho}(\mathbf{\Gamma},s)[\hat{\gamma}_{i,i},\hat{H}^0(\mathbf{\Gamma})]\right) = \sum_j c_{i,j}(\mathbf{\Gamma})\Gamma_{j,j}(s). \tag{4.24}$$

The form of Eq. (4.24) shows us that s acts like the parameter of a continuous orthogonal transformation of the vector $\mathbf{\Gamma}$ to $\mathbf{\Gamma}(s)$, similar to performing a coordinate rotation parameterized by an angle in two or three dimensional vector space. We can freely perform this coordinate "rotation" and rewrite the derivatives with respect to Γ in Eq. (4.19) with derivatives with respect to $\Gamma(s)$, giving us

$$\sum_{i,j}\frac{\partial\hat{\rho}(\mathbf{\Gamma}(s))}{\partial\Gamma^{\mu\nu}_{i,i}(s)}c_{i,j}(\mathbf{\Gamma})\Gamma^{\mu\nu}_{j,j}(s) - [\hat{H}^0(\mathbf{\Gamma}),\hat{\rho}(\mathbf{\Gamma}(s))] = \hat{\mathfrak{F}}(\mathbf{\Gamma}(s)) \tag{4.25}$$

Note that not every appearance of $\mathbf{\Gamma}$ has been "rotated" to $\mathbf{\Gamma}(s)$. This is permissible because the solution of this equation will still be a solution of Eq. (4.19) when $s = 0$. Using Eq. (4.24) we can write

$$i\hbar\sum_i\frac{\partial\hat{\rho}(\mathbf{\Gamma}(s))}{\partial\Gamma^{\mu\nu}_{i,i}(s)}\frac{\partial\Gamma^{\mu\nu}_{i,i}(s)}{\partial s} - [\hat{H}^0(\mathbf{\Gamma}),\hat{\rho}(\mathbf{\Gamma}(s))] = \hat{\mathfrak{F}}(\mathbf{\Gamma}(s)) \tag{4.26}$$

or, more simply,

$$i\hbar\frac{\partial\hat{\rho}(\mathbf{\Gamma}(s))}{\partial s} - [\hat{H}^0(\mathbf{\Gamma}),\hat{\rho}(\mathbf{\Gamma}(s))] = \hat{\mathfrak{F}}(\mathbf{\Gamma}(s)) \tag{4.27}$$

Note that $\hat{\rho}(\mathbf{\Gamma}(s))$ is not the same thing as $\hat{\rho}(\mathbf{\Gamma},s)$. The former is the full density matrix evaluated at $\mathbf{\Gamma}(s)$ and the latter is the evolution of the density matrix under the action of $\hat{H}^0$ for a "time" of length s starting with $\hat{\rho}(\mathbf{\Gamma})$ when $s = 0$. In order to solve Eq. (4.27) perturbatively, we will need a boundary condition which will come from an assumption about the relationship between $\hat{\rho}(\mathbf{\Gamma}(s))$ and $\hat{\rho}(\mathbf{\Gamma},s)$. This boundary condition is

$$\lim_{s\to\infty}\hat{\rho}(\mathbf{\Gamma},s) \equiv \hat{\rho}_0(\mathbf{\Gamma}(s)). \tag{4.28}$$

and can also be written in terms of $\hat{\rho}(\mathbf{\Gamma}(s))$ as

$$\lim_{s\to-\infty}\hat{U}^{0\dagger}(s,0)\hat{\rho}(\mathbf{\Gamma}(s))\hat{U}^0(s,0) = \hat{\rho}_0(\mathbf{\Gamma}). \tag{4.29}$$

The logic behind this boundary condition is based on the Bogoliubov assumption. After a very long

"time" s, phase mixing induced by $\hat{H}^0(\mathbf{\Gamma})$ and relaxation caused by $\hat{H}^1(\mathbf{\Gamma})$ causes the density operator to approach the limiting form $\hat{\rho}_0(\mathbf{\Gamma})$. The density matrix $\hat{\rho}_0(\mathbf{\Gamma})$ represents a sort of "temporary" equilibrium under the s-evolution. It must obey the equation

$$\sum_i \frac{\partial \hat{\rho}_0(\mathbf{\Gamma})}{\partial \Gamma_{i,i}^{\mu\nu}} \mathrm{Tr}\left(\hat{\rho}_0(\mathbf{\Gamma})[\hat{\gamma}_{i,i}, \hat{H}^0(\mathbf{\Gamma})]\right)^{\mu\nu} - [\hat{H}^0(\mathbf{\Gamma}), \hat{\rho}_0(\mathbf{\Gamma})] = 0 \tag{4.30}$$

The perturbative solution to Eq. (4.27) can be found by defining yet another density matrix, an s-interaction picture density matrix, given by

$$\hat{\rho}_I(s) \equiv \hat{U}^{0\dagger}(s,0)\hat{\rho}(\mathbf{\Gamma}(s))\hat{U}^0(s,0). \tag{4.31}$$

By definition, the density matrix $\hat{\rho}_I(s)$ can be seen to obey the differential equation

$$i\hbar \frac{d\hat{\rho}_I(s)}{ds} = \hat{U}^{0\dagger}(s,0)\hat{\mathfrak{F}}(\mathbf{\Gamma}(s)\hat{U}^0(s,0). \tag{4.32}$$

We can write the formal integral solution to this equation as

$$\hat{\rho}_I(0) = \hat{\rho}_I(-s_0) + \frac{1}{i\hbar}\int_{-s_0}^{0} ds \hat{U}^{0\dagger}(s,0)\hat{\mathfrak{F}}(\mathbf{\Gamma}(s))\hat{U}^0(s,0). \tag{4.33}$$

By using the definition (4.31) this becomes

$$\hat{\rho}(\mathbf{\Gamma}) = \hat{U}^{0\dagger}(-s_0,0)\hat{\rho}(\mathbf{\Gamma}(-s_0))\hat{U}^0(-s_0,0) + \frac{1}{i\hbar}\int_{-s_0}^{0} ds \hat{U}^{0\dagger}(s,0)\hat{\mathfrak{F}}(\mathbf{\Gamma}(s))\hat{U}^0(s,0). \tag{4.34}$$

Taking the limit $s_0 \to \infty$ so that the boundary condition (4.29) can be used, we obtain

$$\hat{\rho}(\mathbf{\Gamma}) = \hat{\rho}_0(\mathbf{\Gamma}) + \frac{1}{i\hbar}\int_{-\infty}^{0} ds \hat{U}^{0\dagger}(s,0)\hat{\mathfrak{F}}(\mathbf{\Gamma}(s))\hat{U}^0(s,0). \tag{4.35}$$

4.4 Kinetic Equation

Our task is now to combine Eq. (4.35) and (4.16) to derive a "kinetic equation". We take a kinetic equation to be an equation which describes the evolution of expectation values. Thus a kinetic equation is analogous to the Boltzmann equation. Before we begin, we must first solve Eq. (4.30) and then show that $\mathrm{Tr}\left(\hat{\rho}(\mathbf{\Gamma})\hat{\gamma}_{i,i}\right) = \mathrm{Tr}\left(\hat{\rho}_0(\mathbf{\Gamma})\hat{\gamma}_{i,i}\right)$.

In fact there is not a unique solution to (4.30), allowing us to choose any solution which reproduces the desired expectation values $\Gamma_{i,i} = \mathrm{Tr}\left(\hat{\rho}_0(\mathbf{\Gamma})\hat{\gamma}_{i,i}\right)$. The most convenient form of $\hat{\rho}_0$ is given by

$$\hat{\rho}_0(\mathbf{\Gamma}) = \exp\left[-\sum_i X^i_{\mu\nu}\hat{\gamma}^{\mu\nu}_{i,i} - \Omega\right]. \tag{4.36}$$

where $\Omega = \log\left[\mathrm{Tr}\left(\exp\left[-\sum_i X^i_{\mu\nu}\hat{\gamma}^{\mu\nu}_{i,i} - \Omega\right]\right)\right]$. The quantities X^i are matrices that encode the values of $\Gamma_{i,i}$. This form is convenient because it allows us to derive a type of Wick expansion for high order expectation values.

We can show that $\mathrm{Tr}\left(\hat{\rho}(\mathbf{\Gamma})\hat{\gamma}_{i,i}\right) = \mathrm{Tr}\left(\hat{\rho}_0(\mathbf{\Gamma})\hat{\gamma}_{i,i}\right)$ by showing that $\mathrm{Tr}\left(\hat{\mathfrak{F}}(\mathbf{\Gamma})\hat{\gamma}_{i,i}\right) = 0$. To show this, let us write out the result of taking the trace. We obtain

$$-\sum_j \frac{\partial\Gamma_{i,i}}{\partial\Gamma^{\mu\nu}_{j,j}}\mathrm{Tr}\left(\hat{\rho}(\mathbf{\Gamma})[\hat{\gamma}_{j,j}, \hat{H}^1(\mathbf{\Gamma})]\right)^{\mu\nu} + \mathrm{Tr}\left([\hat{H}^1(\mathbf{\Gamma}), \hat{\rho}(\mathbf{\Gamma})]\hat{\gamma}_{j,j}\right) = 0. \tag{4.37}$$

Since $\frac{\partial\Gamma_{i,i}}{\partial\Gamma_{j,j}} = \delta_{i,j}$, the two terms become equal and opposite, yielding zero. Let us emphasize that this is not a perturbative result and is a true to all orders.

The next step in deriving a kinetic equation is to create several conditions that will define the mean field in the mean field Hamiltonian $\hat{H}^0(\mathbf{\Gamma})$. This condition is

$$\mathrm{Tr}\left(\hat{\rho}_0(\mathbf{\Gamma})[\hat{\gamma}_{i,i}, \hat{H}^1(\mathbf{\Gamma})]\right) = 0, \tag{4.38}$$

which is such that terms of first order in $\hat{H}^1$ do not appear in the kinetic equation.

Now we may finally expand Eq. (4.35) as a power series in $\hat{H}^1$ and insert it into Eq. (4.16). To

second order in the interaction, Eq. (4.16) takes the form

$$\frac{\partial \Gamma_{i,i}(t)}{\partial t} = \frac{1}{i\hbar}\sum_j c_{i,j}(\mathbf{\Gamma})\Gamma_{j,j} + \frac{1}{\hbar^2}\int_{-\infty}^{0} ds \mathrm{Tr}\left(\hat{\rho}_0(\mathbf{\Gamma})[\hat{H}^1(\mathbf{\Gamma}), \hat{U}^{0\dagger}(0,s)[\hat{\gamma}_{i,i}, \hat{H}^1(\mathbf{\Gamma})]\hat{U}^0(0,s)]\right). \quad (4.39)$$

This equation is the starting point of our kinetic theory of Bose-Einstein condensates.

4.5 Summary

In this Chapter we began from a description of an interacting system of bosons as a quantum field and derived a kinetic equation for expectation values that is a quantum analog of the Boltzmann equation. To do this, we first transformed the quantum field Hamiltonian from the position representation to the momentum representation and took our particles to be confined to a rectangular box with periodic boundary conditions. Next, we developed a perturbative solution to the quantum Liouville equation for the density matrix of the system. This solution relied on the Bogoliubov assumption that the number of relevant parameters is reduced in each phase of the relaxation so that the density matrix becomes a function of these parameters and loses its dependence on all others. Finally, we used this perturbative solution to obtain a general kinetic equation for the evolution of expectation values.

5 Characteristic Relaxation Rates of the Uehling-Uhlenbeck Equation

The Uehling-Uhlenbeck (U-U) equation [29], also known as the Boltzmann-Nordheim equation [30], is a semiclassical extension of the Boltzmann equation that accounts for the bosonic nature of the particles. Again, we concern ourselves with its behavior when applied to systems which are spatially uniform and close to thermal equilibrium. These restrictions allow us to linearize the equation about an equilibrium distribution and write it as an eigenvalue equation with a linear collision operator, similar to what we did with the Boltzmann Equation in section 2.4. The eigenvalues of the collision operator are again directly related to the rate of relaxation of the momentum distribution to equilibrium. In subsequent sections, we provide a full analysis of the linearized U-U equation by calculating its kernel functions Q_{UU} and R_{UU} and numerically computing its relaxation rates and relaxation modes. We will also expressing the relaxation of the gas in terms of a spectral decomposition involving these rates and modes, similar to section 2.7. We use the finite ordinate method of section 2.5 to obtain our results.

5.1 Derivation of the Uehling-Uhlenbeck Equation

To derive the U-U equation, we apply the results of the previous Chapter (4.39), taking the unperturbed Hamiltonian $\hat{H}^0$ to be

$$\hat{H}^0 = \sum_1 \epsilon_1 \hat{a}_1^\dagger \hat{a}_1 \tag{5.1}$$

and the interaction Hamiltonian $\hat{H}^1$ to be

$$\hat{H}^1 = \frac{g}{2V} \sum_{1,2,3,4} \delta_{1+2,3+4} \hat{a}_1^\dagger \hat{a}_2^\dagger \hat{a}_3 \hat{a}_4. \tag{5.2}$$

We take the kinetic variables (the $\Gamma_{i,i}$) to be simply the particle occupation numbers N_i defined by

$$\mathrm{Tr}(\hat{\rho}_0 \hat{a}_i^\dagger \hat{a}_j) \equiv N_i \delta_{i,j} \tag{5.3}$$

with

$$\hat{\rho}_0 = \exp\left[-\sum_i \xi_i \hat{a}_i^\dagger \hat{a}_i - \Omega \right]. \tag{5.4}$$

These kinetic variables automatically have the property (4.38) as well as the convenient property that $c_{i,j} = 0$. We then obtain the kinetic equation for a spatially homogeneous gas,

$$\begin{aligned} \frac{dN_i}{dt} =& \frac{g^2}{4V^2\hbar^2} \sum_{1,2,3,4} \sum_{5,6,7,8} \delta_{1+2,3+4} \delta_{5+6,7+8} \\ & \times \int_{-\infty}^{0} ds \mathrm{Tr}\left(\rho_0 [\hat{a}_1^\dagger \hat{a}_2^\dagger \hat{a}_3 \hat{a}_4, [\hat{a}_i^\dagger(s)\hat{a}_i(s), \hat{a}_5^\dagger(s)\hat{a}_6^\dagger(s)\hat{a}_7(s)\hat{a}_8(s)]] \right). \end{aligned} \tag{5.5}$$

Given the form of $\hat{H}^0$, the s-evolution of the operators is simply given by

$$\hat{a}_i^\dagger(s) = e^{-i\epsilon_i s/\hbar} \hat{a}_i^\dagger \qquad \text{and} \qquad \hat{a}_i(s) = e^{i\epsilon_i s/\hbar} \hat{a}_i. \tag{5.6}$$

Using this and working out the commutator and expectation values (which is quite tedious) in Eq. (5.5), we obtain the Uehling-Uhlenbeck equation for a spatially homogeneous gas,

$$\frac{dN_i}{dt} = \frac{4\pi g^2}{V^2\hbar} \sum_{2,3,4} \delta_{i+2,3+4} \delta(\epsilon_i + \epsilon_2 - \epsilon_3 - \epsilon_4) \left[(1 + N_i + N_2) N_3 N_4 - N_i N_2 (1 + N_3 + N_4) \right]. \tag{5.7}$$

The details of this derivation can be found in appendix A.6.

Note that the presence of a Dirac delta function inside of a sum is slightly inconsistent. This arises from our use of the Bogoliubov assumption and the boundary condition (4.29). This inconsistency disappears when we take the thermodynamic limit. Let us do this now by sending $V \to \infty$ and $N \to \infty$ in such a way that the density $n = \frac{N}{V}$ remains constant.

In doing this, we must be careful to remember that N_i is a momentum state occupation number and can not be changed directly into a density because it is dimensionless. The closest analogy to the classical phase space distribution $f(\mathbf{r}, \mathbf{v})$ for a spatially homogeneous system is a Wigner distribution $f(\mathbf{r}, \mathbf{k}) = f(\mathbf{k})$ in the $\{\mathbf{r}, \mathbf{k}\}$ phase space that has no actual position dependence. The distribution

$f(\mathbf{k})$ would be dimensionless since the dimensions of $\mathbf{k}$ are length^{-1}. The proper object to take the place of N_i in the thermodynamic limit is in fact the dimensionless distribution $f(\mathbf{k}_i)$.

The final point to make before taking the thermodynamic limit is on the conversion of sums and Kronecker delta functions to integrals and Dirac delta functions. The sum $\sum_i$ becomes $\frac{V}{(2\pi)^3}\int d\mathbf{k}_i$ and the Kronecker delta functions $\delta_{i,j}$ become $\frac{(2\pi)^3}{V}\delta^3(\mathbf{k}_i - \mathbf{k}_j)$. Taking the thermodynamic limit of Eq. (5.5) therefore results in

$$\begin{aligned}\frac{df_i}{dt} =& \frac{g^2}{16\pi^5\hbar}\int d\mathbf{k}_2 d\mathbf{k}_3 d\mathbf{k}_4 \delta^3(\mathbf{k}_i + \mathbf{k}_2 - \mathbf{k}_3 - \mathbf{k}_4)\delta(\epsilon_i + \epsilon_2 - \epsilon_3 - \epsilon_4) \\ & \times [(1+f_i)(1+f_2)f_3 f_4 - f_i f_2 (1+f_3)(1+f_4)]\end{aligned} \tag{5.8}$$

where again f_i is shorthand for $f(\mathbf{r}, \mathbf{k}_i)$.

5.2 Equilibrium

Our first task on the route to computing the characteristic relaxation rates of the Uehling-Uhlenbeck equation is to determine its equilibrium solution. By inspection, we can see that the U-U equation has five conserved quantities corresponding to the five conserved quantities in a two-body collision, the same as the Boltzmann equation. These quantities are average total particle number, average total momentum and average total energy. The equilibrium distribution will therefore be determined by these five quantities, but the form of the equilibrium distribution will not be a Maxwell-Boltzmann distribution. Inspecting the U-U equation, we see that the chief difference from the Boltzmann equation is the term involving the occupation numbers which in equilibrium appears as,

$$(1+f_i^0)(1+f_2^0)f_3^0 f_4^0 - f_i^0 f_2^0 (1+f_3^0)(1+f_4^0) = 0 \tag{5.9}$$

instead of $f_3^0 f_4^0 - f_i^0 f_2^0 = 0$ as it does in the Boltzmann equation. We can determine the form of the equilibrium distribution by the following trick: consider factoring out the quantity $f_i^0 f_2^0 f_3^0 f_4^0$ from both terms in Eq. (5.9). We will then be left with

$$f_i^0 f_2^0 f_3^0 f_4^0 \left[\frac{1+f_i^0}{f_i^0}\frac{1+f_2^0}{f_2^0} - \frac{1+f_3^0}{f_3^0}\frac{1+f_4^0}{f_4^0}\right]. \tag{5.10}$$

This will be zero if $\frac{1+f^0}{f^0}$ is an exponential of any of the conserved quantities. This leads to a Bose-Einstein equilibrium distribution of the form

$$f^0(\mathbf{r},\mathbf{k}) = \frac{1}{\exp\left[\frac{\hbar^2(\mathbf{k}-\bar{\mathbf{k}})^2}{2mk_BT} - \frac{\mu}{k_BT}\right] - 1}. \tag{5.11}$$

We cannot simply multiply this distribution by a constant to set the overall number of particles in the system as we did for the Boltzmann equation. The approach we must take is to introduce a chemical potential μ whose value is implicitly determined by the average number of particles in the system. Thus μ can be viewed as energy representing particles entering or leaving the open system, or as an undetermined Lagrange multiplier that is associated with a constraint on the system. It is worth noting that this distribution function can also be derived by maximizing the von Neumann entropy $S = -k_B\mathrm{Tr}(\hat{\rho}\log(\hat{\rho}))$ for bosons subject to the constraints on average total particle number, average total momentum and average total energy.

Again we can set $\bar{\mathbf{k}} = 0$ by a coordinate transformation. We will find it more convenient to write the equilibrium distribution in terms of a quantity known as the fugacity z, given by $z = e^{\mu/(k_BT)}$ rather than μ itself. The equilibrium distribution then depends only on the values T and z as

$$f^0(\mathbf{k},z,T) = \frac{z}{e^{\hbar^2k^2/(2mk_BT)} - z}. \tag{5.12}$$

Since the system is spatially uniform, the conserved quantities are given by the particle density $\bar{n} = \int \frac{d\mathbf{k}}{(2\pi)^3} f(\mathbf{k},t)$, the momentum density $\bar{\mathbf{p}} = \int \frac{d\mathbf{k}}{(2\pi)^3}\hbar\mathbf{k}f(\mathbf{k},t)$ and the energy density $\bar{\epsilon} = \int \frac{d\mathbf{k}}{(2\pi)^3}\frac{\hbar^2k^2}{2m}f(\mathbf{k},t)$. The quantities $\bar{n}$, $\bar{\mathbf{p}}$ and $\bar{\epsilon}$, being conserved, are independent of the time t at which they are evaluated. The solutions $f(\mathbf{k},t)$ to Eq. (5.8) have the property $\lim_{t\to\infty} f(\mathbf{k},t) = f^0(\mathbf{k},z,T)$. Since the conserved quantities are independent of time, they can equally well be evaluated using the equilibrium distribution function $f^0(\mathbf{k},z,T)$. Doing this, we find that $\bar{n}$ and $\bar{\epsilon}$ are related to z and T by

$$\bar{n} = \frac{1}{\lambda_T^3}\mathrm{Li}_{\frac{3}{2}}(z) \tag{5.13}$$

and

$$\bar{\epsilon} = \frac{3}{2}\frac{k_BT}{\lambda_T^3}\mathrm{Li}_{\frac{5}{2}}(z) \tag{5.14}$$

where

$$\lambda_T = \frac{h}{\sqrt{2\pi m k_B T}} \tag{5.15}$$

is the thermal wavelength and $\mathrm{Li}_s(z)$ is a polylogarithm function (see Eq. A.2). When presented with an arbitrary initial distribution $f(\mathbf{k}, 0)$ one would determine $\bar{n}$ and $\bar{\epsilon}$ and use Eqs. (5.13) and (5.14) to find its fugacity and temperature.

We can write the U-U equation in dimensionless form if we introduce the dimensionless velocity $\mathbf{c}_i = \frac{\hbar}{\sqrt{2mk_BT}}\mathbf{k}_i$. In terms of this quantity, the U-U equation (5.8) takes the form

$$\begin{aligned}\frac{df_1(t)}{dt} = &-\frac{\gamma_{\mathrm{UU}}}{\pi^2 z}\int d\mathbf{c}_2 d\mathbf{c}_3 d\mathbf{c}_4 \delta(c_1^2 + c_2^2 - c_3^2 - c_4^2)\delta^3(\mathbf{c}_1 + \mathbf{c}_2 - \mathbf{c}_3 - \mathbf{c}_4) \\ &\times \left[f_1(t)f_2(t)(1 + f_3(t) + f_4(t)) - (1 + f_1(t) + f_2(t))f_3(t)f_4(t)\right],\end{aligned} \tag{5.16}$$

where the time constant γ_{UU} is given by

$$\gamma_{\mathrm{UU}} = \frac{32\pi z k_B T}{h}\left(\frac{a}{\lambda_T}\right)^2. \tag{5.17}$$

A factor of z has been incorporated into γ_{UU} to give it the proper behavior as $z \to 0$. Consideration of Eq. (5.13) shows that $\bar{n} = \frac{z}{\lambda_T^3}$ in the limit that $z \to 0$. A few algebraic manipulations reveal that γ_{UU} is also equal to $\bar{n}\bar{v}\sigma$ where $\bar{v} = \sqrt{\frac{8k_BT}{\pi m}}$ is the average particle speed and $\sigma = 8\pi a^2$ is the total cross section for low-energy scattering of two identical bosons [50]. A nearly identical rate constant Eq. (2.19) is found in the Boltzmann equation with $\sigma = \pi a^2$ for classical hard spheres of diameter a [51].

The particular value of γ_{UU} will depend on experimental conditions such as temperature, density and type of particle. If one knows the detailed properties of the system, the rate constant γ_{UU} can be used to get a rough estimate for the relaxation rate. For example, if we consider Sodium atoms in the $F = 1$, $m_F = -1$ state [50] at a density of $\bar{n} = 10^{11}$ cm^{-3} and temperature of $T = 200$ μK [52] we find that $\gamma_{\mathrm{UU}} \simeq 0.093$ s^{-1}. Alternatively, measurement of γ_{UU} by measuring the relaxation rates could provide a way to obtain the scattering length a of the interaction as done in [53].

5.3 Linearization of the Uehling-Uhlenbeck Equation

The linearized U-U equation describes the relaxation of the boson gas when it has been perturbed away from thermodynamic equilibrium, $f^0(\mathbf{c}) = \frac{z}{e^{c^2}-z}$. We choose the linearization scheme

$$f(\mathbf{c},t) = f^0(\mathbf{c}) + f^0(\mathbf{c})(1+f^0(\mathbf{c}))\phi(\mathbf{c},t), \tag{5.18}$$

where $\phi(\mathbf{c},t)$ is a small parameter that approaches zero as the gas equilibrates and thus $f(\mathbf{c},t)$ approaches $f^0(\mathbf{c})$. Applying this scheme to Eq. (5.16) and keeping only terms linear in $\phi(\mathbf{c},t)$, we obtain the linearized U-U equation,

$$\begin{aligned}\frac{d\phi_1(t)}{dt} = -\frac{\gamma_{\mathrm{UU}}}{\pi^2 z}\frac{1}{1+f_1^0}\int d\mathbf{c}_2 d\mathbf{c}_3 d\mathbf{c}_4 \delta^3\left(\mathbf{c}_1+\mathbf{c}_2-\mathbf{c}_3-\mathbf{c}_4\right)\delta(c_1^2+c_2^2-c_3^2-c_4^2) \\ \times f_2^0(1+f_3^0)(1+f_4^0)(\phi_1(t)+\phi_2(t)-\phi_3(t)-\phi_4(t)),\end{aligned} \tag{5.19}$$

where $f_i^0 = f^0(\mathbf{c}_i)$ and $\phi_i(t) = \phi(\mathbf{c}_i,t)$. In all expressions, the classical (Boltzmann) limit can be obtained by considering $z \to 0$. In this limit, $f^0(\mathbf{c}) \to ze^{-c^2}$ and $1+f^0(\mathbf{c}) \to 1$. We have also used the fact that $(1+f_1^0)(1+f_2^0)f_3^0 f_4^0 = f_1^0 f_2^0(1+f_3^0)(1+f_4^0)$ to write Eq. (5.19) in a form where its classical limit is clearly the linearized Boltzmann equation 2.16.

We can see by inspection that Eq. (5.19) admits five forms of $\phi(\mathbf{c},t)$ which result in $\frac{d\phi(\mathbf{c},t)}{dt} = 0$. These are $\phi(\mathbf{c},t) \propto 1$, $\phi(\mathbf{c},t) \propto c^2$ and $\phi(\mathbf{c},t)$ proportional to any of the three components of $\mathbf{c}$. These five functions represent the five conserved quantities of the U-U equation. Each of these modes corresponds to an eigenmode of the collision operator and in section 5.5, we give explicit expressions for these. In section 5.6 we see that each of these modes also has a zero eigenvalue.

Since the right side of Eq. (5.19) is linear in $\phi(\mathbf{c},t)$, it can be written as a convolution of the function $\phi(\mathbf{c},t)$. Doing this, we find that

$$\frac{d\phi_1(t)}{dt} = -\gamma_{\mathrm{UU}}\left[M(\mathbf{c}_1)\phi_1(t) + \frac{1}{\pi^2 z}\frac{1}{1+f_1^0}\int d\mathbf{c}_2 f_2^0\left[Q_{\mathrm{UU}}(\mathbf{c}_1,\mathbf{c}_2) - 2R_{\mathrm{UU}}(\mathbf{c}_1,\mathbf{c}_2)\right]\phi_2(t)\right], \tag{5.20}$$

where the kernels Q_{UU} and R_{UU} are given by

$$Q_{\mathrm{UU}}(\mathbf{c}_1,\mathbf{c}_2) \equiv \int d\mathbf{c}_3 d\mathbf{c}_4 \delta^3\left(\mathbf{c}_1+\mathbf{c}_2-\mathbf{c}_3-\mathbf{c}_4\right)\delta(c_1^2+c_2^2-c_3^2-c_4^2)(1+f_3^0)(1+f_4^0), \tag{5.21}$$

$$R_{\mathrm{UU}}(\mathbf{c}_1,\mathbf{c}_2) \equiv \frac{1+f_2^0}{f_2^0}\int d\mathbf{c}_3 d\mathbf{c}_4 \delta^3\left(\mathbf{c}_1-\mathbf{c}_2+\mathbf{c}_3-\mathbf{c}_4\right)\delta(c_1^2-c_2^2+c_3^2-c_4^2) f_3^0(1+f_4^0) \tag{5.22}$$

and the function M_{UU} is given by

$$M_{\mathrm{UU}}(\mathbf{c}_1) = \frac{1}{\pi^2 z(1+f_1^0)}\int d\mathbf{c}_2 f_2^0 Q_{\mathrm{UU}}(\mathbf{c}_1,\mathbf{c}_2). \tag{5.23}$$

The particular form of the kernels Q_{UU} and R_{UU} have been chosen so that they are symmetric in their two arguments and reduce to their classical expressions in the limit $z \to 0$. It is possible to write these functions in closed form as

$$Q_{\mathrm{UU}}(\mathbf{c}_1,\mathbf{c}_2) = \frac{\pi}{2}\frac{e^{c_1^2+c_2^2}}{e^{c_1^2+c_2^2}-z^2}\left(\frac{2}{|\mathbf{c}_1+\mathbf{c}_2|}\log\left(\frac{e^{\frac{c_1^2}{2}+\frac{c_2^2}{2}+\frac{|\mathbf{c}_1+\mathbf{c}_2||\mathbf{c}_1-\mathbf{c}_2|}{2}}-z}{e^{\frac{c_1^2}{2}+\frac{c_2^2}{2}-\frac{|\mathbf{c}_1+\mathbf{c}_2||\mathbf{c}_1-\mathbf{c}_2|}{2}}-z}\right)-|\mathbf{c}_1-\mathbf{c}_2|\right) \tag{5.24}$$

and

$$R_{\mathrm{UU}}(\mathbf{c}_1,\mathbf{c}_2) = \frac{\pi}{2z|\mathbf{c}_1-\mathbf{c}_2|(e^{-c_1^2}-e^{-c_2^2})}\log\left(\frac{e^{-\frac{|\mathbf{c}_1\times\mathbf{c}_2|^2}{(\mathbf{c}_1-\mathbf{c}_2)^2}}-ze^{-c_2^2}}{e^{-\frac{|\mathbf{c}_1\times\mathbf{c}_2|^2}{(\mathbf{c}_1-\mathbf{c}_2)^2}}-ze^{-c_1^2}}\right) \tag{5.25}$$

The details of this derivation are outlined in appendix A.4.

5.4 Relaxation Rates

Equation (5.20) is again an eigenvalue problem very similar to Eq. (2.20). Its eigenvalues determine how quickly the velocity distribution of the gas relaxes to thermal equilibrium. The properties of the kernels Q_{UU} and R_{UU} determine the form of the eigenvalue spectrum. Since the linearized Boltzmann equation for hard spheres is a limiting case of Eq. (5.20), we expect that the spectrum of the linearized U-U equation will have the same features as the spectrum of the linearized Boltzmann equation. Specifically, there should a total of be five zero eigenvalues representing the five conserved quantities. The subsequent non-zero discrete eigenvalues increase but are bounded from above by a limiting value λ_M as discussed at the end of section 2.4.

Before we begin, we should mention that there are still several ways to discretize Eq. (5.20). In Chapter 2 we discussed two different methods, expansion in a set of orthogonal polynomials and the finite ordinate method. A little thought reveals that the finite ordinate method suffers almost no changes while the polynomial expansion will encounter serious algebraic complexity. The polynomial

expansion that is applied in 2 relies on several special properties of the Burnett functions, namely that they are orthogonal over $d\mathbf{c}$ with a weighting function equal to the equilibrium distribution and have a generating function which is exponential, as discussed in sec. A.2. Either we would have to take up the undesirable task of generating a new set of orthogonal polynomials and finding their generating functions, or we could persist in using the Burnett functions and do the resulting integrals by quadrature. The latter method would result in a multi-dimensional quadrature calculation for each individual matrix element. It is also quite possible that after all of this work, the eigenvalue would show extremely slow convergence as the matrix size is varied [4]. These difficulties have convinced us that the finite ordinate method is the only one worth pursuing.

We will now give an expression for the collision matrix of order l for the linearized Uehling-Uhlenbeck equation. This derivation will closely follow the steps in sec. 2.6. If we inspect the form of Eqs. (5.21) and (5.22), we see that the functions Q_{UU} and S_{UU} are very similar in form to Q_{HS} (2.21) and R_{HS} (2.22). In fact the U-U kernels reduce to the hard spheres kernels in the limit $z \to 0$. We can analyze the eigenvalues of Eq. (5.20) with the methods described in section (2.5). Again comparing Eqs. (2.20) and (2.39), we find

$$\mathcal{M}(\mathbf{c}) = M_{\mathrm{UU}}(\mathbf{c}), \qquad \mathcal{W}(c_2) = \frac{z}{e^{c_2^2} - z}, \qquad \mathcal{V}(c_1) = 1 + \frac{z}{e^{c_1^2} - z} \tag{5.26}$$

and

$$\mathcal{K}(\mathbf{c}_1, \mathbf{c}_2) = \frac{1}{\pi^2 z} \left(Q_{\mathrm{UU}}(\mathbf{c}_1, \mathbf{c}_2) - 2R_{\mathrm{UU}}(\mathbf{c}_1, \mathbf{c}_2) \right). \tag{5.27}$$

The overall timescale factor of γ_{UU} is given in Eq. (5.17). This form of $\mathcal{W}$ and $\mathcal{V}$ gives

$$\psi_n^l(c) = c \frac{\sqrt{z} e^{\frac{1}{2}c_2^2}}{e^{c_2^2} - z} \phi_n^l(c), \tag{5.28}$$

according to Eq. (2.45).

As we did in Eqs. (2.55) and (2.56) we make the definitions

$$Q_{\mathrm{UU}}^l(c_1, c_2) = \int_{-1}^{1} d(\hat{\mathbf{c}}_1 \cdot \hat{\mathbf{c}}_2) Q_{\mathrm{UU}}(\mathbf{c}_1, \mathbf{c}_2) P_l(\hat{\mathbf{c}}_1 \cdot \hat{\mathbf{c}}_2), \tag{5.29}$$

and

$$R^l_{\mathrm{UU}}(c_1, c_2) = \int_{-1}^{1} d(\hat{\mathbf{c}}_1 \cdot \hat{\mathbf{c}}_2) R_{\mathrm{UU}}(\mathbf{c}_1, \mathbf{c}_2) P_l(\hat{\mathbf{c}}_1 \cdot \hat{\mathbf{c}}_2). \tag{5.30}$$

Due to the complicated forms of Q_{UU} and R_{UU} in Eqs. (5.24) and (5.25) we clearly cannot write these functions in closed form. These two functions must be computed by numerical quadrature for each given value of l, c_1 and c_2.

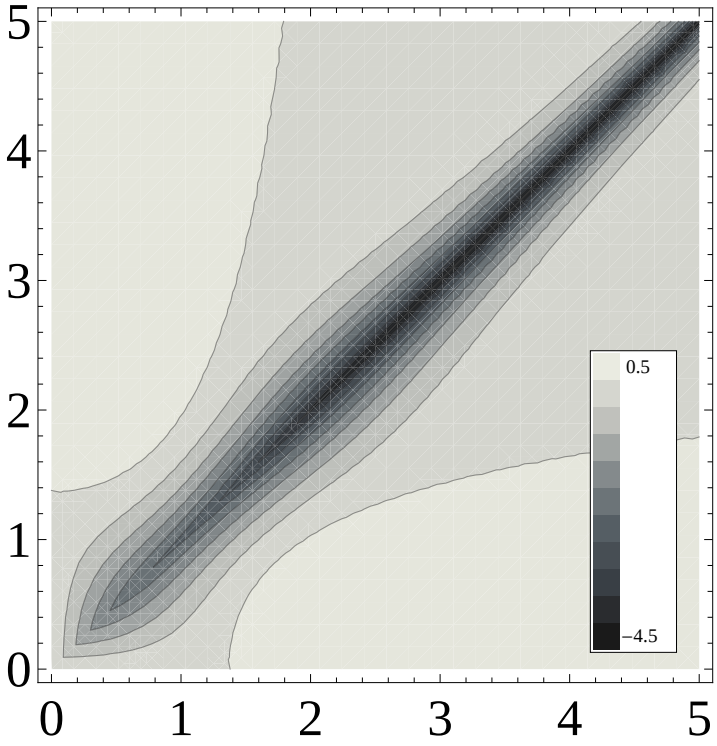

Figure 5.1: Plot of the symmetrized kernel $\frac{1}{\pi^2 z} c_1 c_2 e^{-\frac{c_1^2}{2} - \frac{c_2^2}{2}} \left(Q^0_{\mathrm{UU}}(c_1, c_2) - 2R^0_{\mathrm{UU}}(c_1, c_2) \right)$ versus c_1 and c_2. The function has a cusp when $c_1 = c_2$, but is continuous over its whole domain. In this plot $z = 0.2$.

In Fig. 5.1 we see an example plot of the symmetrized kernel function. The general shape of this function remains the same for all values of z, but differences are noticeable as z approaches 1. This plot illustrates that the kernel functions are well behaved and should support a discrete spectrum of eigenvalues according to ref. [15].

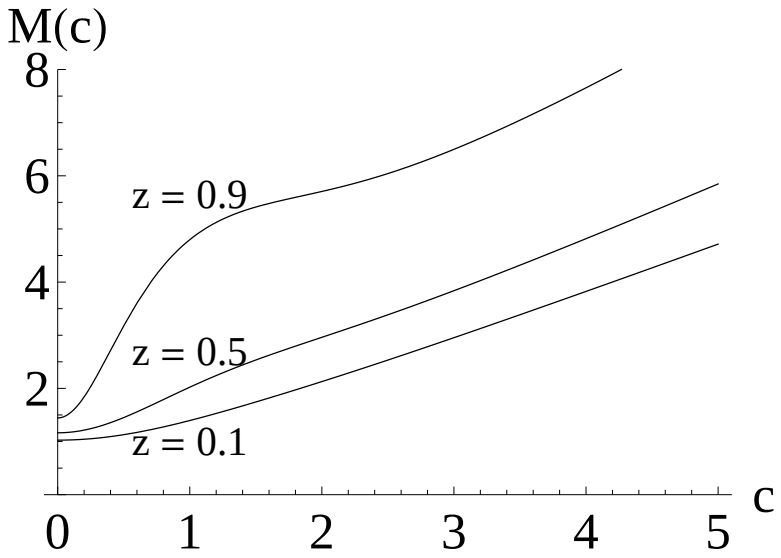

Figure 5.2: Plot of the function $M_{\mathrm{UU}}(c)$ versus c for three values of z. The function is continuous for all positive values of c.

Figure 5.2 shows plots of $M_{\mathrm{UU}}(c)$ for three values of z. The curve with $z = 0.1$ is quite close to the Boltzmann function $M_{\mathrm{HS}}(c)$. Changes are noticeable as z increases, but the minimum value of $M_{\mathrm{UU}}(c)$ still occurs at $c = 0$. This fact allows us to derive an analytic formula for $\lambda_M = M_{\mathrm{UU}}(0)$ in appendix A.5.

The matrix for the Uehling-Uhlenbeck eigenvalues of order l is

$$H^l_{i,j} = M_{\mathrm{UU}}(x_i)\delta_{i,j} + \frac{2}{\pi} w_j x_i x_j e^{-\frac{1}{2}(x_i^2+x_j^2)} \left(Q^l_{\mathrm{UU}}(x_i, x_j) - 2R^l_{\mathrm{UU}}(x_i, x_j) \right). \tag{5.31}$$

Again we can use the angular reduction and the quadrature scheme as a method of calculating $M_{\mathrm{UU}}(c)$. Doing this, we obtain

$$M_{\mathrm{UU}}(x_i) = \frac{2}{\pi}(1 - ze^{-x_i^2}) \sum_{j=1}^{N_Q} w_j x_j^2 \frac{1}{e^{x_j^2} - z} Q^0_{\mathrm{UU}}(x_i, x_j). \tag{5.32}$$

As mentioned at the end of section 2.4, we expect that all of the discrete eigenvalues will fall between zero and a finite limiting value, which we denote here as $\lambda_M(z)$. In appendix A.5, we show that for M_{UU},

$$\lambda_M(z) = \min\left[M_{\mathrm{UU}}(c)\right] = \frac{1}{z}\mathrm{Li}_2(z). \tag{5.33}$$

This expression is very useful because it sets the maximum rate of relaxation for any possible perturbation to the velocity distribution of the gas. It includes the Boltzmann limit, $\lambda_M(z) = 1$ as well as the interesting limit $\lambda_M(1) = \frac{\pi^2}{6}$. This finite value of λ_M for $z = 1$ implies that all eigenvalues remain finite. It is well known that a Bose gas undergoes a phase transition to a Bose-Einstein Condensate when $z = 1$. The absence of any interesting behavior in the eigenvalues spectrum for $z = 1$ indicates that the linearized U-U equation is inadequate for describing this phase transition and is of most interest for $0 < z < 1$.

5.5 Mode Expansion

We can also write a formal solution to the linearized Uehling-Uhlenbeck equation (5.19) analogous to what we did in section 2.7. We begin by stating that the eigenfunctions of linearized Uehling-Uhlenbeck equation are different than those of the linearized Boltzmann equation, but still shared the same orthogonality condition given by

$$\int_0^\infty dc \psi_l^n(c)\psi_l^{n'}(c) = \delta_{n,n'}. \tag{5.34}$$

From our knowledge of the conserved quantities of the U-U equation, the eigenfunction $\psi_0^0(c)$ should produce a deviation $\phi(\mathbf{c})$ that is constant. In addition, the eigenfunction $\psi_1^0(c)$ should produce a deviation proportional to c while the eigenfunction $\psi_0^1(c)$ should produce a deviation that is proportional to $c^2 + B$, where B is a constant. The normalization constants of the eigenfunction and the constant B are determined by the condition in Eq. (2.47). Using this condition, we find that the Uehling-Uhlenbeck eigenfunctions are explicitly given by

$$\psi_0^0(c) = \sqrt{\frac{4z}{\sqrt{\pi}\mathrm{Li}_{\frac{1}{2}}(z)}}\frac{ce^{c^2/2}}{e^{c^2} - z}, \tag{5.35}$$

$$\psi_1^0(c) = \sqrt{\frac{8z}{3\sqrt{\pi}\mathrm{Li}_{\frac{3}{2}}(z)}}\frac{c^2e^{c^2/2}}{e^{c^2} - z} \tag{5.36}$$

and

$$\psi_0^1(c) = \sqrt{\frac{16z\mathrm{Li}_{\frac{1}{2}}(z)}{15\sqrt{\pi}\mathrm{Li}_{\frac{5}{2}}(z)\mathrm{Li}_{\frac{1}{2}}(z) - 9\sqrt{\pi}\mathrm{Li}_{\frac{3}{2}}^2(z)}}\left(c^2 - \frac{3\mathrm{Li}_{\frac{3}{2}}(z)}{2\mathrm{Li}_{\frac{1}{2}}(z)}\right)\frac{ce^{c^2/2}}{e^{c^2} - z}. \tag{5.37}$$

These eigenfunctions reduce to Eqs. (2.61) - (2.63) in the limit $z \to 0$. We can write a formal solution to the original linearized Uehling-Uhlenbeck equation by the mode expansion

$$f(\mathbf{c},t) = f^0(\mathbf{c}) + \frac{1}{c^2}\sum_{n=0}^{\infty}\sum_{l=0}^{\infty}\sum_{m=-l}^{l} A^n_{l,m} e^{-\lambda^n_l \gamma_{\upsilon\upsilon} t}\psi^0_0(c)\psi^n_l(c)Y^m_l(\hat{\mathbf{c}}). \tag{5.38}$$

As in the Boltzmann mode expansion, we only sum over the discrete eigenmodes of the collision operator and exclude the eigenmodes from the continuous spectrum. The coefficients of expansion $A^n_{l,m}$ depend on the initial distribution $f(\mathbf{c},0)$ and are given by

$$A^n_{l,m} = \int d\mathbf{c}\left(f(\mathbf{c},0) - f^0(c)\right)\frac{\psi^n_l(c)}{\psi^0_0(c)}Y^{m*}_l(\hat{\mathbf{c}}) \tag{5.39}$$

The entire time dependence of Eq. (5.38) is carried by the term $e^{-\lambda^n_l\gamma t}$. Using the forms for $\phi^n_l(c)$ in Eqs. (5.35) - (5.37) one can quickly see that $A^0_{0,0}$, $A^1_{0,0}$ and $A^0_{1,m}$ are identically zero due to the conservation laws. This ensures that even through the eigenvalues λ^0_0, λ^1_0 and λ^0_1 are zero, the distribution $f(\mathbf{c},t)$ relaxes to the equilibrium state $f^0(\mathbf{c})$. Eqs. (5.38) and (5.39) allow us to determine the evolution of any distribution function $f(\mathbf{c},t)$ as long as it is close to the equilibrium distribution $f^0(\mathbf{c})$.

5.6 Numerical results for Eigenvalues and Eigenvectors

To compute the eigenvalues and eigenvectors, we must begin by choosing a quadrature scheme as outlined in sections 2.5 and 5.4. This gives us a set of evaluation points x_i and quadrature weights w_i. In general, it is not optimal to choose equally spaced evaluation points for this problem, due to the observed rapid oscillations of the higher-order eigenfunctions near the origin. The issue becomes more pronounced for higher values of z. For our quadrature scheme, we chose a fixed cutoff value of $c = 6$. This effectively assumes that the velocity perturbations are zero beyond $c = 6$. Plots of the eigenfunctions confirm this assumption. We then subdivide the interval $0 < c < 6$ into $\frac{N_Q}{5}$ subintervals, with the width of each subinterval proportional to c^p with $p = 3$ in the final data. In this way we get a much higher density of subintervals near $c = 0$. We then apply a five-point Gaussian quadrature to each subinterval. The use of a five-point method on $\frac{N_Q}{5}$ subintervals results in a total of N_Q evaluation points. This scheme was repeated with differing values p and increasing values of N_Q

to gauge its accuracy. We found that schemes with $p = 3$ produced accurate results without having to resort to large values of N_Q.

	λ_0^0	λ_0^1	λ_0^2	λ_0^3	λ_1^0	λ_1^1	$\lambda_M(z)$
Classical	0	0	0.67123	0.91157	0	0.69503	1
$z = 0.1$	0.0	0.0	0.69096	0.94117	0.0	0.72104	1.02618
$z = 0.2$	0.0	0.0	0.71248	0.97354	0.0	0.74994	1.05502
$z = 0.5$	0.0	0.0	0.79129	1.09410	0.0	0.86163	1.16448
$z = 0.9$	0.0	0.0	0.94759	1.44144	0.0	1.14435	1.44413

Table 5.1: Several of the discrete eigenvalues of the Uehling-Uhlenbeck Equation. The uncertainties of all values are less than 10^{-5}.

In the second step, we choose a particular value of l and z and use a Gauss-Kronrod local adaptive quadrature scheme $(\mathrm{G7, K15})$ [54] to evaluate the integrals in Eqs. (5.29) and (5.30) at the evaluation points x_i, x_j. We use this in combination with Eqs. (5.21) and (5.22) to obtain the $N_Q \times N_Q$ matrices Q_{ij}^0, Q_{ij}^l and S_{ij}^l. From these we compute the values M_i according the Eq. (5.32) and the matrix elements $H_{i,j}^l$ according to Eqs.R (5.31). We then numerically diagonalize the matrix $\mathbf{H}^l$ for increasing N_Q to find its eigenvalues and eigenvectors.

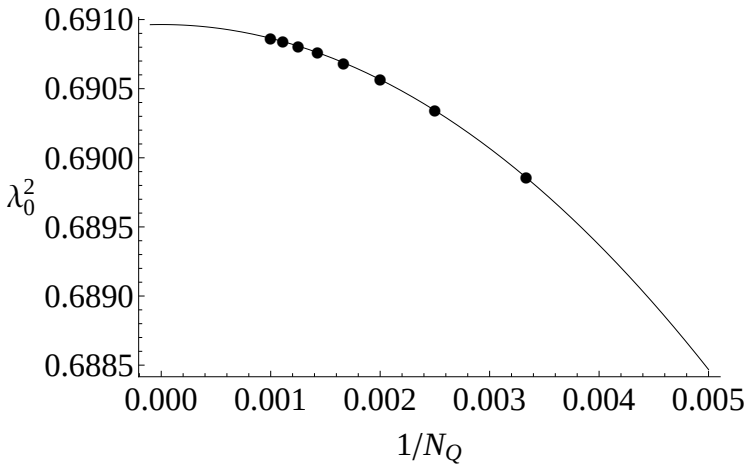

Figure 5.3: Plot of the first non-zero eigenvalue versus inverse matrix size which illustrates the fitting procedure used to estimate the exact eigenvalues. In this plot $z = 0.1$.

To obtain an accurate estimate of the exact eigenvalues, we do not use the numerical eigenvalues of any single matrix. Instead, we plot the numerical eigenvalues versus the inverse matrix size, $\frac{1}{N_Q}$. We then fit this plot with a polynomial in $\frac{1}{N_Q}$ to extrapolate the value of intercept with the vertical axis [3]. This value is what we use for our best estimate of the exact eigenvalues. This procedure is illustrated in figure 5.3 and several eigenvalues are reported in Table 5.1. Our procedure was also able to reproduce the classical results for very small values of z.

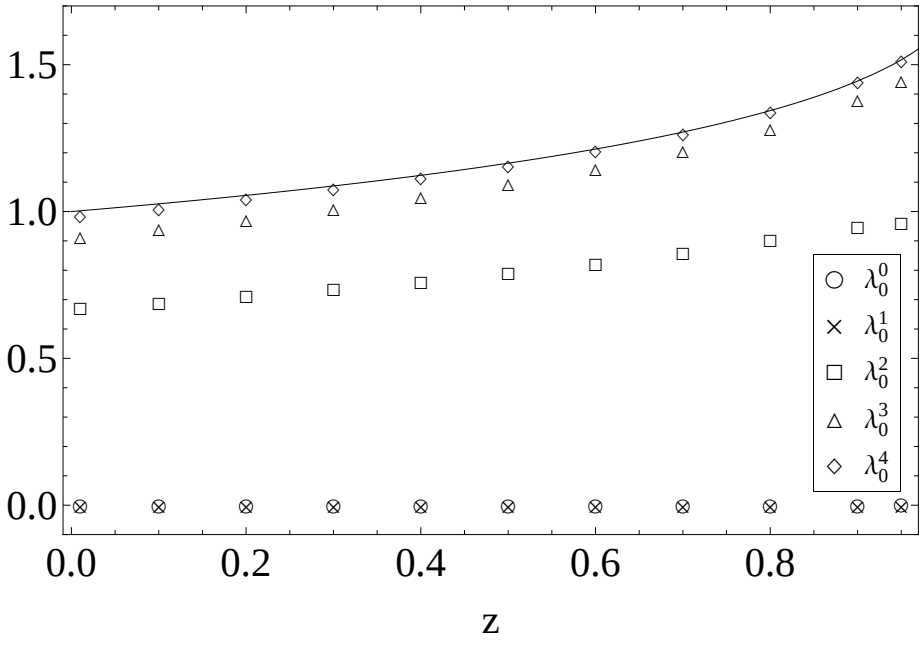

Figure 5.4: Plot showing the dependence of the first few $l = 0$ eigenvalues on z. Note the two zero eigenvalues. The solid curve represents $\lambda_M(z)$, the start of the continuous spectrum.

A plot of interest is the dependence of the eigenvalues on z. In the classical limit, $z \to 0$ we expect our eigenvalues to converge to the known classical eigenvalues in Eqs. (2.34), (2.36) and (2.37). We expect that there will still be zero eigenvalues when $l = 0$ representing conservation of particle number and energy and one zero eigenvalue when $l = 1$ representing conservation of momentum. We also expect that all discrete eigenvalues will be between zero and $\lambda_M(z)$. The plots of λ versus z

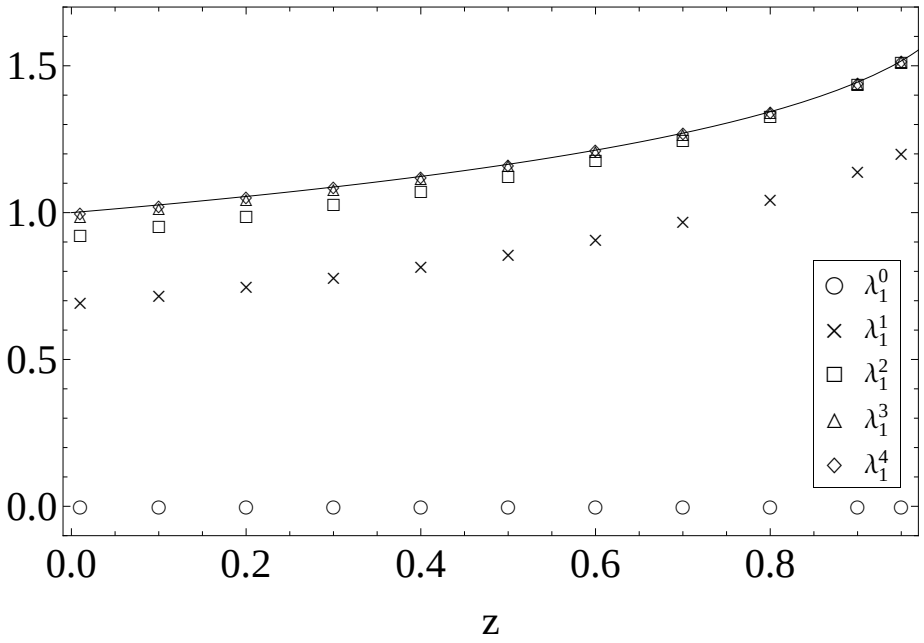

Figure 5.5: Plot showing the dependence of the first few $l = 1$ eigenvalues on z. Note the single zero eigenvalue. The solid curve represents $\lambda_M(z)$, the start of the continuous spectrum.

in figures 5.4 and 5.5 confirm our expectations. These plots also strongly suggest that the discrete eigenvalues approach finite limiting values between zero and $\frac{\pi^2}{6}$ as $z \to 1$. As z approaches 1, the accuracy of the computation decreases substantially. This can be understood by looking at the plots of the eigenfunctions for high values of z. Plots of the eigenvectors ψ_l^n for $z = 0.1$ and $z = 0.9$ are shown in figures 5.6 and 5.7. The eigenvectors appear to be continuous and bounded, but they show increasingly rapid variations near the origin as z is increased. As z becomes greater than about 0.95, the oscillatory features of the higher order eigenfunctions become smaller than the size of our subintervals and accuracy is lost.

5.7 Summary

In this Chapter, we have linearized the Uehling-Uhlenbeck Equation for a Bose gas interacting via a contact potential and derived explicit forms for the kernels Q_{UU} and R_{UU} as functions of the fugacity z. We then compute the spectrum of eigenvalues and their eigenfunctions. The eigenvalue spectrum has the same form as it does for the linearized Boltzmann Equation and the eigenfunctions appear to be

continuous and bounded for $0 \leq z < 1$. Momentum perturbations corresponding to the eigenfunction ψ_l^n relaxes exponentially at a rate of $\gamma_{\mathrm{UU}}\lambda_l^n$ where λ_l^n is the associated eigenvalue and γ_{UU} is defined by Eq. (5.17).

The eigenvalues (and therefore the relaxation rates) increase as z increases, but they remain bounded and also remain within an order of magnitude of their classical values. This increase in relaxation rates is due to the Bose enhancement factors of $1 + f_i(t)$ in the U-U Equation which increases the scattering rate compared to the classical Boltzmann Equation.

A second interesting result is that the eigenvalues of the linearized U-U Equation appear to remain finite in the limit $z \to 1$. The discrete eigenvalues of the linearized U-U Equation all lie between zero and a finite limiting value $\lambda_M(z) = \frac{1}{z}\mathrm{Li}_2(z)$. Since a Bose gas undergoes a phase transition when $z = 1$, we would expect a more interesting behavior of the eigenvalues. The absence of any more interesting behavior indicates that the linearized U-U Equation may be incapable of describing the Bose gas very close to the phase transition.

In conclusion, the Uehling-Uhlenbeck Equation performs best as a refinement to the Boltzmann Equation at the level of quantum corrections. It cannot accurately describe new processes that occur within quantum regime such as Bose-Einstein condensation or superfluidity. However, we find that initial distributions which are close to the quantum regime will relax to equilibrium at a much faster rate than if they were treated classically. We also conclude that the spectrum of the linearized Uehling-Uhlenbeck Equation predicts that distributions near to equilibrium will relax exponentially towards a Bose-Einstein equilibrium distribution.

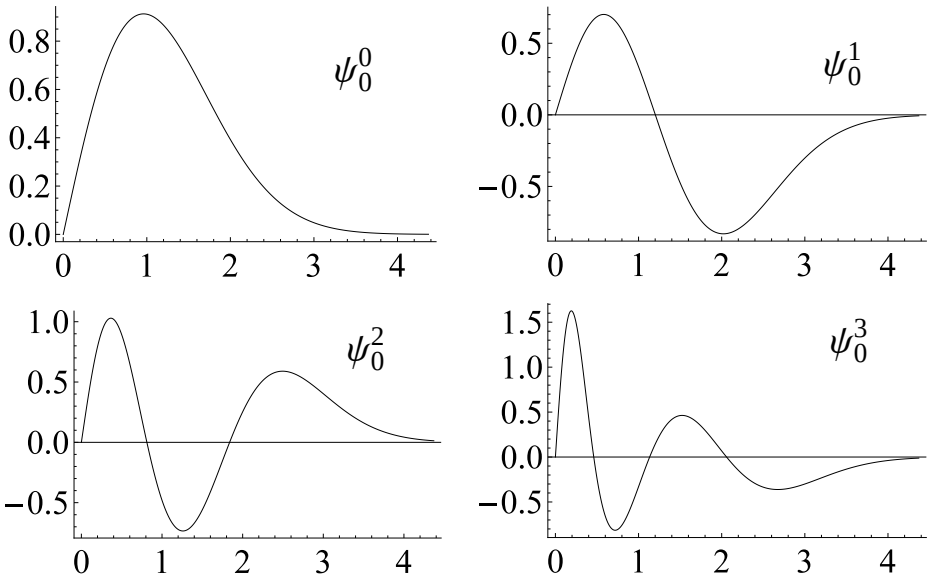

Figure 5.6: A plot of ψ_l^n versus c showing the first few eigenvectors when $l = 0$ and $z = 0.1$.

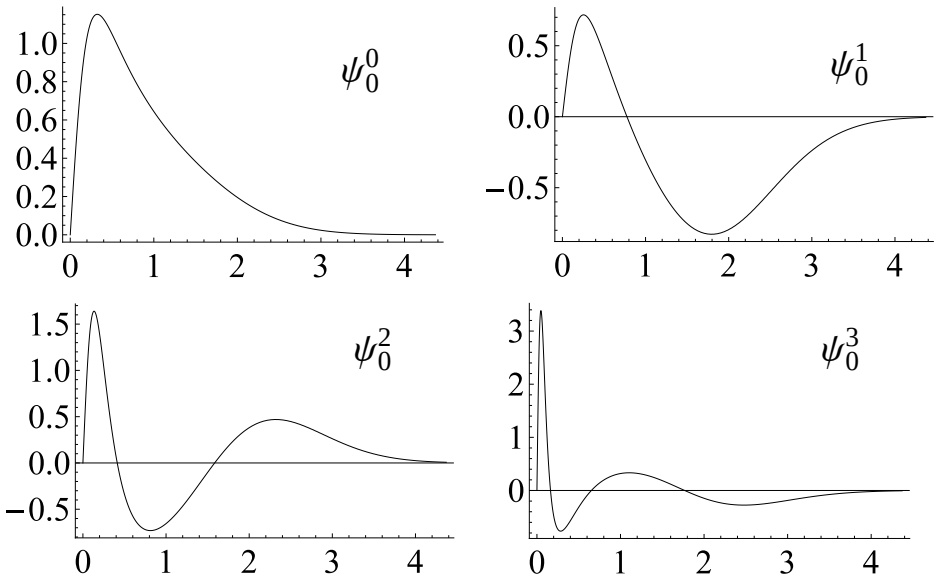

Figure 5.7: A plot of ψ_l^n versus c showing the first few eigenvectors when $l = 0$ and $z = 0.9$.

6 Characteristic Relaxation Rates of the Bogolon Kinetic Equation

6.1 Introduction to the Bogolon Kinetic Equation

The Uehling-Uhlenbeck Equation, though it offers an extension of the Boltzmann Equation to quantum particles, it still is not capable of describing a gas of Bosons where a Bose-Einstein condensate (BEC) is present. The reason for this limitation is essentially the choice of $\hat{H}^0$ and $\hat{H}^1$ in Eqs. (5.1) and (5.2). In fact this choice is somewhat of a trivial choice in the context of what is allowed for in Chapter 4. The Hamiltonians of Chapter 5 are actually not mean field Hamiltonians at all.

As a dilute Bose gas is cooled to low temperatures, the well known phenomena of Bose-Einstein condensation occurs. In spatially homogeneous Bose-Einstein condensation, a macroscopic number of particles occupies the ground state and the ground state acquires an overall phase. Theoretically, this transition is realized by a broken $U(1)$ gauge symmetry and the appearance of an order parameter. The state ($\hat{\rho}_0$) becomes such that the averages $\hat{a}_i\hat{a}_j$ and $\hat{a}_i^\dagger\hat{a}_j^\dagger$ take on non-zero values. These facts must be explicitly built in to the mean field Hamiltonian $\hat{H}^0$ for them to appear in the theory. This alteration of the mean field Hamiltonian $\hat{H}^0$ makes a description in terms of the particle operators $\hat{a}_i^\dagger$ and $\hat{a}_i$ inappropriate. We perform a Bogoliubov transformation to diagonalize the mean field Hamiltonian $\hat{H}^0$ and obtain a description in terms of Bogoliubov excitations or bogolons. We will use the methods of Chapter 4 to derive a kinetic equation for evolution of the bogolon momentum distribution.

6.2 Mean Field Hamiltonian and Bogoliubov Transformation

We can write the Hamiltonian for the BEC in a way that accounts for the broken $U(1)$ gauge symmetry and conserves the *average* number of particles N. We also want to design the form of $\hat{H}^1$ so that the

condition (4.38) is satisfied. The mean field Hamiltonian that satisfies all of these conditions can be written as

$$\hat{H}_0 = \sum_i \left[(\epsilon_i - \mu + \nu)\hat{a}_i^\dagger \hat{a}_i + \frac{\Delta}{2}(\hat{a}_i^\dagger \hat{a}_{-i}^\dagger + \hat{a}_{-i}\hat{a}_i) \right] \tag{6.1}$$

where ν and Δ are the mean fields and μ is the chemical potential. The interaction Hamiltonian takes the form

$$\hat{H}^1 = \frac{g}{2V}\sum_{ijkl}\delta_{i+j,k+l}\hat{a}_i^\dagger \hat{a}_j^\dagger \hat{a}_k \hat{a}_l - \sum_i \left[\nu \hat{a}_i^\dagger \hat{a}_i + \frac{\Delta}{2}(\hat{a}_i^\dagger \hat{a}_{-i}^\dagger + \hat{a}_{-i}\hat{a}_i) \right]. \tag{6.2}$$

The requirement (4.38) results in two self-consistency equations for the mean fields,

$$\nu = \frac{2g}{V}\sum_i \mathrm{Tr}(\hat{\rho}_0 \hat{a}_i^\dagger \hat{a}_i) = \frac{2gN}{V}, \tag{6.3}$$

and

$$\Delta = \frac{g}{V}\sum_i \mathrm{Tr}(\hat{\rho}_0 \hat{a}_i^\dagger \hat{a}_{-i}^\dagger) = \frac{g}{V}\sum_i \mathrm{Tr}(\hat{\rho}_0 \hat{a}_{-i}\hat{a}_i). \tag{6.4}$$

These relations are of importance for the equilibrium properties (sec. 6.6) as well as the relaxation rates (sec. 6.5) of the gas.

When the gauge symmetry is broken, a macroscopic number of particles condenses into the state $i = 0$. We therefore replace $\hat{a}_0^\dagger$ and $\hat{a}_0$ by c-numbers so $\hat{a}_0^\dagger = \sqrt{N_0}$ and $\hat{a}_0 = \sqrt{N_0}$ where N_0 is the average number of particles in the state $i = 0$ [55, 56, 57]. We can then diagonalize the mean field Hamiltonian in Eq. (6.1) by a Bogoliubov transformation

$$\hat{b}_i^\dagger = u_i \hat{a}_i^\dagger + v_i \hat{a}_{-i} \qquad \text{and} \qquad \hat{b}_i = u_i \hat{a}_i + v_i \hat{a}_{-i}^\dagger, \tag{6.5}$$

where $\hat{b}_i^\dagger$ and $\hat{b}_i$ are creation and annihilation operators for the Bogoliubov excitations which we call bogolons. The Bogoliubov transformation does not apply when $i = 0$. The replacement $\hat{a}_0^\dagger = \hat{a}_0 = \sqrt{N_0}$ must be accompanied by the constraint $\nu - \mu = \Delta$ to be consistent [32]. Without these replacements, the only solution to Eq. (6.4) is $\Delta = 0$, which indicates a non-condensed system. In terms of bogolon operators, the Hamiltonian $\hat{H}^0$ takes on the simple form

$$\hat{H}^0 = {\sum_i}' E_i \hat{b}_i^\dagger \hat{b}_i + E_G, \tag{6.6}$$

where primed summations do not include $i = 0$ and the bogolon energy E_i is given by

$$E_i = \sqrt{(\epsilon_i + \Delta)^2 - \Delta^2}. \tag{6.7}$$

The term E_G gives the ground state energy of the condensed Bose gas [55, 58]. The transformation factors u_i and v_i are given by

$$u_i = \frac{1}{\sqrt{2}}\sqrt{\frac{\epsilon_i + \Delta}{E_i} + 1} \qquad \text{and} \qquad v_i = \frac{1}{\sqrt{2}}\sqrt{\frac{\epsilon_i + \Delta}{E_i} - 1}. \tag{6.8}$$

A useful parametrization of u_i and v_i is

$$u_i = \cosh\theta_i \qquad \text{and} \qquad v_i = \sinh\theta_i \qquad \text{where} \qquad \theta_i = \frac{1}{2}\tanh^{-1}\left(\frac{\Delta}{\epsilon_i + \Delta}\right). \tag{6.9}$$

The Bogoliubov transformation allows us to calculate the s-evolution of particle and bogolon operators quite easily. The only relations that we will need are

$$\hat{b}_i^\dagger(s) = e^{-iE_i s/\hbar}\hat{b}_i^\dagger \qquad \text{and} \qquad \hat{b}_i(s) = e^{iE_i s/\hbar}\hat{b}_i. \tag{6.10}$$

We also write the density matrix $\hat{\rho}_0$ in terms of bogolon operators as

$$\hat{\rho}_0 = \exp\left[-{\sum_i}' \xi_i \hat{b}_i^\dagger \hat{b}_i - \Omega\right]. \tag{6.11}$$

The quantity ξ_i is a c-number. It determines the out-of-equilibrium expectation value of $\hat{b}_i^\dagger\hat{b}_i$ which is the number of bogolons in state i.

6.3 Kinetic Equations for Bose Condensed Gas

In this section, we derive the kinetic equations for the bogolon momentum distribution. First note that by using the parametrization (6.9) the time derivative of the bogolon momentum distribution

can be written

$$\begin{aligned}\frac{d\langle\hat{b}_i^\dagger\hat{b}_i\rangle}{dt} =& u_i^2\frac{d\langle\hat{a}_i^\dagger\hat{a}_i\rangle}{dt} + v_i^2\frac{d\langle\hat{a}_{-i}\hat{a}_{-i}^\dagger\rangle}{dt} + u_iv_i\frac{d\langle\hat{a}_i^\dagger\hat{a}_{-i}^\dagger\rangle}{dt} + u_iv_i\frac{d\langle\hat{a}_{-i}\hat{a}_i\rangle}{dt} \\ &+ \left[2u_iv_i\langle\hat{a}_i^\dagger\hat{a}_i\rangle + 2u_iv_i\langle\hat{a}_{-i}\hat{a}_{-i}^\dagger\rangle + (u_i^2+v_i^2)\langle\hat{a}_i^\dagger\hat{a}_{-i}^\dagger\rangle + (u_i^2+v_i^2)\langle\hat{a}_{-i}\hat{a}_i\rangle\right]\frac{d\theta_i}{dt}.\end{aligned} \tag{6.12}$$

By re-expressing the term in square brackets in terms of bogolon operators, it can be show that it is equal to $\langle\hat{b}_i^\dagger\hat{b}_{-i}^\dagger\rangle + \langle\hat{b}_{-i}\hat{b}_i\rangle$ which is exactly zero. Therefore, we have

$$\frac{d\langle\hat{b}_i^\dagger\hat{b}_i\rangle}{dt} = u_i^2\frac{d\langle\hat{a}_i^\dagger\hat{a}_i\rangle}{dt} + v_i^2\frac{d\langle\hat{a}_{-i}^\dagger\hat{a}_{-i}\rangle}{dt} + u_iv_i\frac{d\langle\hat{a}_i^\dagger\hat{a}_{-i}^\dagger\rangle}{dt} + u_iv_i\frac{d\langle\hat{a}_{-i}\hat{a}_i\rangle}{dt}. \tag{6.13}$$

In obtaining this, terms involving time derivatives of u_i and v_i are both proportional to the time derivative of Δ. When all such terms are grouped together and written in terms of $\langle\hat{b}_i^\dagger\hat{b}_i\rangle$, the resulting coefficient of $\frac{d\Delta}{dt}$ is zero. Due to the above relationship, we define

$$\mathrm{Tr}(\hat{\rho}_0\hat{a}_i^\dagger\hat{a}_j) \equiv \langle\hat{a}_i^\dagger\hat{a}_j\rangle \equiv N_i\delta_{i,j} \qquad F_i \equiv N_i + 1, \tag{6.14}$$

$$\frac{1}{2}\mathrm{Tr}\left[\hat{\rho}_0\left(\hat{a}_i^\dagger\hat{a}_j^\dagger + \hat{a}_i\hat{a}_j\right)\right] \equiv \Lambda_i\delta_{i,-j} \tag{6.15}$$

and

$$\mathrm{Tr}\left(\hat{\rho}_0\hat{b}_i^\dagger\hat{b}_j\right) \equiv \langle\hat{b}_i^\dagger\hat{b}_j\rangle \equiv \mathcal{N}_i\delta_{i,j} \qquad \mathcal{F}_i \equiv 1 + \mathcal{N}_i. \tag{6.16}$$

Due to the diagonal exponent of $\hat{\rho}_0$ in Eq. (6.11), expectation values of products of bogolon operators containing unequal numbers of creation and annihilation operators are zero. Expectation values of products containing four or more bogolon operators can be shown to satisfy Wick's theorem and can be written in terms of all possible pairwise averages of bogolon operators. For example,

$$\langle\hat{b}_1^\dagger\hat{b}_2^\dagger\hat{b}_3\hat{b}_4\rangle = \langle\hat{b}_1^\dagger\hat{b}_3\rangle\langle\hat{b}_2^\dagger\hat{b}_4\rangle + \langle\hat{b}_1^\dagger\hat{b}_4\rangle\langle\hat{b}_2^\dagger\hat{b}_3\rangle. \tag{6.17}$$

This greatly reduces the number of possible expectation values we must calculate. We also note that these rules strictly only apply to indices other than zero. Whenever zero appears in an index, $\hat{a}_0^\dagger$ and $\hat{a}_0$ must be replaced with $\sqrt{N_0}$ before expectation values are taken.

We can now use Eqs. (6.2), (6.16) and (6.17) to evaluate the right hand side of Eq. (4.39). To

accomplish this, all particle operators except $\hat{a}_0^\dagger$ and $\hat{a}_0$ are expressed in terms of bogolon operators and the s-evolution of the bogolon operators is applied according to Eq. (6.10). All commutators are evaluated and the remaining operators are put in normal order. Then expectation values are taken with respect to $\hat{\rho}_0$. This process generates anywhere from 5000 to 40000 individual terms, depending on how much simplification is done after each step. The individual terms possess a high degree of symmetry with respect to their indices and can be simplified considerably. We used a custom computer algebra code to complete these calculations in a reasonable amount of time. The operation of this code is discussed in appendix B.

The kinetic equation for the average number of particles in the state i takes the form

$$\frac{dN_i}{dt} = \mathcal{C}_i^{12}\{\mathcal{N}\} + \mathcal{C}_i^{22}\{\mathcal{N}\} + \mathcal{C}_i^{31}\{\mathcal{N}\}, \tag{6.18}$$

where $\mathcal{C}_i^{12}$, $\mathcal{C}_i^{22}$ and $\mathcal{C}_i^{31}$ are collision operators defined in appendix A.7. We also write a kinetic equation for the anomalous average $\Lambda_i \equiv \frac{1}{2}\left(\langle \hat{a}_i^\dagger \hat{a}_{-i}^\dagger \rangle + \langle \hat{a}_{-i}\hat{a}_i \rangle\right)$ and find a structure similar to Eq. (6.18) but with different collision operators,

$$\frac{d\Lambda_i}{dt} = \mathcal{D}_i^{12}\{\mathcal{N}\} + \mathcal{D}_i^{22}\{\mathcal{N}\} + \mathcal{D}_i^{31}\{\mathcal{N}\}, \tag{6.19}$$

where $\mathcal{D}_i^{12}$, $\mathcal{D}_i^{22}$ and $\mathcal{D}_i^{31}$ are again collision integrals which can be found in appendix A.7. The collision integrals describe collisions between bogolons that conserve energy and momentum but not bogolon number. There are three basic collision processes for bogolons. In the first ($\mathcal{C}^{12}$ and $\mathcal{D}^{12}$), two bogolons collide and become one, or vice versa. The rate of this process is proportional to N_0. The second process ($\mathcal{C}^{22}$ and $\mathcal{D}^{22}$) involves an elastic collision of two bogolons. The third process ($\mathcal{C}^{31}$ and $\mathcal{D}^{31}$) is three bogolons colliding to become one and vice versa. The first and third processes allow for the creation and destruction of bogolons as they thermalize.

To obtain an equation for the evolution of $\mathcal{N}_i$, we use Eq. (6.13), (6.18) and (6.19). Putting these together results in a closed kinetic equation for the bogolon distribution $\mathcal{N}_i$,

$$\frac{d\mathcal{N}_i}{dt} = \mathcal{G}_i^{12}\{\mathcal{N}\} + \mathcal{G}_i^{22}\{\mathcal{N}\} + \mathcal{G}_i^{31}\{\mathcal{N}\} \tag{6.20}$$

where the bogolon collision operators are given by

$$\begin{aligned}\mathcal{G}_i^{12}\{\mathcal{N}\} = &\frac{8\pi N_0 g^2}{\hbar V^2}{\sum_{2,3}}' \delta_{i+2,3}\delta(E_i + E_2 - E_3)(W^{12}_{i,2,3})^2(\mathcal{F}_i\mathcal{F}_2\mathcal{N}_3 - \mathcal{N}_i\mathcal{N}_2\mathcal{F}_3)\\ &+\frac{4\pi N_0 g^2}{\hbar V^2}{\sum_{2,3}}' \delta_{i,2+3}\delta(E_i - E_2 - E_3)(W^{12}_{3,2,i})^2(\mathcal{F}_i\mathcal{N}_2\mathcal{N}_3 - \mathcal{N}_i\mathcal{F}_2\mathcal{F}_3),\end{aligned} \tag{6.21}$$

$$\mathcal{G}_i^{22}\{\mathcal{N}\} = \frac{4\pi g^2}{\hbar V^2}{\sum_{2,3,4}}' \delta_{i+2,3+4}\delta(E_i + E_2 - E_3 - E_4)(W^{22}_{i,2,3,4})^2(\mathcal{F}_i\mathcal{F}_2\mathcal{N}_3\mathcal{N}_4 - \mathcal{N}_i\mathcal{N}_2\mathcal{F}_3\mathcal{F}_4) \tag{6.22}$$

and

$$\begin{aligned}\mathcal{G}_i^{31}\{\mathcal{N}\} = &\frac{4\pi g^2}{3\hbar V^2}{\sum_{2,3,4}}' \delta_{i,2+3+4}\delta(E_i - E_2 - E_3 - E_4)(W^{31}_{1,2,3,4})^2(\mathcal{F}_i\mathcal{N}_2\mathcal{N}_3\mathcal{N}_4 - \mathcal{N}_i\mathcal{F}_2\mathcal{F}_3\mathcal{F}_4)\\ &+\frac{4\pi g^2}{\hbar V^2}{\sum_{2,3,4}}' \delta_{i+2+3,4}\delta(E_i + E_2 + E_3 - E_4)(W^{31}_{4,3,2,i})^2(\mathcal{F}_i\mathcal{F}_2\mathcal{F}_3\mathcal{N}_4 - \mathcal{N}_i\mathcal{N}_2\mathcal{N}_3\mathcal{F}_4).\end{aligned} \tag{6.23}$$

The weighting functions are given in terms of u and v by

$$W^{12}_{1,2,3} = u_1u_2u_3 - u_1v_2u_3 - v_1u_2u_3 + u_1v_2v_3 + v_1u_2v_3 - v_1v_2v_3, \tag{6.24}$$

$$W^{22}_{1,2,3,4} = u_1u_2u_3u_4 + u_1v_2u_3v_4 + u_1v_2v_3u_4 + v_1u_2u_3v_4 + v_1u_2v_3u_4 + v_1v_2v_3v_4 \tag{6.25}$$

and

$$W^{31}_{1,2,3,4} = u_1u_2u_3v_4 + u_1u_2v_3u_4 + u_1v_2u_3u_4 + v_1v_2v_3u_4 + v_1v_2u_3v_4 + v_1u_2v_3v_4. \tag{6.26}$$

Each of these weighting functions has specific symmetry with respect to interchanges of its indices that is shared by its collision integral. In the limit that $\Delta \to 0$, the weighting functions W^{12} and W^{22} approach 1 while the weighting function W_{31} approaches zero. However, $\mathcal{G}^{12}$ still approaches zero overall since it is multiplied by N_0 which approaches zero.

The collision integral $\mathcal{G}^{12}$ is the same as is found in ref. [26]. The collision integral $\mathcal{G}^{22}$ is analogous to the Uehling-Uhlenbeck equation. To the best of our knowledge, the collision integral $\mathcal{G}^{31}$ is a new result. We would also like to note that Eq. (6.20) can also be obtained by expressing the original mean field Hamiltonians $\hat{H}^0$ and $\hat{H}^1$ in terms of bogolon operators, separating out the $i = 0$ terms from the sums, and applying the results of Chapter 4.

6.4 Conservation of Particle Number

Given that we are going to be working with a kinetic equation for the bogolon occupation numbers, it is a worthwhile to stop and consider particle number conservation. We should have total average particle number conservation since the original Hamiltonian $\hat{H}^0+\hat{H}^1$ commutes with the total particle number operator $\sum_i \hat{a}_i^\dagger \hat{a}_i$. This information should be contained in the form of the collision operators in Eq. (6.18).

In order to discuss conservation of particle number, consider the quantity

$$\frac{dN_{ex}}{dt} = \frac{d}{dt}{\sum_1}' n_1 \tag{6.27}$$

which represents the rate of change of the number of particles not in the condensate. From the explicit forms of the collision operators $\mathcal{C}^{12}$ (A.42), $\mathcal{C}^{22}$ (A.43) and $\mathcal{C}^{31}$ (A.44) found in appendix A.7, we can show that

$$\begin{aligned}\frac{dN_{ex}}{dt} =& -\frac{4\pi N_0 g^2}{\hbar V^2}{\sum_{1,2,3}}' \delta_{1,2+3}\delta(E_1-E_2-E_3)(\mathcal{F}_1\mathcal{N}_2\mathcal{N}_3-\mathcal{N}_1\mathcal{F}_2\mathcal{F}_3)\\ &\times W^{12}_{3,2,1}(u_1u_2u_3+u_1v_2u_3+u_1u_2v_3+v_1v_2v_3+v_1u_2v_3+v_1v_2u_3).\end{aligned} \tag{6.28}$$

It is not unexpected that the time rate of change of the number of excited particles is not zero. Indeed the portion which contributes is $\mathcal{C}^{12}$, which describes collisions involving transfers to the ground state N_0.

Examination of the quantity $\frac{dN_0}{dt}$ should yield a result consistent with conservation of particle number. We must be careful in doing this, since Eq. (6.18) is strictly only valid for particles not in the ground state. Nevertheless, it is illuminating to use Eq. (6.18) to calculate $\frac{dN_0}{dt}$ in a formal sense. We do this by setting index 1 to zero in Eq. (6.18) and setting $\mathcal{N}_0 = \mathcal{F}_0 = N_0$, $u_0 = 1$ and $v_0 = 0$, because the Bogoliubov transformation does not act on the operators with $i = 0$. Interestingly, the collision integral $\mathcal{C}^{12}$ involving transfer to the ground state becomes zero due to the conservation of momentum and energy requirements and the terms involving two body collisions, $\mathcal{C}^{22}$ and $\mathcal{C}^{31}$, merge

to take on a familiar form. The final result is

$$\begin{aligned}\frac{dN_0}{dt} =& \frac{4\pi N_0 g^2}{\hbar V^2} \sum_{1,2,3}{}' \delta_{1,2+3}\delta(E_1 - E_2 - E_3)(\mathcal{F}_1\mathcal{N}_2\mathcal{N}_3 - \mathcal{N}_1\mathcal{F}_2\mathcal{F}_3) \\ & \times W^{12}_{3,2,1}(u_1u_2u_3 + u_1v_2u_3 + u_1u_2v_3 + v_1v_2v_3 + v_1u_2v_3 + v_1v_2u_3).\end{aligned} \tag{6.29}$$

This is the exact opposite of eq (6.28), showing that the total particle number is conserved.

This leads us to thing that we may be able to treat N_0 as a dynamical variable. However we will find that after linearizing the kinetic equations, treating N_0 as a dynamical variable has no effect on the evolution of the $\mathcal{N}_i$. The reason for this is that when we linearize, only $\mathcal{C}^{12}$ will contribute to the evolution of N_0, and we will end up with ϕ_0 multiplied by $\mathcal{C}^{12}$ applied to the equilibrium distributions $\mathcal{N}_i^0$, which will give zero.

6.5 Relaxation Rates from the Linearized Bogolon Kinetic Equation

At equilibrium, $\hat{\rho}_0 = \exp\left[-\hat{H}^0/(k_BT) - \Omega\right]$ so the momentum distribution of bogolons is

$$\mathcal{N}_i^0 = \frac{1}{e^{\frac{E_i}{k_BT}} - 1} \qquad\qquad \mathcal{F}_i^0 = 1 + \mathcal{N}_i^0 \tag{6.30}$$

Indeed, when this distribution is used in the bogolon collision operators (6.21, 6.22, 6.23) it gives identically zero. Therefore, the distribution (6.30) is a stationary solution of the kinetic equation (6.20).

To obtain the characteristic relaxation rates for the momentum distribution of the Bogolon gas, We linearize the kinetic equation about this equilibrium distribution by writing the bogolon distribution as

$$\mathcal{N}_i = \mathcal{N}_i^0 + \mathcal{N}_i^0\mathcal{F}_i^0\phi_i \tag{6.31}$$

and neglecting terms beyond first order in ϕ. This linearization scheme along with energy conservation produces, for example,

$$\mathcal{F}_1\mathcal{F}_2\mathcal{N}_3\mathcal{N}_4 - \mathcal{N}_1\mathcal{N}_2\mathcal{F}_3\mathcal{F}_4 \to \mathcal{N}_1^0\mathcal{N}_2^0\mathcal{F}_3^0\mathcal{F}_4^0(-\phi_1 - \phi_2 + \phi_3 + \phi_4). \tag{6.32}$$

Similar results apply to the other products of distributions found in the collision operators.

To continue the analysis, we convert to a continuum description by introducing a continuous dimensionless momentum vector $\mathbf{c} = \sqrt{\frac{\hbar^2}{2mk_BT}}\mathbf{k}$ and making the replacements $\mathcal{N}_i = \mathcal{N}(\mathbf{c}_i)$. We take the thermodynamic limit by letting $V \to \infty$, $N \to \infty$ and such that the densities $n = \frac{N}{V}$ and $n_0 = \frac{N_0}{V}$ remain constant. The other quantities affected by the change to the continuum are

$$\sum_1{}' \to \frac{V}{(2\pi)^3}\left(\frac{2mk_BT}{\hbar^2}\right)^{3/2}\int d\mathbf{c}_1 \tag{6.33}$$

and

$$\delta_{1,2} \to \frac{(2\pi)^3}{V}\left(\frac{\hbar^2}{2mk_BT}\right)^{3/2}\delta^3(\mathbf{c}_1 - \mathbf{c}_2). \tag{6.34}$$

In making the integrals dimensionless, we collect many of the physical quantities as coefficients of the collision operators. We define $b = \frac{\Delta}{k_BT}$ as the dimensionless ratio between the mean field and the temperature, $\mathcal{E}_i \equiv \frac{E_i}{k_BT} = \sqrt{c_i^4 + 2bc_i^2}$ as the dimensionless bogolon energy for momentum c_i and $\epsilon_a = \frac{h^2}{2\pi ma^2}$ as an energy scale set solely by the choice of particle mass m and particle scattering length a. Also two coefficients appear in the collision operators. The dimensionless coefficient

$$\alpha = n_0a^3\left(\frac{\pi\epsilon_a}{k_BT}\right)^{3/2} \tag{6.35}$$

appears in front of the $\mathcal{G}^{12}$ collision integral and is proportional to the density of particles in the ground state, and

$$\gamma = \frac{32\pi(k_BT)^2}{h\epsilon_a} \tag{6.36}$$

is an overall rate coefficient that multiplies every collision integral with units of inverse time.

These notations also allow us to conveniently write the linearized bogolon collision operator $\mathcal{G}^{12}\{\phi\}$ as

$$\begin{aligned}\mathcal{G}_i^{12}\{\phi\} = &-\frac{\gamma\alpha}{\pi^2}\mathcal{N}_1^0\phi_1\int d\mathbf{c}_2\mathcal{N}_2^0\left[2T^A(\mathbf{c}_1,\mathbf{c}_2) + T_B(\mathbf{c}_1,\mathbf{c}_2)\right]\\ &-\frac{\gamma\alpha}{\pi^2}\mathcal{N}_1^0\int d\mathbf{c}_2\mathcal{N}_2^0\left[2T_A(\mathbf{c}_1,\mathbf{c}_2) - 2T_B(\mathbf{c}_1,\mathbf{c}_2) - 2T_B(\mathbf{c}_2,\mathbf{c}_1)\right]\phi_2,\end{aligned} \tag{6.37}$$

where

$$T_A(\mathbf{c}_1,\mathbf{c}_2) = \int d\mathbf{c}_3\delta^3(\mathbf{c}_1 + \mathbf{c}_2 - \mathbf{c}_8)\delta(\mathcal{E}_1 + \mathcal{E}_2 - \mathcal{E}_3)(W_{1,2,3}^{12})^2\mathcal{F}_3^0 \tag{6.38}$$

and

$$T_B(\mathbf{c}_1,\mathbf{c}_2)=\frac{\mathcal{F}_2^0}{\mathcal{N}_2^0}\int d\mathbf{c}_3\delta^3(\mathbf{c}_1-\mathbf{c}_2-\mathbf{c}_3)\delta(\mathcal{E}_1-\mathcal{E}_2-\mathcal{E}_3)(W^{12}_{3,2,1})^2\mathcal{F}_3^0. \tag{6.39}$$

The linearized bogolon collision operator $\mathcal{G}^{22}\{\phi\}$ can be written as

$$\begin{aligned}\mathcal{G}_1^{22}\{\phi\}=&-\frac{\gamma}{\pi^2}\mathcal{N}_1^0\phi_1\int d\mathbf{c}_2\mathcal{N}_2^0\left[Q_A(\mathbf{c}_1,\mathbf{c}_2)\right]\\&-\frac{\gamma}{\pi^2}\mathcal{N}_1^0\int d\mathbf{c}_2\mathcal{N}_2^0\left[Q_A(\mathbf{c}_1,\mathbf{c}_2)-2R_A(\mathbf{c}_1,\mathbf{c}_2)\right]\phi_2,\end{aligned} \tag{6.40}$$

where

$$Q_A(\mathbf{c}_1,\mathbf{c}_2)=\int d\mathbf{c}_3d\mathbf{c}_4\delta^3(\mathbf{c}_1+\mathbf{c}_2-\mathbf{c}_3-\mathbf{c}_4)\delta(\mathcal{E}_1+\mathcal{E}_2-\mathcal{E}_3-\mathcal{E}_4)(W^{22}_{1234})^2\mathcal{F}_3^0\mathcal{F}_4^0 \tag{6.41}$$

and

$$R_A(\mathbf{c}_1,\mathbf{c}_2)=\frac{\mathcal{F}_2^0}{\mathcal{N}_2^0}\int d\mathbf{c}_3d\mathbf{c}_4\delta^3(\mathbf{c}_1-\mathbf{c}_2+\mathbf{c}_3-\mathbf{c}_4)\delta(\mathcal{E}_1-\mathcal{E}_2+\mathcal{E}_3-\mathcal{E}_4)(W^{22}_{1324})^2\mathcal{N}_3^0\mathcal{F}_4^0. \tag{6.42}$$

Lastly, the linearized bogolon collision operator $\mathcal{G}^{31}\{\phi\}$ can be written as

$$\begin{aligned}\mathcal{G}_1^{31}\{\phi\}=&-\frac{\gamma}{\pi^2}\mathcal{N}_1^0\phi_1\int d\mathbf{c}_2\mathcal{N}_2^0\left[Q_B(\mathbf{c}_1,\mathbf{c}_2)+\frac{1}{3}Q_C(\mathbf{c}_1,\mathbf{c}_2)\right]\\&-\frac{\gamma}{\pi^2}\mathcal{N}_1^0\int d\mathbf{c}_2\mathcal{N}_2^0\left[2Q_B(\mathbf{c}_1,\mathbf{c}_2)-Q_C(\mathbf{c}_1,\mathbf{c}_2)-Q_C(\mathbf{c}_2,\mathbf{c}_1)\right]\phi_2\end{aligned} \tag{6.43}$$

where

$$Q_B(\mathbf{c}_1,\mathbf{c}_2)=\int d\mathbf{c}_3d\mathbf{c}_4\delta^3(\mathbf{c}_1+\mathbf{c}_2+\mathbf{c}_3-\mathbf{c}_4)\delta(\mathcal{E}_1+\mathcal{E}_2+\mathcal{E}_3-\mathcal{E}_4)(W^{31}_{4,3,2,1})^2\mathcal{N}_3^0\mathcal{F}_4^0 \tag{6.44}$$

and

$$Q_C(\mathbf{c}_1,\mathbf{c}_2)=\frac{\mathcal{F}_2^0}{\mathcal{N}_2^0}\int d\mathbf{c}_3d\mathbf{c}_4\delta^3(\mathbf{c}_1-\mathbf{c}_2-\mathbf{c}_3-\mathbf{c}_4)\delta(\mathcal{E}_1-\mathcal{E}_2-\mathcal{E}_3-\mathcal{E}_4)(W^{31}_{1,2,3,4})^2\mathcal{F}_3^0\mathcal{F}_4^0. \tag{6.45}$$

We call the six functions Q_A, R_A, Q_B, Q_C, T_A and T_B the kernel functions. The functions Q_A, R_A, Q_B, and T_A are symmetric with respect to interchange of their two arguments. The functions Q_C and T_B are not symmetric; they are zero for $|\mathbf{c}_1|<|\mathbf{c}_2|$, but they appear in a symmetric way in the bogolon

collision operators. From the forms of the collision kernels, one can see that the collision operators $\mathcal{G}^{12}$, $\mathcal{G}^{22}$ and $\mathcal{G}^{31}$ conserve bogolon energy and momentum.

We can now write the linearized kinetic equation as an evolution equation for the deviations ϕ compactly as

$$\frac{d\phi(\mathbf{c}_1)}{dt} = -\gamma\left[M(\mathbf{c}_1)\phi(\mathbf{c}_1) + \int d\mathbf{c}_2 \frac{\mathcal{N}_2^0}{\mathcal{F}_1^0}\kappa(\mathbf{c}_1,\mathbf{c}_2)\phi(\mathbf{c}_2)\right], \tag{6.46}$$

where

$$\begin{aligned} M(\mathbf{c}_1) = \frac{1}{\pi^2}\int d\mathbf{c}_2 \frac{\mathcal{N}_2^0}{\mathcal{F}_1^0}\Big[&Q_A(\mathbf{c}_1,\mathbf{c}_2) + Q_B(\mathbf{c}_1,\mathbf{c}_2) + \frac{1}{3}Q_C(\mathbf{c}_1,\mathbf{c}_2) \\ &+ 2\alpha T_A(\mathbf{c}_1,\mathbf{c}_2) + \alpha T_B(\mathbf{c}_1,\mathbf{c}_2)\Big] \end{aligned} \tag{6.47}$$

and

$$\begin{aligned} \kappa(\mathbf{c}_1,\mathbf{c}_2) = \frac{1}{\pi^2}\Big[&Q_A(\mathbf{c}_1,\mathbf{c}_2) + 2Q_B(\mathbf{c}_1,\mathbf{c}_2) - Q_C(\mathbf{c}_1,\mathbf{c}_2) - Q_C(\mathbf{c}_2,\mathbf{c}_1) \\ &- 2R_A(\mathbf{c}_1,\mathbf{c}_2) + 2\alpha T_A(\mathbf{c}_1,\mathbf{c}_2) - 2\alpha T_B(\mathbf{c}_1,\mathbf{c}_2) - 2\alpha T_B(\mathbf{c}_2,\mathbf{c}_1)\Big]. \end{aligned} \tag{6.48}$$

We can make the same identifications here that we have made in sections 2.6 and 5.4

$$\mathcal{M}(\mathbf{c}) = M(\mathbf{c}), \qquad \mathcal{W}(c_2) = \mathcal{N}_2^0, \qquad \mathcal{V}(c_1) = \mathcal{F}_1^0 \tag{6.49}$$

and

$$\mathcal{K}(\mathbf{c}_1,\mathbf{c}_2) = \kappa(\mathbf{c}_1,\mathbf{c}_2). \tag{6.50}$$

We can also form the matrices $H_{i,j}^l$ in the same manner as Eqs. (2.57) and (5.31) to obtain

$$H_{i,j}^l = M(x_i)\delta_{i,j} + 2\pi w_j x_i x_j \sqrt{\frac{\mathcal{N}_i^0\mathcal{N}_j^0}{\mathcal{F}_i^0\mathcal{F}_j^0}}\kappa^l(x_i,x_j), \tag{6.51}$$

where

$$\kappa^l(c_1,c_2) = \int_{-1}^{1} d(\hat{\mathbf{c}}_1\cdot\hat{\mathbf{c}}_2)P_l(\hat{\mathbf{c}}_1\cdot\hat{\mathbf{c}}_2)\kappa(\mathbf{c}_1,\mathbf{c}_2) \tag{6.52}$$

All of the eigenvalues of $\mathbf{H}^l$ should be either zero or positive with each zero eigenvalue corresponding to a conserved quantity and all others representing exponential relaxation to equilibrium. The overall physical rate of relaxation of a mode ψ_l^n is $e^{-\lambda_l^n\gamma t}$ where γ has units of inverse time and is given in Eq.

(6.36). Note that unlike the Boltzmann and Uehling-Uhlenbeck eigenvalues, λ_n^l depends not only on the properties of the particles, but also on the temperature and the density through the parameters α and b. The computation of the matrix elements $\kappa^l(x_i, x_j)$ consumes the majority of the calculation time. In appendix A.8 we give the explicit results that we used to compute these values.

The eigenfunctions of the linearized bogolon collision operator also have an orthogonality condition given by

$$\int_0^\infty dc \psi_l^n(c) \psi_l^{n'}(c) = \delta_{n,n'}. \tag{6.53}$$

Because the average total number of bogolons is not conserved, and because of energy conservation, we expect that the eigenvalue $\lambda_0^0 = 0$ and the mode ψ_0^0 should produce a deviation ϕ that is proportional to $\mathcal{E}(c)$, not constant as it was for the Boltzmann and U-U equations. Momentum conservation is unchanged and predicts that the eigenvalue $\lambda_1^0 = 0$ and that the mode ψ_1^0 should produce a deviation proportional to c. Using these conditions and the orthogonality relation, we can write these eigenfunctions explicitly as

$$\psi_0^0(c) \propto c\sqrt{c^4 + 2bc^2} \frac{e^{\frac{1}{2}\sqrt{c^4+2bc^2}}}{e^{\sqrt{c^4+2bc^2}} - 1} \tag{6.54}$$

and

$$\psi_1^0(c) \propto c^2 \frac{e^{\frac{1}{2}\sqrt{c^4+2bc^2}}}{e^{\sqrt{c^4+2bc^2}} - 1} \tag{6.55}$$

Due to the presence of the square roots, normalization of these eigenfunctions must be done numerically.

We can use the eigenmodes to write the bogolon distribution in the linear regime as

$$\mathcal{N}(\mathbf{c}) = \mathcal{N}^0(\mathbf{c}) + \frac{1}{c^2 \mathcal{E}(c)} \sum_{n=0}^{\infty} \sum_{l=0}^{\infty} \sum_{m=-l}^{l} \mathcal{A}_{l,m}^n e^{-\lambda_l^n \gamma t} \psi_0^0(c) \psi_l^n(c) Y_l^m(\hat{\mathbf{c}}) \tag{6.56}$$

where

$$\mathcal{A}_{l,m}^n = \int d\mathbf{c} \mathcal{E}(c) \left[\mathcal{N}(\mathbf{c}) - \mathcal{N}^0(c)\right] \frac{\psi_l^n(c)}{\psi_0^0(c)} Y_l^{m*}(\hat{\mathbf{c}}) \tag{6.57}$$

This mode expansion is slightly different from the Uehling-Uhlenbeck mode expansion [41] because of the presence of $\mathcal{E}(c)$. This makes the lowest order expansion coefficient $\mathcal{A}_{0,0}^0$ correspond to an energy rather than an amount of particles. Since the effects of energy and momentum conservation are already included in $\mathcal{N}^0(\mathbf{c})$, the expansion coefficients $\mathcal{A}_{0,0}^0$ and $\mathcal{A}_{1,m}^0$ are exactly zero.

6.6 Self-Consistency Equations

Since we have linearized the kinetic equation about equilibrium, the eigenvalues of linearized collision operator will depend upon the equilibrium state that we choose. For a given particle, the equilibrium state can chosen by specifying any two of the parameters: average total density n, condensate density n_0, temperature T or mean field Δ. The mean field self-consistency equations (6.3, 6.4) provide the relations between the quantities n, n_0, T and Δ. They also give us information about the equilibrium behavior of the gas. Explicit formulas for the self-consistency equations that are used for calculation can be found in appendix A.9.

Note that different levels of approximation are found in the literature [55, 56, 59]. Most involve performing the calculations at zero temperature and/or assuming that $n_0 \approx n$. We keep all finite temperature effects and non-analytic interaction effects. The inclusion of these effects is particularly important for the linearization about thermal equilibrium that we carry out in Sec. 6.5, since thermal equilibrium occurs at finite temperature.

Particle	b	T (μK)	$na^3(10^{-3})$	n_0/n	α	γ (s^{-1})
^{23}Na	0.1	1.0	0.004455	0.774	37.5875	133.901
^{23}Na	0.5	1.0	0.016904	0.952	175.291	133.901
^{23}Na	1.0	1.0	0.032401	0.974	343.738	133.901
^{23}Na	0.1	81.0	1.176625	0.377	6.63369	878523
^{23}Na	0.5	81.0	1.967583	0.698	20.5220	878523
^{23}Na	1.0	81.0	2.909002	0.787	34.1993	878523
^{87}Rb	0.1	0.1	0.006026	0.752	33.2949	17.4201
^{87}Rb	0.5	0.1	0.022161	0.945	153.828	17.4201
^{87}Rb	1.0	0.1	0.042232	0.970	300.812	17.4201
^{87}Rb	0.1	8.1	1.698619	0.360	6.15674	114293
^{87}Rb	0.5	8.1	2.682890	0.671	18.1373	114293
^{87}Rb	1.0	8.1	3.843073	0.760	29.4298	114293

Table 6.1: Sample of the parameter values that are used in generating the data sets for figures 6.4, 6.5 and tables 6.2, 6.3 and 6.4. The first three columns are specified while the remaining follow from the self-consistency equations.

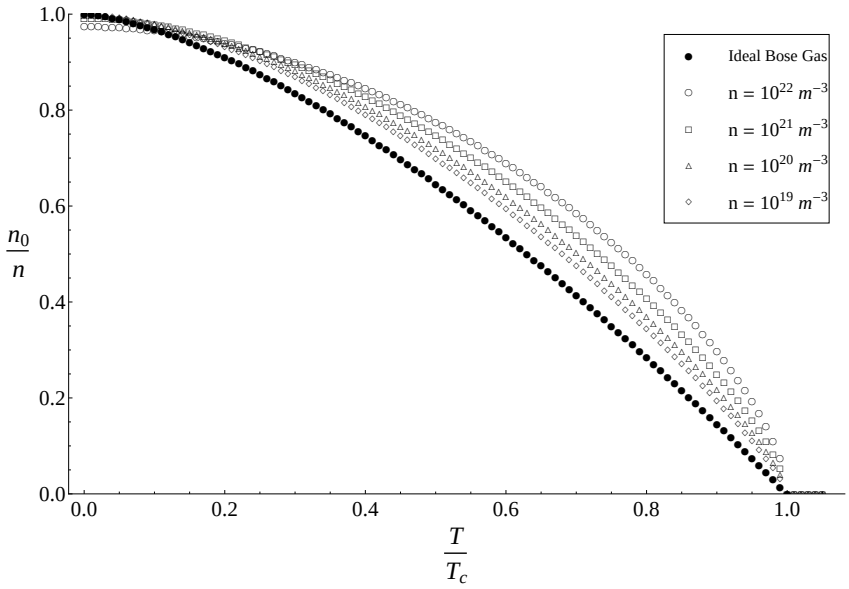

Figure 6.1: Condensate fraction versus temperature for different densities. The ideal Bose gas is the non-interacting or low density limit. Note that the temperature is scaled against the critical temperature, which is different for each density. This data is for ^{23}Na in the lower hyperfine state.

To match these up to an experiment, we must choose first the type of particle to fix a and m and to calculate ϵ_a. Then we would determine the density n and the temperature T that best describe the experiment. Eq. (6.3 must then be solved numerically for $\frac{\Delta}{\epsilon_a}$. This result can be used to find $b = \frac{\Delta}{k_B T}$ which is the key parameter in computation of the collision matrix. Finally, Eq. (6.4 is used to obtain $n_0 a^3$ which can be used to get the condensate fraction $\frac{n_0}{n}$ as well as α.

From a computational perspective, we choose a type of particle to get a and m and then choose values for b and $\frac{k_B T}{\epsilon_a}$. For reasons discussed in appendix A.9, it is important that these choices yield $na^3 \ll 1$. [59] From these we calculate the parameters α and γ that are needed to make predictions. We also look at $\frac{n_0}{n}$ to make sure that we are in a reasonable regime. To give numerical results, we compute data for two atomic species that are commonly used experimentally [52, 60], ^{23}Na in the lower hyperfine state with $a = 55a_0$ and ^{87}Rb in the lower hyperfine state with $a = 102a_0$ [61]. In these expressions, a_0 is the Bohr radius.

The linearized collision operator depends on the two parameters b and α. The matrix elements themselves all depend on b as it appears in the bogolon energy relation while α only acts as a coefficient on the $\mathcal{G}^{12}$ portion. While it may be more intuitive to specify the equilibrium state by n and T or some

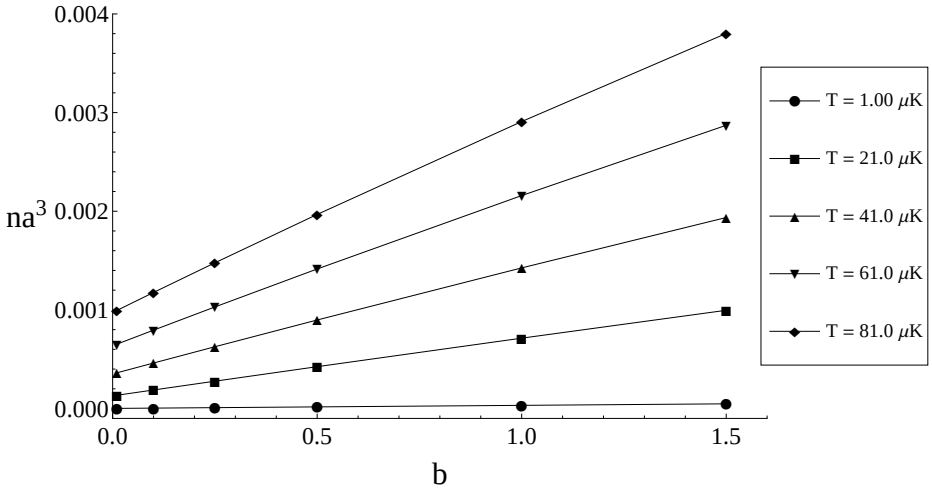

Figure 6.2: Dimensionless density versus dimensionless mean field to temperature ratio. The non-zero intercept on the vertical axis signifies the phase transition: temperature must be low enough and density must be high enough to allow a solution with $\Delta \neq 0$.

other pair, this would inevitably produce a different value of b for each choice, thus necessitating an entirely new matrix for each data point. To be economical, we instead choose several values of b and compute their corresponding matrices. We then choose several values for T that generate reasonable values of na^3 and n_0/n. The α values for these b and T pairs are found by using the self-consistency equations discussed in appendix A.9. Table 6.1 contains a sampling of parameters that were used to generate some of the data seen in the plots.

Figures 6.1 and 6.2 show two of the many possible plots that can be generated from the self-consistency equations. In figure 6.1 we choose to plot condensate fraction versus temperature. The temperature is scaled by the critical temperature for Bose-Einstein condensation for the ideal Bose gas. The "Ideal Bose Gas" curve is simply $1 - (T/T_C)^{3/2}$. Note that since T_C depends on the density n, each curve would occur at a much different scale on an absolute temperature axis. The effect of interactions is seen in the other four curves. At moderate temperatures, the condensate fraction is enhanced by interaction, while at low temperatures the condensate fraction is reduced. This low temperature effect is the well-known depletion of the condensate by interactions. [32, 55, 57, 58]

Figure 6.2 illustrates the procedure that must be taken to solve the self-consistency equations. For each chosen temperature, one obtains a curve for na^3 versus b. A desired value of na^3 gives a horizontal curve and the intersection point between these two curves gives the value of b. Not every

choice of T and na^3 will result in an intersection between these two curves. This indicates that there is a phase transition for the Bose gas. Above a certain temperature and below a certain density, there is no solution to the self-consistency equations and it is inconsistent to assume the presence of a condensate.

6.7 Calculation of Eigenvalues

In this section, we explain how we numerically obtain eigenvalues and eigenvectors from Eq. (6.51) and give the results of these calculations. For our calculations, we choose a midpoint method with an upper cutoff $c_{\max}$ for the quadrature scheme. Typically we set $c_{\max} = 15$ which captures the important features of the kernel and eigenvectors, though smaller values were used for some data sets. This scheme works well enough when the details of the eigenvectors are not known. A better quadrature scheme would concentrate more quadrature points where the eigenvectors have rapid variations.

In order to gauge the accuracy of the calculated eigenvalues we perform the discretization with matrix sizes N_Q of 500, 1000, 1500 and 2000. The eigenvalues that we report are found by performing a quadratic regression of the eigenvalue versus $1/N_Q$. This fit is then extrapolated to $1/N_Q = 0$ to find the best estimate of the eigenvalue and its estimated error, similar to the procedure illustrated in Fig. 5.3. Note that the reported error includes only this, and not errors that may arise from the numerical computation of the matrix elements $K_l(x_i, x_j)$. We compute these values using a Gauss-Kronrod (G3-K7) adaptive quadrature scheme with a value of 10^{-6} for the local relative tolerance [54]. The eigenvectors shown are from the largest matrix size $N_Q = 2000$.

Tables 6.2 and 6.3 show the computed eigenvalues for ^{23}Na at the temperatures of $T = 1$ μK and $T = 81$ μK, respectively. Calculations for ^{87}Rb are shown in Table 6.4. The value λ_M is the maximum discrete eigenvalue as discussed in section 2.4.

b	0.01	0.10	0.25	0.50	1.00	1.50
α	4.71521	37.5875	89.8281	175.291	343.738	510.248
λ_0^0	-0.16(53)	0.008(21)	0.0005(17)	-0.000064(11)	-0.00022(31)	-0.00035(50)
λ_0^1	2.09(30)	8.9664(27)	16.9935(23)	21.739(43)	20.668(46)	18.531(44)
λ_0^2	4.06(11)	14.179(23)	22.406(53)	26.440(11)	27.028(54)	24.902(34)
λ_1^0	-0.19(41)	0.004(19)	0.00001(45)	-0.00031(33)	-0.00043(61)	-0.00056(80)
λ_1^1	2.40(40)	8.327(13)	14.9693(16)	20.45(10)	22.080(16)	20.812(14)
λ_2^0	5.07(64)	8.90125(33)	8.58061(20)	7.359(24)	5.4926(25)	4.40442(35)
λ_M	16.96(17)	30.575(23)	33.88(12)	34.779(17)	32.530(25)	29.360(38)

Table 6.2: Numerical results for ^{23}Na with $a = 55a_0$ at $T = 1.0$ μK giving $\gamma = 133.9$ s^{-1}. Specific values of mean field to temperature ratio result in different dimensionless density, condensate fraction, $\mathcal{G}^{12}$ coefficient α and eigenvalues. The numbers in parentheses indicated the uncertainty in the last two digits, as found from the λ vs. $\frac{1}{N_Q}$ fitting procedure.

b	0.01	0.10	0.25	0.50	1.00	1.50
α	1.61983	6.63369	12.4435	20.5220	34.1993	45.9407
λ_0^0	-0.07(22)	0.0014(36)	0.00002(14)	-0.00011(15)	-0.00022(32)	-0.00034(50)
λ_0^1	1.23(12)	2.51317(71)	3.656180(80)	4.84983(50)	5.89098(95)	6.0961(15)
λ_0^2	2.754(27)	4.5453(33)	6.11473(28)	7.69000(76)	8.8345(16)	8.8718(24)
λ_1^0	-0.06(19)	0.0006(19)	-0.00025(31)	-0.00033(42)	-0.00043(61)	-0.00056(79)
λ_1^1	1.81(17)	2.9027(19)	3.81954(27)	4.78276(63)	5.67724(94)	5.9352(11)
λ_2^0	4.27(29)	4.4976(21)	4.0070058(54)	3.425(14)	2.84942(12)	2.58657(19)
λ_M	12.752(71)	13.7746(27)	14.482803(93)	13.93524(44)	12.43392(53)	11.5080(16)

Table 6.3: Numerical results for ^{23}Na with $a = 55a_0$ at $T = 81.0$ μK giving $\gamma = 8.785 \times 10^5$ s^{-1}. Specific values of mean field to temperature ratio result in different dimensionless density, condensate fraction, $\mathcal{G}^{12}$ coefficient α and eigenvalues. The numbers in parentheses indicated the uncertainty in the last two digits, as found from the λ vs. $\frac{1}{N_Q}$ fitting procedure.

For comparison, see the eigenvalues of the Uehling-Uhlenbeck equation in Table 5.1. The Uehling-Uhlenbeck equation describes a Bose gas that has no condensate fraction and therefore, all of our eigenvalues should converge to the Uehling-Uhlenbeck eigenvalues as Δ approaches zero. It is interesting that the bogolon eigenvalues as $\Delta \to 0$ and the U-U eigenvalues as $z \to 1$ appear to converge to the same values. Our treatment breaks down close to the critical point, and the uncertainties in the eigenvalues become large as the critical point is approached from above and below. The plots in Figs. 6.4 and 6.5 show the behavior of the bogolon eigenvalues as b is varied.

The rapid increase in the eigenvalues as Δ increases from zero is quite interesting. The first effect of the appearance of the condensate is a rapid increase in the rate of relaxation for perturbations. For

b	0.01	0.1	0.25	0.5	1.0	1.5
α	4.28606	33.2949	79.0967	153.828	300.812	445.860
λ_0^0	-0.15(49)	0.007(19)	0.0005(15)	-0.000071(30)	-0.00022(32)	-0.00035(50)
λ_0^1	1.98(28)	8.0779(27)	15.19159(86)	20.123(32)	19.495(43)	17.546(41)
λ_0^2	3.890(97)	12.855(20)	20.852(42)	24.427(23)	25.302(27)	23.393(17)
λ_1^0	-0.11(38)	0.004(11)	-0.00003(35)	-0.00031(35)	-0.00043(62)	-0.00056(80)
λ_1^1	2.32(37)	7.577(12)	13.4661(12)	18.5196(73)	20.331(12)	19.296(11)
λ_2^0	4.96(59)	8.34279(36)	7.98589(19)	6.848(24)	5.15730(25)	4.18163(33)
λ_M	16.35(16)	29.02(15)	31.929(28)	32.620(54)	30.3921(98)	27.43353(58)

Table 6.4: Numerical results for ^{87}Rb with $a = 102a_0$ at $T = 0.1$ μK giving $\gamma = 17.4201$ s^{-1}. Specific values of mean field to temperature ratio result in different dimensionless density, condensate fraction, $\mathcal{G}^{12}$ coefficient α and eigenvalues. The numbers in parentheses indicated the uncertainty in the last two digits, as found from the λ vs. $\frac{1}{N_Q}$ fitting procedure.

larger Δ we approach the strongly condensed regime with $n_0/n > 0.95$. Calculations in this regime become difficult, because the kernel functions composing the matrix elements $K_l(x_i, x_j)$ develop very sharp peaks, slowing the quadrature algorithm. However, this regime is well described by the Gross-Pitaevskii equation and other low-temperature approximations.

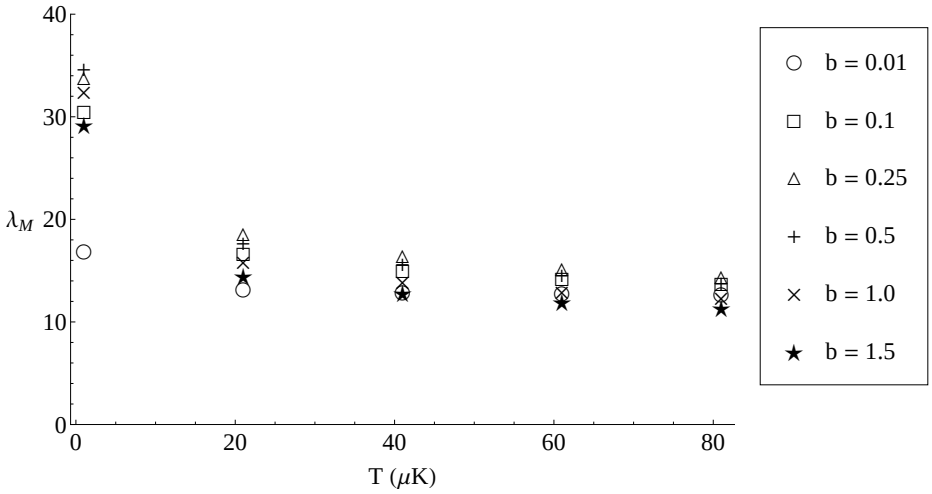

Figure 6.3: Largest discrete dimensionless eigenvalue λ_M versus temperature for different values of the dimensionless mean field to temperature ratio for ^{23}Na. The decrease with increasing temperature is largely due to the decrease in condensate density.

In Fig. 6.3 we see the dependence of λ_M as the temperature is varied for different values of b. Immediately we note that the value λ_M is quite a bit larger than for the Boltzmann and U-U

equations. This indicates that the gas as a whole relaxes much faster once a condensate appears. The discrete eigenvalues still appear to converge to this value, so we still consider it to represent the maximum discrete eigenvalue as it did for the Boltzmann and U-U equations. Note that the value λ_M first increases as b increases, reaches a maximum around $b = 0.5$ and then decreases. We currently do not have an explanation for this behavior, but it may be due to a competition between the effects of having a condensate present and the natural slowing caused by lowering the temperature. The physical processes at the root of this effect are difficult to discern because the parameter b depends implicitly on N_0 as well as temperature.

The eigenvectors shown in Figs. 6.6 and 6.7 for $b = 0.5$ already show interesting behavior. The behavior appears to be rapid oscillation up to a certain momentum, followed by an abrupt shift to slower oscillation. This may be related to the transition from a linear energy-momentum dispersion to a quadratic one. It may also be related to the behavior of the function $M(c)$. We have not fully investigated either of these possibilities. One confirmation of our expectations is that the numerically computed eigenvectors ψ_0^0 and ψ_1^0 match exactly with those predicted in Eqs. (6.54) and (6.55).

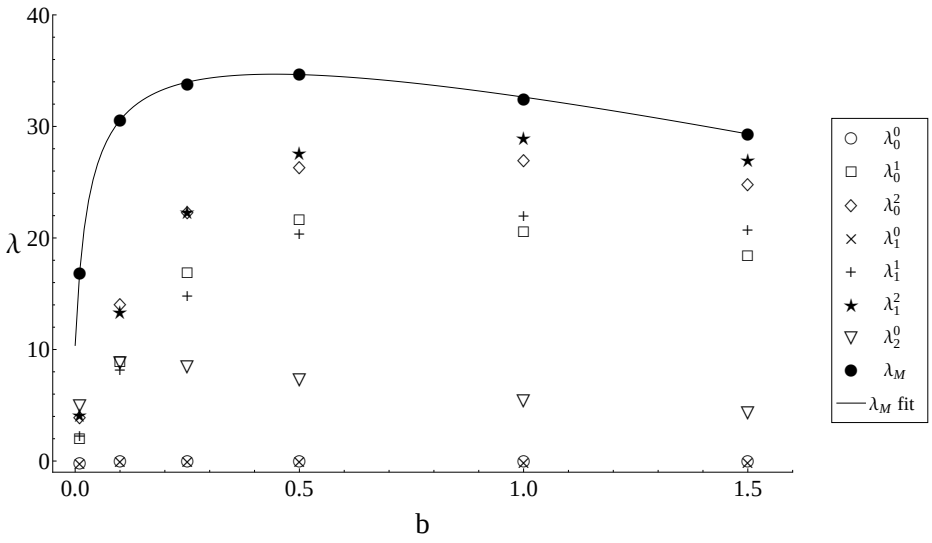

Figure 6.4: Several of the lower dimensionless eigenvalues versus the dimensionless mean field to temperature ration at $T = 1\mu K$ for ^{23}Na. Note the two zero eigenvalues corresponding to energy and momentum conservation. The line is an interpolation of the largest discrete eigenvalue.

6.8 Summary

We have derived a kinetic equation for the momentum distribution of Bogoliubov excitations (bogolons) in a spatially uniform condensed Bose gas using the self-consistent mean-field theory of Chapter 4. This kinetic equation conserves average total particle number, but does not conserve total bogolon number. It does conserves bogolon energy and momentum.

We find that there are three collision operators representing three different processes among bogolons: collision of two bogolons resulting in one and vice versa, elastic collision of two bogolons and collision of three bogolons resulting in one. The $2 \to 1$ collision integral is proportional to the number of condensed particles. The equilibrium distribution of bogolons is a Bose-Einstein distribution in bogolon energy, with the mean-field self-consistency equations relating the parameters of atomic species, density, condensate density, temperature and mean field strength.

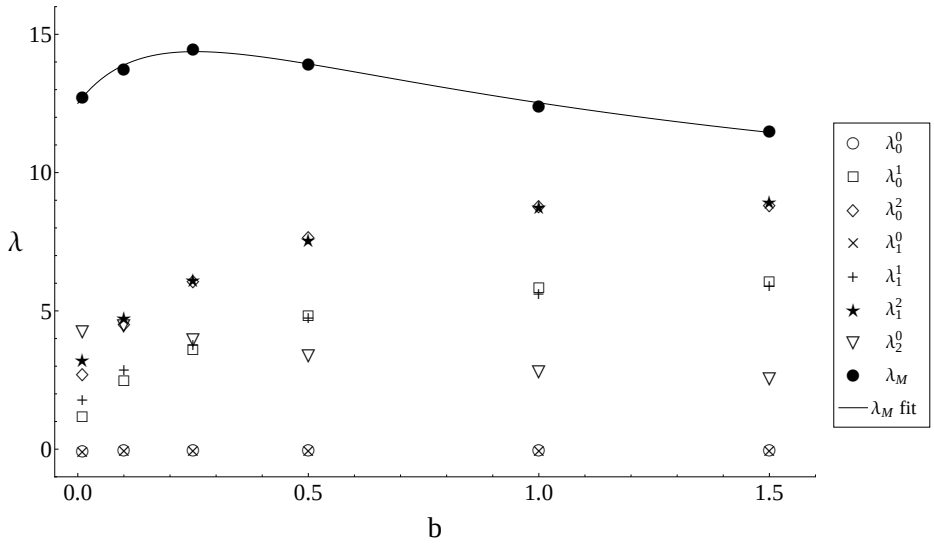

Figure 6.5: Several of the lower dimensionless eigenvalues versus the dimensionless mean field to temperature ratio at $T = 81\mu K$ for ^{23}Na. Note the two zero eigenvalues corresponding to energy and momentum conservation. The line is an interpolation of the largest discrete eigenvalue.

Linearizing the bogolon kinetic equation for small perturbations about equilibrium generates a linear integral equation which can be treated as an eigenvalue equation for the characteristic relaxation

eigenmodes and relaxation rates. We numerically compute the eigenvalues and eigenvectors of the associated matrix equation. These eigenvalues and eigenvectors give us a mode expansion for the relaxation of the momentum distribution to equilibrium. This can be used to make predictions about the behavior of the gas for a wide range of condensate fractions. This is advantageous since typical theoretical methods rely on the assumption of a strongly condensed gas with a condensate fraction approximately equal to unity.

We find that the presence of four zero eigenvalues supports only energy and momentum conservation for bogolons. The numerical associated eigenvectors exactly match the forms predicted by using the conservation law directly. The eigenvalues also seem to have the appropriate behavior as the mean field strength goes to zero. They all approach the same value, which is also the same value approached by the Uehling-Uhlenbeck eigenvalues as the fugacity approaches 1.

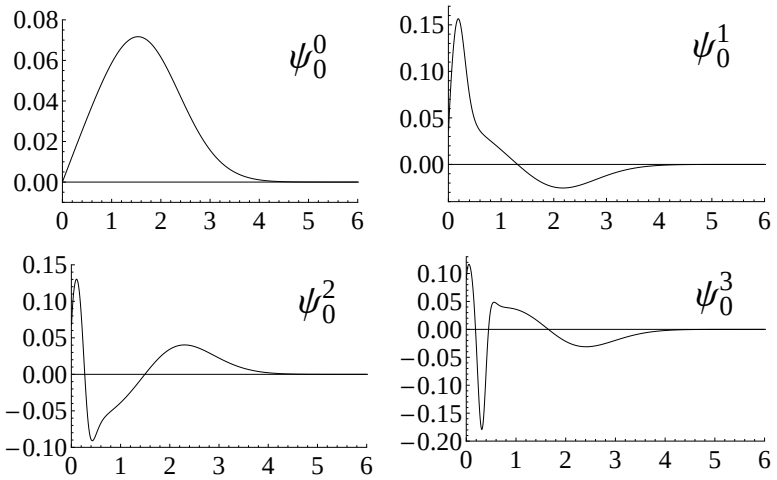

Figure 6.6: Plots of the first few $l = 0$ eigenvectors versus dimensionless momentum c. These plots are for ^{23}Na at $T = 1$ μK with $b = 0.5$.

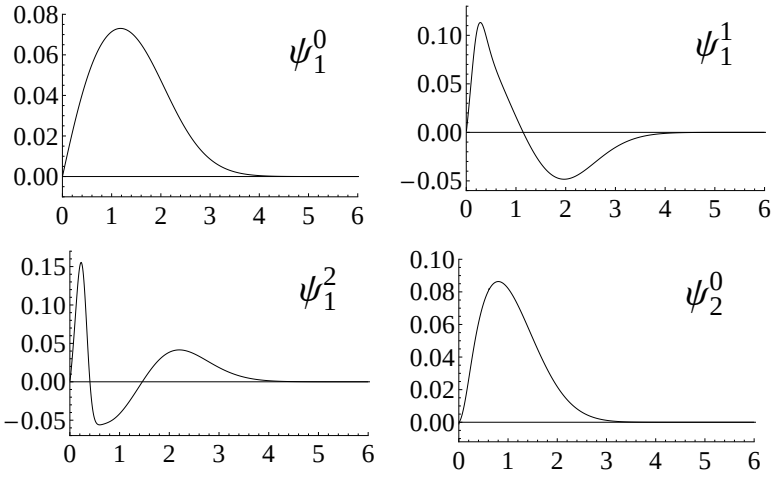

Figure 6.7: Plots of some higher order eigenvectors versus dimensionless momentum c. These plots are for ^{23}Na at $T = 1$ μK with $b = 0.5$.

7 Conclusions

In this report we have computed the characteristic relaxation rates and relaxation modes of a Bose gas in the classical regime, the quantum non-condensed regime and the condensed regime. Each of these regimes required us to use a different kinetic equation describing the evolution of the gas. In the classical regime, this equation was the Boltzmann equation and the quantum non-condensed regime it was the Uehling-Uhlenbeck equation. In the condensed regime, we derived a new kinetic equation describing the evolution of the momentum distribution for Bogoliubov excitations or bogolons. To the best of our knowledge, this bogolon kinetic equation is a new result.

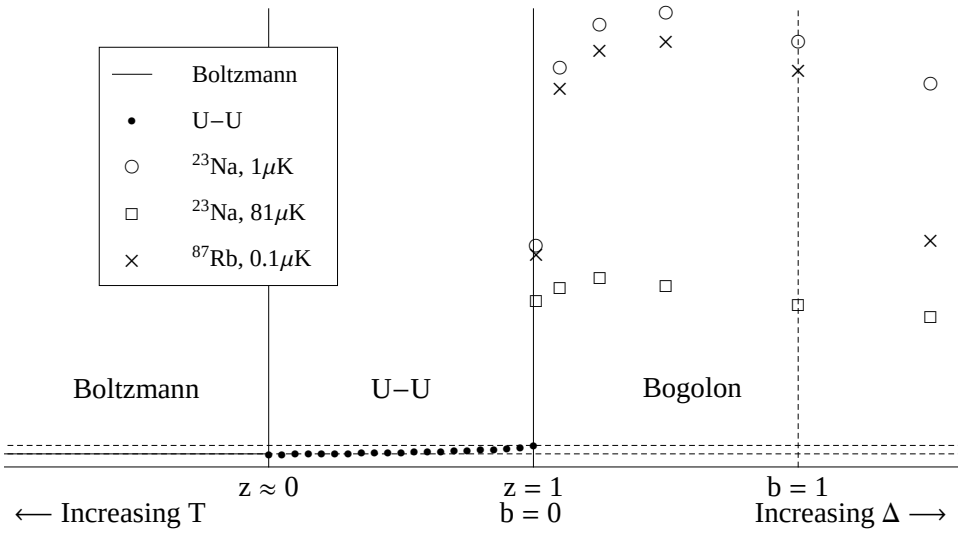

Figure 7.1: The behavior of the maximum discrete eigenvalue in the three regimes that were analyzed. Note that z never becomes zero, so the vertical line labeled $z \approx 0$ indicates the classical limit. The lower horizontal dashed line is at $\lambda_M = 1$ and the upper is $\lambda_M = \frac{\pi^2}{6}$. In the "Bogolon" regime, eigenvalues depend on particle species and temperature. Discrete eigenvalues fall between the plotted points and zero.

For each of these equations, we linearized its collision integral about its equilibrium distribution to generate a linearized evolution equation. These linearized evolution equations were converted into

matrix equations with a collision matrix containing the information from the linearized collision operator. We numerically computed the eigenvalues and eigenvectors of these collision matrices and showed how these results are related to the evolution of the gas.

The eigenvalues determine the rate at which the gas relaxes to equilibrium, with larger eigenvalues representing faster relaxation. In passing to the quantum regimes, the eigenvalues increase over their classical values. The gross behavior of the eigenvalues can be seen in figure 7.1. The eigenvalues of all three regimes match up with each other at the boundary points, indicating that our calculations are consistent with each other. As discussed in the introduction, the eigenvalues and eigenvectors are a bridge from the microscopic dynamics of the gas particles to the macroscopic behavior of the gas, such as transport coefficients.

Each collision matrix has a number of zero eigenvalues, with each zero eigenvalue corresponding to a conserved quantity in the system. For the Boltzmann and Uehling-Uhlenbeck equations, there were five zero eigenvalues, representing the five conserved quantities of particle number, momentum and energy. For the bogolon kinetic equation, the number of conserved quantities shrank to just four. The missing zero eigenvalue is due to the fact that bogolon number is not conserved in collision processes. Indeed, the bogolon kinetic equation contains terms where bogolons are created or destroyed by the collision process.

In Chapter 3, we "measured" the smallest non-zero eigenvalue of the collision operator for a hard sphere gas by performing a simulation containing 1000 particles by. The value we obtain agrees with the theoretical prediction, to within the error induced by fluctuations due to the small number of particles in the simulation. In Chapter 4 we developed a method for deriving self-consistent mean field kinetic equations beginning with the Hamiltonian of the interacting system.

In Chapter 5, we used the results of Chapter 4 to derive the Uehling-Uhlenbeck equation. We then proceeded to linearize it and derived explicit forms for its kernel functions, Q_{UU} and R_{UU} as functions of the fugacity z. We then computed the spectrum of eigenvalues and their eigenfunction. The eigenvalue spectrum of the U-U equations had the same form as it did for the linearized Boltzmann equation and the eigenfunctions appeared to be continuous and bounded for $0 \leq z < 1$. The eigenvalues (and therefore the relaxation rates) increased as z increased, but they remained bounded and also remained within an order of magnitude of their classical values. The increase in relaxation rates was

primarily due to the Bose enhancement factors of $1 + f_i(t)$ in the U-U equation which increased the scattering rate compared to the classical Boltzmann equation.

A second interesting result of Chapter 5 is that the eigenvalues appeared to remain finite and quite well behaved in the limit $z \to 1$. Since a Bose gas undergoes a phase transition when $z = 1$, we would expect a more interesting behavior of the eigenvalues. The absence of this behavior indicates that the U-U equation performs best as a refinement to the Boltzmann equation at the level of quantum corrections. It cannot accurately describe new processes that occur within quantum regime such as Bose-Einstein condensation or superfluidity. However, we find that initial distributions which are close to the quantum regime will relax to equilibrium at a much faster rate than if they were treated classically. We also conclude that spectrum of the linearized Uehling-Uhlenbeck equation predicts that distributions near to equilibrium will relax exponentially towards a Bose-Einstein equilibrium distribution.

In Chapter 6 we derived a kinetic equation for the momentum distribution of Bogoliubov excitations (bogolons) in a spatially uniform condensed Bose gas using the self-consistent mean-field theory of Chapter 4. This kinetic equation conserves average total particle number, but does not conserve total bogolon number. It does conserves bogolon energy and momentum.

We find that there are three collision operators representing three different processes among bogolons: collision of two bogolons resulting in one and vice versa, elastic collision of two bogolons and collision of three bogolons resulting in one. The $2 \to 1$ collision integral is proportional to the number of condensed particles. The equilibrium distribution of bogolons is a Bose-Einstein distribution in bogolon energy, with the mean-field self-consistency equations relating the parameters of atomic species, density, condensate density, temperature and mean field strength.

Linearizing the bogolon kinetic equation for small perturbations about equilibrium generates a linear integral equation which can be treated as an eigenvalue equation for the characteristic relaxation eigenmodes and relaxation rates. We numerically compute the eigenvalues and eigenvectors of the associated matrix equation. These eigenvalues and eigenvectors give us a mode expansion for the relaxation of the momentum distribution to equilibrium. This can be used to make predictions about the behavior of the gas for a wide range of condensate fractions. This is advantageous since typical theoretical methods rely on the assumption of a strongly condensed gas with a condensate fraction approximately equal to unity.

We find that the presence of four zero eigenvalues supports only energy and momentum conservation for bogolons. The numerical associated eigenvectors exactly match the forms predicted by using the conservation law directly. The eigenvalues also seem to have the appropriate behavior as the mean field strength goes to zero. They all approach the same value, which is also the same value approached by the Uehling-Uhlenbeck eigenvalues as the fugacity approaches 1.

Appendix A

Selected Proofs and Derivations

Here we present several proofs and derivations which are involved enough that they would disrupt the flow of the text.

A.1 Identities

In this section we state several mathematical identities which are used at various places throughout the report.

Spherical Harmonic Addition Theorem.

$$\sum_{m=-l}^{l} Y_l^{m*}(\hat{\mathbf{c}}_1) Y_l^m(\hat{\mathbf{c}}_2) = \frac{2l+1}{4\pi} P_l(\hat{\mathbf{c}}_1 \cdot \hat{\mathbf{c}}_2) \tag{A.1}$$

Definition of the Polylogarithm function.

$$\mathrm{Li}_s(z) = \sum_{j=1}^{\infty} \frac{z^j}{j^s}. \tag{A.2}$$

Evaluation of integrals leading to Polylogarithm functions.

$$\int_0^{\infty} \frac{z x^n}{e^x - z} dx = \Gamma(n+1)\mathrm{Li}_{n+1}(z) \tag{A.3}$$

Second order Polylogarithm identity.

$$\mathrm{Li}_2(z^2) = 2\mathrm{Li}_2(z) + 2\mathrm{Li}_2(-z) \tag{A.4}$$

Ordinary Generating Function for the Laguerre Polynomials.

$$\sum_{n=0}^{\infty} L_n^k(c^2)x^n = \frac{1}{(1-x)^{k+1}} e^{-\frac{xc^2}{1-x}} \tag{A.5}$$

Exponential Generating Function for the Legendre Polynomials.

$$\sum_{l=0}^{\infty} P_l(\hat{\mathbf{c}}_1 \cdot \hat{\mathbf{c}}_2)\frac{t^l}{l!} = \frac{1}{2\pi} e^{t\hat{\mathbf{c}}_1\cdot\hat{\mathbf{c}}_2} \int_0^{2\pi} e^{it|\hat{\mathbf{c}}_1\times\hat{\mathbf{c}}_2|\cos\phi} d\phi \tag{A.6}$$

Generalized Geometric Series.

$$\frac{1}{(1-A-B)^{\nu}} = \sum_{j=0}^{\infty}\sum_{k=0}^{\infty} \frac{\Gamma(\nu+j+k)}{\Gamma(\nu)j!k!} A^j B^k \tag{A.7}$$

Limit involving logarithm of a rational function.

$$\lim_{z\to 0} \frac{1}{z} \log\left(\frac{a-bz}{a-cz}\right) = \frac{c-b}{a} \tag{A.8}$$

A.2 Generating Functions of Collision Matrix Elements

In this section, we demonstrate how to obtain the matrix elements $C^l_{n,n'}$ analytically by using a generating function. For a formal introduction to the methods of generating functions, consult Wilf [62]. We begin with Eq. (2.31) and introduce a unnormalized matrix element $J^l_{n,n'}$ which is defined

$$\begin{aligned} J^l_{n,n'} = &\int d\mathbf{c}_1 d\mathbf{c}_2 e^{-c_1^2-c_2^2} c_1^l c_2^l L_n^{l+\frac{1}{2}}(c_1^2) L_{n'}^{l+\frac{1}{2}}(c_2^2) P_l(\hat{\mathbf{c}}_1\cdot\hat{\mathbf{c}}_2) \\ &\times \left(e^{c_2^2} M_{\mathrm{HS}}(\mathbf{c}_1)\delta^3(\mathbf{c}_1-\mathbf{c_2}) + \frac{1}{\pi^2} Q_{\mathrm{HS}}(\mathbf{c}_1,\mathbf{c}_2) - \frac{2}{\pi^2} R_{\mathrm{HS}}(\mathbf{c}_1,\mathbf{c}_2)\right) \end{aligned} \tag{A.9}$$

so that

$$C^l_{n,n'} = \frac{1}{4\pi}\sqrt{\frac{4n!n'!}{\Gamma(n+l+\frac{3}{2})\Gamma(n'+l+\frac{3}{2})}} J^l_{n,n'}. \tag{A.10}$$

The functions M_{HS}, Q_{HS} and R_{HS} are defined in Eqs. (2.23), (2.21) and (2.22). The generating function for $J^l_{n,n'}$ can be written

$$J(x,y;t) \equiv \sum_{n=0}^{\infty}\sum_{n'=0}^{\infty}\sum_{l=0}^{\infty} J^l_{n,n'} x^n y^{n'} \frac{t^l}{l!}. \tag{A.11}$$

Using the generating function identities (A.5) and (A.6) for the Laguerre and Legendre Polynomials, we obtain

$$J(x,y;t) = \frac{1}{2\pi\left[(1-x)(1-y)\right]^{\frac{3}{2}}}\int d\mathbf{c}_1\int d\mathbf{c}_2\int_0^{2\pi} d\phi e^{-c_1^2-c_2^2}e^{-\frac{xc_1^2}{1-x}-\frac{yc_2^2}{1-y}+\frac{t\mathbf{c}_1\cdot\mathbf{c}_2}{(1-x)(1-y)}}e^{\frac{it|\mathbf{c}_1\times\mathbf{c}_2|\cos\phi}{(1-x)(1-y)}} \\ \times\left(e^{c_2^2}M_{\rm HS}(\mathbf{c}_1)\delta^3(\mathbf{c}_1-\mathbf{c}_2)+\frac{1}{\pi^2}Q_{\rm HS}(\mathbf{c}_1,\mathbf{c}_2)-\frac{2}{\pi^2}R_{\rm HS}(\mathbf{c}_1,\mathbf{c}_2)\right). \tag{A.12}$$

For the hard sphere collision kernels $Q_{\rm HS}$ and $R_{\rm HS}$ the integrals in Eq. (A.12) can be done analytically. Using Eqs. (2.21), (2.22) and (2.23), we can obtain

$$J(x,y;t) = \pi^{3/2}\sqrt{2-x-y-t}\left(\frac{1}{(1-xy-t)^2}+1-\frac{2}{1-xy-t+\frac{t^2}{4}}\right) \tag{A.13}$$

The fact that $J(x,y;t)$ is symmetric in x and y confirms that the collision matrix is symmetric and that the functions $Q_{\rm HS}(\mathbf{c}_1,\mathbf{c}_2)$ and $R_{\rm HS}(\mathbf{c}_1,\mathbf{c}_2)$ are symmetric under interchange of $\mathbf{c}_1$ and $\mathbf{c}_2$. The generating function $J(x,y;t)$ can be expanded in a power series in parameters x, y and t. The coefficient of the term $x^n y^{n'} t^l$ is equal to $J^l_{n,n'}/l!$. Using the identity (A.7), we re-expand $J(x,y;t)$ in powers of x, y and t to obtain

$$J^l_{n,n'} = \frac{\pi}{\sqrt{2}}\sum_{j=0}^{n,n'}\sum_{k=0}^{l}\frac{\Gamma\left(-\frac{1}{2}+n+n'+l-2j-k\right)l!}{(n-j)!(n'-j)!(l-k)!2^{n+n'+l-2j-k}}B_j^k, \tag{A.14}$$

where $B_j^k = -\frac{(j+k+1)!}{j!k!}-\delta_{j0}\delta_{k0}+2\frac{(2j+k+1)!}{(2j+1)!k!2^k}$. Substituting back into Eq. (A.10), we obtain Eq. (2.32).

A.3 Relaxation Rates of the "Maxwell Molecules" Gas

For a Maxwell gas, the inter-particle potential is given by $V(r) = V_4\left(\frac{a}{r}\right)^4$ and the collision cross section for particles of mass m is given by $I(u,\theta) = \frac{a^2}{8}\sqrt{\frac{2V_4}{m}}\frac{1}{u}F(\theta)$, where

$$F(\theta) = \frac{4}{\sin\theta}\frac{\sqrt{\cos 2\psi}}{\sin 2\psi\left[\cos 2\psi E(\sin^2\psi)-\cos^2\psi K(\sin^2\psi)\right]} = \frac{2}{\sin\theta\sin^2 2\psi}\left(\frac{d\theta}{d\psi}\right)^{-1}. \tag{A.15}$$

The angle ψ is defined implicitly by the equation $\theta(\psi) = \pi - 2\sqrt{\cos 2\psi}K(\sin^2\psi)$. Here, K and E are complete elliptic integrals of the first and second kinds, respectively. Though this cross section is

complicated, the $\frac{1}{u}$ dependance results in $\chi_{n,l,m}$ (2.24) being the exact eigenfunctions of the collision operator in (2.16) for the Maxwell gas [1]. The collision matrix $C^l_{n,n'}$ is therefore diagonal and the eigenvalues can be written

$$\lambda^l_n = \frac{2\pi}{\tau_{\rm MM}} \int_0^\pi G^l_n(\theta) F(\theta) \sin\theta d\theta, \tag{A.16}$$

where

$$G^l_n(\theta) = 1 + \delta_{n,0}\delta_{l,0} - \cos^{2n+l}\left(\frac{\theta}{2}\right) P_l\left(\cos\frac{\theta}{2}\right) - \sin^{2n+l}\left(\frac{\theta}{2}\right) P_l\left(\sin\frac{\theta}{2}\right). \tag{A.17}$$

and $\frac{1}{\tau_{\rm MM}} = n_0 a^2 \sqrt{\frac{4V_4}{m}}$.

For the purposes of computation, we can use the fact that $F(\theta)$ is proportional to $\left(\frac{d\theta}{d\psi}\right)^{-1}$ and cancel this factor with a change of integration variables from θ to ψ. This results in

$$\lambda^l_n = \frac{4\pi}{\tau_{\rm MM}} \int_0^{\frac{\pi}{4}} \frac{G^l_n(\theta(\psi))}{\sin^2(2\psi)} d\psi \tag{A.18}$$

which is much better suited to numerical integration than Eq. (A.16).

For the Maxwell gas, the placement of the zero eigenvalues is the same as in the hard sphere case, meaning that particle number, momentum and energy are conserved. Below we list eigenvalues for the first few values of n and l, calculated using Eq. (A.18).

$$\lambda^0_{\rm MM} = \frac{1}{\tau_{\rm MM}} \Big(0, \quad 0, \quad 1.93796, \quad 2.90695, \quad 3.57015, \quad 4.08046, \quad 4.49834, \quad \cdots\Big) \tag{A.19}$$

$$\lambda^1_{\rm MM} = \frac{1}{\tau_{\rm MM}} \Big(0, \quad 1.93796, \quad 2.90695, \quad 3.57015, \quad 4.08046, \quad 4.49834, \quad 4.85402, \quad \cdots\Big) \tag{A.20}$$

$$\lambda^2_{\rm MM} = \frac{1}{\tau_{\rm MM}} \Big(2.90695, \quad 3.39144, \quad 3.90175, \quad 4.33562, \quad 4.70728, \quad 5.03186, \quad \cdots\Big) \tag{A.21}$$

Note that unlike the hard spheres eigenvalues, the Maxwell gas eigenvalues continue to increase without bound. The degeneracy of eigenvalues in $\lambda^0_{\rm MM}$ and $\lambda^1_{\rm MM}$ arises from the dependence of $G^l_n(\theta)$ on indices n and l.

A.4 Evaluation of the Functions $Q_{\rm UU}$ and $R_{\rm UU}$

In this appendix we outline the derivation of the analytic forms for the functions $Q_{\rm UU}$ and $R_{\rm UU}$ given in Eqs. (5.24) and (5.25). We also show that the classical (Boltzmann) limit of these functions gives in the classical results seen in Eqs. (2.50) and (2.51).

We here outline the steps to arrive at Eq. (5.24) from Eq. (5.21). We begin by defining a symmetric set of integration variables, $\mathbf{p} = \frac{1}{2}(\mathbf{c}_3 + \mathbf{c}_4)$ and $\mathbf{q} = \mathbf{c}_3 - \mathbf{c}_4$. In terms of these, Eq. (5.21) becomes

$$\begin{aligned} Q_{\rm UU}(\mathbf{c}_1, \mathbf{c}_2) = \int d\mathbf{p} d\mathbf{q} \delta^3 \left(\mathbf{c}_1 + \mathbf{c}_2 - 2\mathbf{p}\right) \delta(c_1^2 + c_2^2 - 2p^2 - \frac{q^2}{2}) \\ \times \left(1 + \frac{z}{e^{(\mathbf{p}+\frac{\mathbf{q}}{2})^2} - z}\right) \left(1 + \frac{z}{e^{(\mathbf{p}-\frac{\mathbf{q}}{2})^2} - z}\right). \end{aligned} \tag{A.22}$$

The delta functions cancel several of the integrals, leaving us with

$$Q_{\rm UU}(\mathbf{c}_1, \mathbf{c}_2) = \frac{q\pi}{4} \int_{-1}^{1} d\alpha \left(1 + \frac{z}{e^{p^2 + \frac{q^2}{4}} e^{pq\alpha} - z}\right) \left(1 + \frac{z}{e^{p^2 + \frac{q^2}{4}} e^{-pq\alpha} - z}\right) \tag{A.23}$$

where $p = \frac{1}{2}|\mathbf{c}_1 + \mathbf{c}_2|$, $q = |\mathbf{c}_1 - \mathbf{c}_2|$ and $\alpha = \hat{\mathbf{c}}_1 \cdot \hat{\mathbf{c}}_2$. Using a partial fractions expansion and performing the integration over α results in

$$Q_{\rm UU}(\mathbf{c}_1, \mathbf{c}_2) = \frac{\pi}{2} \frac{e^{2p^2 + \frac{q^2}{2}}}{e^{2p^2 + \frac{q^2}{2}} - z^2} \left(\frac{1}{p} \log\left(\frac{e^{p^2 + pq + \frac{q^2}{4}} - z}{e^{p^2 - pq + \frac{q^2}{4}} - z}\right) - q\right). \tag{A.24}$$

Re-writing this in terms of $\mathbf{c}_1$ and $\mathbf{c}_2$ gives us Eq. (5.24). The function $Q_{\rm UU}$ is manifestly symmetric in an interchange of $\mathbf{c}_1$ and $\mathbf{c}_2$. In the classical limit when $z \to 0$, we can just replace z by zero in the expression for $Q_{\rm UU}$. The result simplifies to the classical expression for hard spheres,

$$Q_{\rm HS}(\mathbf{c}_1, \mathbf{c}_2) = \frac{\pi}{2} |\mathbf{c}_1 - \mathbf{c}_2|. \tag{A.25}$$

For evaluation of the function $R_{\rm UU}$ from Eq. (5.25), we again express the integration in terms of

$\mathbf{p}$ and $\mathbf{q}$, giving

$$\begin{aligned} R_{\mathrm{UU}}(\mathbf{c}_1,\mathbf{c}_2) =& \frac{1}{z}e^{c_2^2}\int d\mathbf{p}d\mathbf{q}\delta^3\left(\mathbf{c}_1-\mathbf{c}_2+\mathbf{q}\right)\delta(c_1^2-c_2^2+2\mathbf{p}\cdot\mathbf{q}) \\ &\times\frac{z}{e^{(\mathbf{p}+\frac{1}{2}\mathbf{q})^2}-z}\left(1+\frac{z}{e^{(\mathbf{p}-\frac{1}{2}\mathbf{q})^2}-z}\right). \end{aligned} \tag{A.26}$$

It is easiest to evaluate the $\mathbf{q}$ integration first and then evaluate the $\mathbf{p}$ integration in cylindrical coordinates with the z-axis oriented in the direction of $\mathbf{q}$. After doing this, we obtain

$$R_{\mathrm{UU}}(\mathbf{c}_1,\mathbf{c}_2)=\frac{\pi}{qz}e^{c_2^2}\int_0^\infty p_\rho dp_\rho\left(1+\frac{z}{e^{p_\rho^2+p_z^2+\frac{q^2}{4}-p_zq}-z}\right)\frac{z}{e^{p_\rho^2+p_z^2+\frac{q^2}{4}+p_zq}-z} \tag{A.27}$$

where $p_z=\frac{c_2^2-c_1^2}{2q}$ and $q=|\mathbf{c}_1-\mathbf{c}_2|$.

The remaining integral over p_ρ can be evaluated by defining $u=e^{p_\rho^2}$ and using a partial fractions expansion. Rewriting this result in terms of $\mathbf{c}_1$ and $\mathbf{c}_2$ gives us Eq. (5.25). This equation is also symmetric under interchange of $\mathbf{c}_1$ and $\mathbf{c}_2$. In the $z\to 0$ limit we cannot simply replace z in Eq. (5.25) by zero due to the appearance of z in the denominator. A quick inspection reveals that the numerator also goes to zero as z approaches zero. Using the identity (A.8) applied to the logarithm in Eq. (5.25), we find that

$$R_{\mathrm{UU}}(\mathbf{c}_1,\mathbf{c}_2)=\frac{\pi}{2z|\mathbf{c}_1-\mathbf{c}_2|(e^{-c_1^2}-e^{-c_2^2})}\left[e^{\frac{|\mathbf{c}_1\times\mathbf{c}_2|^2}{(\mathbf{c}_1-\mathbf{c}_2)^2}}\left(e^{-c_1^2}-e^{-c_2^2}\right)z+O(z^2)\right] \tag{A.28}$$

which is indeed equal to the classical result for hard spheres.

$$R_{\mathrm{HS}}(\mathbf{c}_1,\mathbf{c}_2)=\frac{\pi}{2|\mathbf{c}_1-\mathbf{c}_2|}e^{\frac{|\mathbf{c}_1\times\mathbf{c}_2|^2}{(\mathbf{c}_1-\mathbf{c}_2)^2}}. \tag{A.29}$$

A.5 Maximum Discrete Eigenvalue λ_M for the U-U Equation

The value λ_M is the maximum discrete eigenvalue for hard sphere collision operators and is conjectured to be equal to the minimum of the function $M_{\mathrm{UU}}(c)$ (5.23) for the Uehling-Uhlenbeck equation. This conjecture is a proven fact for the Boltzmann equation and the minimum of $M_{\mathrm{HS}}(c)$ (2.23) is simply 1. In this appendix, we outline the steps necessary to obtain Eq. (5.33). From Fig. 5.2 we can see that the minimum of M_{UU} still occurs at $c=0$.

We begin the calculation with the definition,

$$\lambda_M(z) = M_{\mathrm{UU}}(0). \tag{A.30}$$

After substituting in from Eqs. (5.12), (5.24), (5.29) and (5.23) we get

$$\lambda_M(z) = \frac{1-z}{z}\int_0^\infty dc_2 c_2^2 \frac{z}{e^{c_2^2}-z}\int_{-1}^{1} d(\cos\theta) P_0(\cos\theta)\frac{e^{c_2^2}}{e^{c_2^2}-z^2}\left(\frac{2}{c_2}\log\left(\frac{e^{c_2^2}-z}{1-z}\right)-c_2\right). \tag{A.31}$$

The integral over θ is trivial and the integral over c_2 can be evaluated analytically in terms of the polylogarithm function $\mathrm{Li}_2(z)$ (see Eq. (A.3). The result is

$$\lambda_M(z) = \frac{1}{z}\left[-2\mathrm{Li}_2(-z) - \mathrm{Li}_2(z) + \mathrm{Li}_2(z^2)\right] \tag{A.32}$$

Using the identity (A.4) which can be easily proved from the definition (A.2), this simplifies to

$$\lambda_M(z) = \frac{\mathrm{Li}_2(z)}{z}. \tag{A.33}$$

Figures 5.4 and 5.5 show a plot of $\lambda_M(z)$ along with several of the Uehling-Uhlenbeck eigenvalues.

A.6 Details of the Uehling-Uhlenbeck Derivation

In this section, we describe the method necessary to go from Eq. (5.5) to Eq. (5.7). Let us begin by again looking at Eq. (5.5).

$$\begin{aligned}\frac{dN_i}{dt} =& \frac{g^2}{4V^2\hbar^2}\sum_{1,2,3,4}\sum_{5,6,7,8}\delta_{1+2,3+4}\delta_{5+6,7+8} \\ &\times\int_{-\infty}^{0} ds \mathrm{Tr}\left(\rho_0[\hat{a}_1^\dagger\hat{a}_2^\dagger\hat{a}_3\hat{a}_4,[\hat{a}_i^\dagger(s)\hat{a}_i(s),\hat{a}_5^\dagger(s)\hat{a}_6^\dagger(s)\hat{a}_7(s)\hat{a}_8(s)]]\right).\end{aligned} \tag{A.34}$$

The first step in simplifying this is to work out the inner commutator. We can write this in a concise form as

$$[\hat{a}_i^\dagger(s)\hat{a}_i(s),\hat{a}_5^\dagger(s)\hat{a}_6^\dagger(s)\hat{a}_7(s)\hat{a}_8(s)] = (\delta_{i,5}+\delta_{i,6}-\delta_{i,7}-\delta_{i,8})\hat{a}_5^\dagger(s)\hat{a}_6^\dagger(s)\hat{a}_7(s)\hat{a}_8(s). \tag{A.35}$$

Since we are using the Hamiltonian $\hat{H}^0$ defined in Eq. (5.1), we can use Eq. (5.6) for the s-evolution of the particle operators. Doing this, we obtain

$$\begin{aligned}\frac{dN_i}{dt} =& \frac{g^2}{4V^2\hbar^2}\sum_{1,2,3,4}\sum_{5,6,7,8}\delta_{1+2,3+4}\delta_{5+6,7+8}(\delta_{i,5}+\delta_{i,6}-\delta_{i,7}-\delta_{i,8}) \\ &\times\int_{-\infty}^{0} ds e^{-i(\epsilon_5+\epsilon_6-\epsilon_7-\epsilon_8)s/\hbar}\mathrm{Tr}\left(\rho_0[\hat{a}_1^\dagger\hat{a}_2^\dagger\hat{a}_3\hat{a}_4,\hat{a}_5^\dagger\hat{a}_6^\dagger\hat{a}_7\hat{a}_8]\right).\end{aligned} \tag{A.36}$$

The next step is to work out the final commutator and put the result in normal order, that is, all $\hat{a}_i^\dagger$ appear on the left and all $\hat{a}_i$ appear on the right. This step is quite tedious and generates several terms that do not contribute to the final result. We will simply give the results of this step which is

$$\begin{aligned}\frac{dN_i}{dt} =& \frac{g^2}{4V^2\hbar^2}\sum_{1,2,3,4}\delta_{1+2,3+4}^2(\delta_{i,4}+\delta_{i,3}-\delta_{i,2}-\delta_{i,1}) \\ &\times\int_{-\infty}^{0} ds e^{-i(\epsilon_5+\epsilon_6-\epsilon_7-\epsilon_8)s/\hbar}\left[4(N_1N_2(1+N_3)(1+N_4)-(1+N_1)(1+N_2)N_3N_4)\right]\end{aligned} \tag{A.37}$$

Finally, we can perform the final delta functions to obtain

$$\begin{aligned}\frac{dN_i}{dt} = \frac{g^2}{V^2\hbar^2}\int_{-\infty}^{0} ds\Big[& \\ &\sum_{1,2,3}\delta_{1+2,3+i}^2 e^{-i(\epsilon_i+\epsilon_3-\epsilon_2-\epsilon_1)s/\hbar}\left[N_1N_2(1+N_3)(1+N_i)-(1+N_1)(1+N_2)N_3N_i\right] \\ &+\sum_{1,2,4}\delta_{1+2,i+4}^2 e^{-i(\epsilon_4+\epsilon_i-\epsilon_2-\epsilon_1)s/\hbar}\left[N_1N_2(1+N_i)(1+N_4)-(1+N_1)(1+N_2)N_iN_4\right] \\ &-\sum_{1,3,4}\delta_{1+i,3+4}^2 e^{-i(\epsilon_4+\epsilon_3-\epsilon_i-\epsilon_1)s/\hbar}\left[N_1N_i(1+N_3)(1+N_4)-(1+N_1)(1+N_i)N_3N_4\right] \\ &-\sum_{2,3,4}\delta_{i+2,3+4}^2 e^{-i(\epsilon_4+\epsilon_3-\epsilon_2-\epsilon_i)s/\hbar}\left[N_iN_2(1+N_3)(1+N_4)-(1+N_i)(1+N_2)N_3N_4\right]\Big]\end{aligned} \tag{A.38}$$

The last step which is often needed is the rename the summation indices so that the terms can be combined. The choice of what to rename requires some intuition about the symmetries of the terms. For example, we rename $1\to 4$, $2\to 3$ and $4\to 2$ in the second term. Doing this, we can combine terms to obtain an integral of the form $\int_0^\infty ds\left(e^{iEs/\hbar}+e^{-iEs/\hbar}\right)$ which is equal to $2\pi\hbar\delta(E)$. Upon doing

this, we finally obtain

$$\frac{dN_i}{dt} = \frac{4\pi g^2}{V^2\hbar} \sum_{2,3,4} \delta^2_{i+2,3+4} \delta(\epsilon_i + \epsilon_2 - \epsilon_3 - \epsilon_4) \left[(1+N_i)(1+N_2)N_3 N_4 - N_i N_2 (1+N_3)(1+N_4) \right], \quad \text{(A.39)}$$

which is the result given in Eq. (5.7).

A.7 Bogolon Collision Operators

In this appendix, we give explicit forms for the collision operators $\mathcal{C}$ and $\mathcal{D}$ found in Eqs. (6.18) and (6.19). To generate the kinetic equations for the quantities N_i and Λ_i, we use Eq. (4.39) to get

$$\begin{aligned} \frac{dN_i}{dt} =& \frac{g^2}{4\hbar^2 V^2} \sum_{1,2,3,4} \sum_{5,6,7,8} \delta_{1+2,3+4} \delta_{5+6,7+8} \\ & \times \int_{-\infty}^{0} ds \langle [\hat{a}_1^\dagger \hat{a}_2^\dagger \hat{a}_3 \hat{a}_4, [\hat{a}_i^\dagger(s) \hat{a}_i(s), \hat{a}_5^\dagger(s) \hat{a}_6^\dagger(s) \hat{a}_7(s) \hat{a}_8(s)]] \rangle \end{aligned} \quad \text{(A.40)}$$

and

$$\begin{aligned} \frac{d\Lambda_i}{dt} =& \frac{g^2}{8\hbar^2 V^2} \sum_{1,2,3,4} \sum_{5,6,7,8} \delta_{1+2,3+4} \delta_{5+6,7+8} \\ & \times \int_{-\infty}^{0} ds \langle [\hat{a}_1^\dagger \hat{a}_2^\dagger \hat{a}_3 \hat{a}_4, [\hat{a}_i^\dagger(s) \hat{a}_{-i}^\dagger(s), \hat{a}_5^\dagger(s) \hat{a}_6^\dagger(s) \hat{a}_7(s) \hat{a}_8(s)]] \rangle \\ & + \frac{g^2}{8\hbar^2 V^2} \sum_{1,2,3,4} \sum_{5,6,7,8} \delta_{1+2,3+4} \delta_{5+6,7+8} \\ & \times \int_{-\infty}^{0} ds \langle [\hat{a}_1^\dagger \hat{a}_2^\dagger \hat{a}_3 \hat{a}_4, [\hat{a}_{-i}(s) \hat{a}_i(s), \hat{a}_5^\dagger(s) \hat{a}_6^\dagger(s) \hat{a}_7(s) \hat{a}_8(s)]] \rangle \end{aligned} \quad \text{(A.41)}$$

The calculation of the commutations and traces in Eqs. (A.40) and (A.41) is quite arduous. Not only must we perform the same steps as in appendix A.6, but the particles operators must be expressed in terms of bogolon operators at the outset. To speed up the process, we developed a custom symbolic algebra code. The primary capabilities of this code are storage and manipulation of large expressions containing both operators and c-number variables. The specific manipulations that the code is capable

of include expanding commutators and expectation values, performing sums over Kronecker delta functions and permuting indices to recombine terms in a compact form. More details on this code can be found in appendix B. The code then generates an output file containing an algebraic expression that is anywhere from 70 to 500 terms long. The final simplification and factorization must be done by hand. Following this process, we obtain the Eq. (6.18) with

$$\begin{aligned}\mathcal{C}_1^{12}\{\mathcal{N}\} =&\frac{4\pi N_0 g^2}{\hbar V^2}\sum_{2,3}{}'\delta_{1,2+3}\delta(\mathcal{E}_1-\mathcal{E}_2-\mathcal{E}_3)W^{12}_{3,2,1}\\ &\times\left[\Upsilon^A_{1,2,3}(\mathcal{F}_1\mathcal{N}_2\mathcal{N}_3-\mathcal{N}_1\mathcal{F}_2\mathcal{F}_3)+\tilde{\Upsilon}^A_{1,2,3}(\mathcal{F}_{-1}\mathcal{N}_{-2}\mathcal{N}_{-3}-\mathcal{N}_{-1}\mathcal{F}_{-2}\mathcal{F}_{-3})\right]\\ &+\frac{8\pi N_0 g^2}{\hbar V^2}\sum_{2,3}{}'\delta_{1+2,3}\delta(\mathcal{E}_1+\mathcal{E}_2-\mathcal{E}_3)W^{12}_{1,2,3}\\ &\times\left[\Upsilon^B_{1,2,3}(\mathcal{F}_1\mathcal{F}_2\mathcal{N}_3-\mathcal{N}_1\mathcal{N}_2\mathcal{F}_3)+\tilde{\Upsilon}^B_{1,2,3}(\mathcal{F}_{-1}\mathcal{F}_{-2}\mathcal{N}_{-3}-\mathcal{N}_{-1}\mathcal{N}_{-2}\mathcal{F}_{-3})\right],\end{aligned} \tag{A.42}$$

$$\begin{aligned}\mathcal{C}_1^{22}\{\mathcal{N}\} =&\frac{4\pi g^2}{\hbar V^2}\sum_{2,3,4}{}'\delta_{1+2,3+4}\delta(\mathcal{E}_1+\mathcal{E}_2-\mathcal{E}_3-\mathcal{E}_4)W^{22}_{1,2,3,4}\\ &\times\left[\Upsilon^C_{1,2,3,4}(\mathcal{F}_1\mathcal{F}_2\mathcal{N}_3\mathcal{N}_4-\mathcal{N}_1\mathcal{N}_2\mathcal{F}_3\mathcal{F}_4)-\tilde{\Upsilon}^C_{1,2,3,4}(\mathcal{F}_{-1}\mathcal{F}_{-2}\mathcal{N}_{-3}\mathcal{N}_{-4}-\mathcal{N}_{-1}\mathcal{N}_{-2}\mathcal{F}_{-3}\mathcal{F}_{-4})\right]\end{aligned} \tag{A.43}$$

and

$$\begin{aligned}\mathcal{C}_1^{31}\{\mathcal{N}\} =&\frac{4\pi g^2}{3\hbar V^2}\sum_{2,3,4}{}'\delta_{1,2+3+4}\delta(\mathcal{E}_1-\mathcal{E}_2-\mathcal{E}_3-\mathcal{E}_4)W^{31}_{1,2,3,4}\\ &\times\left[\Upsilon^D_{1,2,3,4}(\mathcal{F}_1\mathcal{N}_2\mathcal{N}_3\mathcal{N}_4-\mathcal{N}_1\mathcal{F}_2\mathcal{F}_3\mathcal{F}_4)-\tilde{\Upsilon}^D_{1,2,3,4}(\mathcal{F}_{-1}\mathcal{N}_{-2}\mathcal{N}_{-3}\mathcal{N}_{-4}-\mathcal{N}_{-1}\mathcal{F}_{-2}\mathcal{F}_{-3}\mathcal{F}_{-4})\right]\\ &+\frac{4\pi g^2}{\hbar V^2}\sum_{2,3,4}{}'\delta_{1+2+3,4}\delta(\mathcal{E}_1+\mathcal{E}_2+\mathcal{E}_3-\mathcal{E}_4)W^{31}_{4,3,2,1}\\ &\times\left[\Upsilon^E_{1,2,3,4}(\mathcal{F}_1\mathcal{F}_2\mathcal{F}_3\mathcal{N}_4-\mathcal{N}_1\mathcal{N}_2\mathcal{N}_3\mathcal{F}_4)-\tilde{\Upsilon}^E_{1,2,3,4}(\mathcal{F}_{-1}\mathcal{F}_{-2}\mathcal{F}_{-3}\mathcal{N}_{-4}-\mathcal{N}_{-1}\mathcal{N}_{-2}\mathcal{N}_{-3}\mathcal{F}_{-4})\right]\end{aligned} \tag{A.44}$$

where

$$\Upsilon^{A}_{1,2,3} = u_1u_2u_3 - u_1v_2u_3 - u_1u_2v_3 \tag{A.45}$$

$$\Upsilon^{B}_{1,2,3} = u_1u_2u_3 + u_1v_2v_3 - u_1v_2u_3 \tag{A.46}$$

$$\Upsilon^{C}_{1,2,3,4} = u_1u_2u_3u_4 + u_1v_2v_3u_4 + u_1v_2u_3v_4 \tag{A.47}$$

$$\Upsilon^{D}_{1,2,3,4} = u_1v_2u_3u_4 + u_1u_2v_3u_4 + u_1u_2u_3v_4 \tag{A.48}$$

$$\Upsilon^{E}_{1,2,3,4} = u_1u_2v_3u_4 + u_1v_2u_3u_4 + u_1v_2v_3v_4 \tag{A.49}$$

and $\tilde{\Upsilon}$ is Υ with each u and v interchanged.

For Λ_i we obtain Eq. (6.19) with

$$\begin{aligned}\mathcal{D}^{12}_1\{\mathcal{N}\} =& -\frac{4\pi N_0 g^2}{\hbar V^2}{\sum_{2,3}}'\delta(\mathcal{E}_1+\mathcal{E}_2-\mathcal{E}_3)\delta_{1+2,3}W^{12}_{1,2,3}\Omega^{A}_{1,2,3}\\ &\times(\mathcal{F}_1\mathcal{F}_2\mathcal{N}_3-\mathcal{N}_1\mathcal{N}_2\mathcal{F}_3+\mathcal{F}_{-1}\mathcal{F}_{-2}\mathcal{N}_{-3}-\mathcal{N}_{-1}\mathcal{N}_{-2}\mathcal{F}_{-3})\\ &+\frac{2\pi N_0 g^2}{\hbar V^2}{\sum_{2,3}}'\delta(\mathcal{E}_1-\mathcal{E}_2-\mathcal{E}_3)\delta_{1,2+3}W^{12}_{3,2,1}\Omega^{B}_{1,2,3}\\ &\times(\mathcal{F}_1\mathcal{N}_2\mathcal{N}_3-\mathcal{N}_1\mathcal{F}_2\mathcal{F}_3+\mathcal{F}_{-1}\mathcal{N}_{-2}\mathcal{N}_{-3}-\mathcal{N}_{-1}\mathcal{F}_{-2}\mathcal{F}_{-3}),\end{aligned} \tag{A.50}$$

$$\begin{aligned}\mathcal{D}^{22}_1\{\mathcal{N}\} =&\frac{2\pi g^2}{\hbar V^2}{\sum_{2,3,4}}'\delta(\mathcal{E}_1+\mathcal{E}_2-\mathcal{E}_3-\mathcal{E}_4)\delta_{1+2,3+4}W^{22}_{1,2,3,4}\Omega^{C}_{1,2,3,4}\\ &\times(\mathcal{F}_1\mathcal{F}_2\mathcal{N}_3\mathcal{N}_4-\mathcal{N}_1\mathcal{N}_2\mathcal{F}_3\mathcal{F}_4+\mathcal{F}_{-1}\mathcal{F}_{-2}\mathcal{N}_{-3}\mathcal{N}_{-4}-\mathcal{N}_{-1}\mathcal{N}_{-2}\mathcal{F}_{-3}\mathcal{F}_{-4})\end{aligned} \tag{A.51}$$

and

$$\begin{aligned}\mathcal{D}^{31}_1\{\mathcal{N}\} =& -\frac{2\pi g^2}{3\hbar V^2}{\sum_{2,3,4}}'\delta(\mathcal{E}_1-\mathcal{E}_2-\mathcal{E}_3-\mathcal{E}_4)\delta_{1,2+3+4}W^{31}_{1,2,3,4}\Omega^{D}_{1,2,3,4}\\ &\times(\mathcal{F}_1\mathcal{N}_2\mathcal{N}_3\mathcal{N}_4-\mathcal{N}_1\mathcal{F}_2\mathcal{F}_3\mathcal{F}_4+\mathcal{F}_{-1}\mathcal{N}_{-2}\mathcal{N}_{-3}\mathcal{N}_{-4}-\mathcal{N}_{-1}\mathcal{F}_{-2}\mathcal{F}_{-3}\mathcal{F}_{-4})\\ &+\frac{2\pi g^2}{\hbar V^2}{\sum_{2,3,4}}'\delta(\mathcal{E}_1+\mathcal{E}_2+\mathcal{E}_3-\mathcal{E}_4)\delta_{1+2+3,4}W^{31}_{4,3,2,1}\Omega^{E}_{1,2,3,4}\\ &\times(\mathcal{F}_1\mathcal{F}_2\mathcal{F}_3\mathcal{N}_4-\mathcal{N}_1\mathcal{N}_2\mathcal{N}_3\mathcal{F}_4+\mathcal{F}_{-1}\mathcal{F}_{-2}\mathcal{F}_{-3}\mathcal{N}_{-4}-\mathcal{N}_{-1}\mathcal{N}_{-2}\mathcal{N}_{-3}\mathcal{F}_{-4})\end{aligned} \tag{A.52}$$

where

$$\Omega^A_{1,2,3} = u_1v_2v_3 + v_1v_2v_3 - v_1v_2u_3 + v_1u_2u_3 + u_1u_2u_3 - u_1u_2v_3 \tag{A.53}$$

$$\Omega^B_{1,2,3} = v_1v_2u_3 - u_1v_2v_3 + u_1u_2v_3 + u_1v_2u_3 + v_1u_2v_3 - v_1u_2u_3 \tag{A.54}$$

$$\Omega^C_{1,2,3,4} = u_1v_2v_3v_4 + u_1u_2v_3u_4 + u_1u_2u_3v_4 - v_1v_2v_3u_4 - v_1u_2u_3u_4 - v_1v_2u_3v_4 \tag{A.55}$$

$$\Omega^D_{1,2,3,4} = v_1v_2u_3u_4 + v_1u_2v_3u_4 + v_1u_2u_3v_4 - u_1u_2v_3v_4 - u_1v_2u_3v_4 - u_1v_2v_3u_4 \tag{A.56}$$

$$\Omega^E_{1,2,3,4} = u_1u_2u_3u_4 + u_1v_2u_3v_4 + u_1v_2u_3v_4 - v_1u_2v_3u_4 - v_1u_2v_3u_4 - v_1v_2v_3v_4. \tag{A.57}$$

When these two results are combined using Eq. (6.13), we obtain Eq. (6.20).

A.8 Bogolon Collision Kernels

In this appendix, we show a method of calculating the kernel function $Q^l_A(c_1, c_2)$ as seen in Eq. (6.41). We give expressions for the five other kernel functions: R_A, Q_B, Q_C, T_A and T_B. Throughout this appendix we use the notation $b = \Delta/(k_BT)$ as the key parameter on which all kernels depend.

The function $Q^l_A(c_1, c_2)$ refers to the portion of $\kappa_l(c_1, c_2)$ (6.52) that comes from $Q_A(\mathbf{c}_1, \mathbf{c}_2)$ when $\kappa(\mathbf{c}_1, \mathbf{c}_2)$ from Eq. (6.48) is substituted into Eq. (6.52). It is given by

$$Q^l_A(c_1, c_2) = \int_{-1}^{1} d(\hat{\mathbf{c}_1} \cdot \hat{\mathbf{c}_2}) P_l(\hat{\mathbf{c}_1} \cdot \hat{\mathbf{c}_2}) Q_A(\mathbf{c}_1, \mathbf{c}_2) \tag{A.58}$$

where $Q_A(\mathbf{c}_1, \mathbf{c}_2)$ is given in Eq. (6.41).

We begin by working with $Q_A(\mathbf{c}_1, \mathbf{c}_2)$, doing the $\mathbf{c}_4$ integration by using the delta function and then writing the $\mathbf{c}_3$ integration in spherical coordinates. For the spherical coordinates, we orient the z-axis parallel to $\mathbf{c}_p \equiv \mathbf{c}_1 + \mathbf{c}_5$ and let $z = \mathbf{c}_p \cdot \mathbf{c}_3$. This gives us

$$Q_A(\mathbf{c}_1, \mathbf{c}_2) = 2\pi \int_0^\infty c_3^2 dc_3 \int_{-1}^{1} dz \delta(\mathcal{E}_1 + \mathcal{E}_2 - \mathcal{E}_3 - \mathcal{E}_4)(W^{22}_{1,2,3,4})^2 \mathcal{F}^0_3 \mathcal{F}^0_4 \tag{A.59}$$

where $c_4 = \sqrt{c_p^2 - 2c_p c_3 z + c_3^2}$. We now change integration variables from z to c_4 to obtain

$$Q_A(\mathbf{c}_1, \mathbf{c}_2) = 2\pi \int_0^\infty c_3^2 dc_3 \int_{|c_p - c_3|}^{c_p + c_3} \frac{c_4 dc_4}{c_p c_3} \delta(\mathcal{E}_1 + \mathcal{E}_2 - \mathcal{E}_3 - \mathcal{E}_4)(W^{22}_{1,2,3,4})^2 \mathcal{F}_3^0 \mathcal{F}_4^0 \tag{A.60}$$

To get $Q^l_A(c_1, c_2)$, this expression must be integrated over the angle between $\mathbf{c}_1$ and $\mathbf{c}_2$. We can change this to an integration over c_p by using $c_p = \sqrt{c_1^2 + 2c_1 c_2 x + c_2^2}$ where x is the cosine of the angle between $\mathbf{c}_1$ and $\mathbf{c}_2$. Written in terms of an integration over c_p, $Q^l_A(c_1, c_2)$ takes the form

$$Q^l_A(c_1, c_2) = 2\pi \int_{|c_1 - c_2|}^{c_1 + c_2} \frac{c_p dc_p}{c_1 c_2} P_l(x) \int_0^\infty c_3^2 dc_3 \int_{|c_p - c_3|}^{c_p + c_3} \frac{c_4 dc_4}{c_p c_3} \delta(\mathcal{E}_1 + \mathcal{E}_2 - \mathcal{E}_3 - \mathcal{E}_4)(W^{22}_{1,2,3,4})^2 \mathcal{F}_3^0 \mathcal{F}_4^0. \tag{A.61}$$

The trick is to notice that c_p does not appear in the integrands except through $P_l(x)$ This means we can switch the order of integration and do the c_p integration first. Doing this, we get

$$\begin{aligned} Q^l_A(c_1, c_2) =& \frac{2\pi}{c_1 c_2} \int dc_3 dc_4 c_3 c_4 \delta(\mathcal{E}_1 + \mathcal{E}_2 - \mathcal{E}_3 - \mathcal{E}_4)(W^{22}_{1,2,3,4})^2 \mathcal{F}_3^0 \mathcal{F}_4^0 \\ & \times \int_{\max(|c_1 - c_2|, |c_3 - c_4|)}^{\min(c_1 + c_2, c_3 + c_4)} dc_p P_l \left(\frac{c_p^2 - c_1^2 - c_2^2}{2c_1 c_2} \right). \end{aligned} \tag{A.62}$$

The c_p integration appears in all of the other kernels, so we call it

$$\omega^l_{1,2,3,4} \equiv \int_{\max(|c_1 - c_2|, |c_3 - c_4|)}^{\min(c_1 + c_2, c_3 + c_4)} dc_p P_l \left(\frac{c_p^2 - c_1^2 - c_2^2}{2c_1 c_2} \right). \tag{A.63}$$

Finally, we do the energy delta function

$$Q^l_A(c_1, c_2) = \frac{\pi}{c_1 c_2} \int dc_3 \frac{c_3 \mathcal{E}_4}{c_4^2 + b} (W^{22}_{1,2,3,4})^2 \mathcal{F}_3^0 \mathcal{F}_4^0 \omega^l_{1,2,3,4} \tag{A.64}$$

where $c_4 = \sqrt{\sqrt{(\mathcal{E}_1 + \mathcal{E}_2 - \mathcal{E}_3)^2 + b^2} - b}$. The limits of the c_3 integration are naturally set by the vanishing of $\omega^l_{1,2,3,4}$.

Following these steps for the other five kernel functions, we obtain

$$R_A^l(c_1,c_2)=\frac{\mathcal{F}_2^0}{\mathcal{N}_2^0}\frac{(-1)^l\pi}{c_1c_2}\int dc_3\frac{c_3\mathcal{E}_7}{c_7^2+b}(W^{22}_{1,3,2,7})^2\mathcal{N}_3^0\mathcal{F}_7^0\omega^l_{1,2,3,7}, \tag{A.65}$$

where $c_7=\sqrt{\sqrt{(\mathcal{E}_1-\mathcal{E}_2+\mathcal{E}_3)^2+b^2}-b}$,

$$Q_B^l(c_1,c_2)=\frac{\pi}{c_1c_2}\int dc_3\frac{c_3\mathcal{E}_5}{c_5^2+b}(W^{31}_{5,3,2,1})^2\mathcal{N}_3^0\mathcal{F}_5^0\omega^l_{1,2,3,5} \tag{A.66}$$

where $c_5=\sqrt{\sqrt{(\mathcal{E}_1+\mathcal{E}_2+\mathcal{E}_3)^2+b^2}-b}$,

$$Q_C^l(c_1,c_2)=\frac{\mathcal{F}_2^0}{\mathcal{N}_2^0}\frac{(-1)^l\pi}{c_1c_2}\int dc_3\frac{c_3\mathcal{E}_6}{c_6^2+b}(W^{31}_{1,2,3,6})^2\mathcal{F}_3^0\mathcal{F}_6^0\omega^l_{1,2,3,6} \tag{A.67}$$

where $c_6=\sqrt{\sqrt{(\mathcal{E}_1-\mathcal{E}_2-\mathcal{E}_3)^2+b^2}-b}$,

$$T_A^l(c_1,c_2)=\frac{\mathcal{E}_1+\mathcal{E}_2}{2c_1c_2(c_8^2+b)}(W^{12}_{1,2,8})^2\mathcal{F}_8^0P_l\left(\frac{c_8^2-c_1^2-c_2^2}{2c_1c_2}\right), \tag{A.68}$$

where $c_8=\sqrt{\sqrt{(\mathcal{E}_1+\mathcal{E}_2)^2+b^2}-b}$, and

$$T_B^l(c_1,c_2)=(-1)^l\frac{\mathcal{F}_2^0}{N_2^0}\frac{\mathcal{E}_1-\mathcal{E}_2}{2c_1c_2(c_9^2+b)}(W^{12}_{9,2,1})^2\mathcal{F}_9^0\theta(c_1>c_2)P_l\left(\frac{c_9^2-c_1^2-c_2^2}{2c_1c_2}\right), \tag{A.69}$$

where $c_9=\sqrt{\sqrt{(\mathcal{E}_1-\mathcal{E}_2)^2+b^2}-b}$.

The factor of $(-1)^l$ appears in some kernels because $\mathbf{c}_1$ and $\mathbf{c}_2$ appear in the combination $\mathbf{c}_1-\mathbf{c}_2$ instead of $\mathbf{c}_1+\mathbf{c}_2$. This has the effect of changing the sign of the argument of the Legendre polynomial, producing a factor of $(-1)^l$.

The kernel $R_A^l(c_1,c_2)$ as it is written is undefined when $c_1=c_2$. This is not actually a physical problem since the kernel is multiplied by an eigenvector and integrated in the kinetic equation. The problem arises from our choice of the discretization method. For the matrix elements in Eq. (6.51), a value is needed for $R_A^l(x_i,x_i)$. We handle this by noticing that

$$\int_0^\infty dc_2c_2^2\mathcal{N}^0(c_2)(Q_A^l(c_1,c_2)-R_A^l(c_1,c_2))=0. \tag{A.70}$$

This fact can be used with the quadrature scheme of Eq. (6.51) to fix the value of $R^l_A(x_i, x_i)$. The physical basis for this fact is that $\mathcal{G}^{22}$ alone conserves bogolon number, and we demand that the matrix representation of the linearized collision operators reflects this.

A.9 Mean Field Self-Consistency Equations

In this appendix, we give explicit forms of the self-consistency equations (6.3, 6.4) that can be used for calculation. We begin by using the equilibrium expectation values of the particle operators to obtain

$$\frac{N}{V} = \frac{N_0}{V} + \frac{1}{(2\pi)^3}\int d\mathbf{k}\frac{\epsilon_k + \Delta}{E_k(e^{\mathcal{E}_k} - 1)} + \frac{1}{(2\pi)^3}\int d\mathbf{k}\left(\frac{\epsilon_k + \Delta}{2E_k} - \frac{1}{2}\right) \tag{A.71}$$

and

$$\frac{gN_0}{V} = \Delta + \frac{g}{(2\pi)^3}\int d\mathbf{k}\frac{\Delta}{E_k(e^{\mathcal{E}_k} - 1)} + \frac{g}{(2\pi)^3}\int d\mathbf{k}\left(\frac{\Delta}{2E_k} - \frac{\Delta}{2\epsilon_k}\right). \tag{A.72}$$

Note that in the third term on the right hand side of Eq. (A.72) we have subtracted off the divergent part by subtracting $\frac{\Delta}{2\epsilon_k}$ from the integrand. This is a well-known divergence for the Bose gas and is caused by the use of an effective low-energy contact interaction. A similar divergence appears when calculating higher order corrections to the ground state energy [58] and corrections beyond the Born approximation to the s-wave scattering length a [55]. The justification for dealing with the divergence in this manner is discussed in ref. [59] and relies on the fact that the gas is dilute, that is, $\sqrt{na^3} << 1$. We must keep this condition satisfied when choosing equilibrium states that are specified by values other than n.

The two self-consistency equations, when simplified and combined, are

$$na^3 = \frac{\Delta}{2\epsilon_a} + \left(\frac{k_BT}{\epsilon_a}\right)^{3/2}[F(b) + G(b)] - \frac{8}{3\sqrt{2\pi}}\left(\frac{\Delta}{\epsilon_a}\right)^{3/2} \tag{A.73}$$

and

$$n_0a^3 = \frac{\Delta}{2\epsilon_a} + \left(\frac{k_BT}{\epsilon_a}\right)^{3/2}G(b) - \frac{4}{\sqrt{2\pi}}\left(\frac{\Delta}{\epsilon_a}\right)^{3/2}, \tag{A.74}$$

where

$$F(b) \equiv \frac{4}{\sqrt{\pi}}\int_0^\infty dx\frac{x^2(x^2+b)}{\sqrt{x^4+2bx^2}(e^{\sqrt{x^4+2bx^2}} - 1)} \tag{A.75}$$

and

$$G(b) \equiv \frac{4}{\sqrt{\pi}} \int_0^\infty dx \frac{x^2 b}{\sqrt{x^4 + 2bx^2}(e^{\sqrt{x^4+2bx^2}} - 1)}. \tag{A.76}$$

These equations are used to generate Figs. 6.1 and 6.2 as well as Table 6.1.

Appendix B

Symbolic Algebra Code

B.1 Motivation

In quantum mechanical computations, one must often evaluate the commutator of two operators. This in itself is not a difficult task, as the definition of the commutator is generally part of the statement of the problem or a postulate of the theory. For example, when dealing with many-body systems one works with the creation and annihilation operators $\hat{a}_i^\dagger$ and $\hat{a}_i$ which create and destroy particles in the quantum state i. If the particles are bosons, the commutator is given by

$$[\hat{a}_i, \hat{a}_j^\dagger] = \delta_{i,j}. \tag{B.1}$$

This process begins to become cumbersome when one deals with commutators of products of operators such as

$$[\hat{a}_i\hat{a}_j, \hat{a}_k^\dagger] = \hat{a}_j\delta_{i,k} + \hat{a}_i\delta_{j,k}. \tag{B.2}$$

The rule for evaluating commutators of products of operators is simple if only three operators are involved; it is

$$[AB, C] = A[B, C] + [A, C]B. \tag{B.3}$$

This is still not too bad if we only need to do it once. However, consider the evaluation of a commutator such as $[ABC, DEF]$. Certainly, one could repeatedly use (B.3) to evaluate it, but due to the iterative nature of such a process it quickly becomes very tedious.

When attempting to derive quantum kinetic equations for Bosonic systems, one encounters commutators such as $[\hat{a}_1^\dagger\hat{a}_2^\dagger\hat{a}_3\hat{a}_4, \hat{a}_5^\dagger\hat{a}_6^\dagger\hat{a}_7\hat{a}_8]$, and other similar terms. The need to do long, tedious, repetitive

and error prone calculations such as this is the first main motivation for developing a symbolic algebra code.

A second motivation for using a symbolic algebra code is the need to compute expectation values of operators. In bosonic systems, the simplest expectation value that gives a non-zero value is $\langle \hat{a}_i^\dagger \hat{a}_j \rangle$. Under certain simplifying conditions which we discuss elsewhere, this can be directly evaluated as

$$\langle \hat{a}_i^\dagger \hat{a}_j \rangle = n_i \delta_{i,j}. \tag{B.4}$$

An average such as this is known as a wick average and the quantity n_i is known as the occupation number of the quantum state i. Again we see that this is quite straightforward in the case of only two operators, but any non-trivial computations will require the expectation value of more than just two operators.

Consider the expectation value $\langle \hat{a}_i^\dagger \hat{a}_j^\dagger \hat{a}_k \hat{a}_l \rangle$. This can be computed using the general rule

$$\langle \hat{a}_i^\dagger \hat{a}_j^\dagger \hat{a}_k \hat{a}_l \rangle = \langle \hat{a}_i^\dagger \hat{a}_j^\dagger \rangle \langle \hat{a}_k \hat{a}_l \rangle + \langle \hat{a}_i^\dagger \hat{a}_k \rangle \langle \hat{a}_j^\dagger \hat{a}_l \rangle + \langle \hat{a}_i^\dagger \hat{a}_l \rangle \langle \hat{a}_j^\dagger \hat{a}_k \rangle. \tag{B.5}$$

This is bordering on laborious and there are only four terms. Derivations of quantum kinetic equations require the wick averages of six or even eight operators. Evaluation of wick averages quickly and accurately is our second motivation for using a symbolic algebra code.

The third major motivation (but not the last) for using a symbolic algebra system is just having it do the algebra. In particular, the Bogoliubov transformation

$$\hat{b}_i = u_i \hat{a}_i + v_i \hat{a}_{-i}^\dagger \tag{B.6}$$

results in a large number of terms coming from simple products of operators.

Another practical part of having the computer do the algebra is after the transformations, commutators and wick averages are done, the result typically contains over 10,000 terms which would take months to simplify by hand. The symbolic algebra system can search for like terms in this output and combine them together, reducing the total output of the code to a manageable 200-600 terms. Although the symbolic algebra code saves a lot of time and work, the output must still be checked

and simplified by hand as the final step. One must be content to deal with 320 terms instead 36,000 and always take the final steps by hand.

We have chosen to write this symbolic algebra code in Microsoft Visual Basic 2008 Express Edition which is available free for download at

http://www.microsoft.com/express/

This language was chosen for its adaptability in creating user-defined types and classes, its ability to pass user-defined classes as arguments to functions, its ability to overload function arguments and its simplicity in creating and indexing multi-dimensional dynamically allocated arrays. It it our opinion that the true merit of any programming language is the total time taken to solve a problem, and great amounts of time and effort were saved by choosing a language that is familiar.

B.2 Formulae

The previous section may have led one to believe that the symbolic algebra code applies simple rules such as (B.3) and (B.5) recursively. While it is true that recursive algorithms are generally short, they are also dangerous and tricky to code. In this section, we state the generalizations of (B.3) and (B.5) that the code actually uses.

To deal with multiple commutators, we begin with (B.3). After inspection of this rule, one can convince oneself that the generalization is

$$\left[B, \prod_{i=1}^{N} A_i\right] = \sum_{j=1}^{N} \left(\prod_{i=1}^{j-1} A_i\right) [B, A_j] \left(\prod_{i=j+1}^{N} A_i\right) \tag{B.7}$$

If B itself is a product of operators, we simply write it as such,

$$\left[\prod_{k=1}^{M} B_k, \prod_{i=1}^{N} A_i\right] = \sum_{j=1}^{N} \left(\prod_{i=1}^{j-1} A_i\right) \left[\prod_{k=1}^{M} B_k, A_j\right] \left(\prod_{i=j+1}^{N} A_i\right), \tag{B.8}$$

and use (B.7) again expand the commutator to get

$$\left[\prod_{k=1}^{M} B_k, \prod_{i=1}^{N} A_i\right] = \sum_{j=1}^{N} \sum_{k=1}^{M} \left(\prod_{i=1}^{j-1} A_i\right) \left(\prod_{l=1}^{k-1} B_l\right) [B_k, A_j] \left(\prod_{l=k+1}^{M} B_l\right) \left(\prod_{i=j+1}^{N} A_i\right). \tag{B.9}$$

This is the formula that we use in practice when computing all commutators that contain more than two operators.

To deal with wick averages of many operators, we do not use a recursive routine based on (B.5). Instead, we generalize this rule by beginning with a version of (B.5) for just four operators.

$$\langle B_1 B_2 B_3 B_4 \rangle = \langle B_1 B_2 \rangle \langle B_3 B_4 \rangle + \langle B_1 B_3 \rangle \langle B_2 B_4 \rangle + \langle B_1 B_4 \rangle \langle B_2 B_3 \rangle \tag{B.10}$$

The key to generalizing this is noticing that we can write this as

$$\langle B_1 B_2 B_3 B_4 \rangle = \langle \langle B_1 B_2 \rangle B_3 B_4 + \langle B_1 B_3 \rangle B_2 B_4 + \langle B_1 B_4 \rangle B_2 B_3 \rangle, \tag{B.11}$$

which can now easily be generalized to

$$\left\langle \prod_{i=1}^{N} B_i \right\rangle = \left\langle \sum_{i=2}^{N} \langle B_1 B_i \rangle \prod_{j=2, j\neq i}^{N} B_j \right\rangle. \tag{B.12}$$

Application of this rule to a term with N operators results in an sum of $N-1$ terms, each containing $N-2$ operators. This process is repeated until no more operators are detected in the expression. Note that in a typical expression, many of the terms will average to zero. However, it is better to do the wick expansion with (B.12) first and then worry about which ones are zero.

B.3 Data Structures

The symbolic algebra code is based off of three structures. The most primitive structure is called a `Var`. A `Var` represents a single variable, number or operator. A `Var` can have up to four indices. Example of things which can be represented by a single `Var` are 5, n_k, $\hat{a}_i^\dagger$ or V_{5678}. The second structure is called a `Term`. A `Term` is an ordered sequence of `Var`s, assumed to be multiplied together. In the code, a `Term` is actually a class, which provides some methods for manipulating the sequence of `Var`s, getting information about them and generating new `Term`s from subsets. The third and final structure is called an `Expr`. An `Expr` is an ordered sequence of `Term`s, assumed to be added together. An `Expr` is also a class, providing methods for rearranging, simplifying and displaying `Expr`s.

One can always convert data types upwards, but never downwards. A single `Var` can be converted to a `Term`, and that `Term` will have one element. A single `Term` can be converted to an `Expr` and that `Expr` will have again, one element. Though technically a single element `Term` or `Expr` could be converted back to the lower type, we do not allow this in the interest of preventing bugs.

The conversion of data types is easily handled by the language's capability for *overloading*. Overloading essentially means that one can give a single subroutine multiple definitions, each for a different type of input, but having the same name. The program then decides which subroutine to use based on the data types of its inputs. This results in a large time and effort savings because when one wants to multiply, one simply writes `mult(A, B)` regardless of the specific types of `A` and `B`. Of course, one must still know what to expect so that the result can be assigned to an appropriate data structure.

VarType		
element	enumeration	purpose
num	0	indicates that the var is a constant integer.
var	1	indicates that the var is a variable.
ope	2	indicates that the var is an operator.

Table B.1: The elements of the enumerated data type, VarType.

Enumerated data types are used as members of `Var`s. They give the user or the code information about what the `Var` represents. There are two enumerated data types defined in the symbolic algebra code. The first is the data type `VarType` and its definitions are show in Table B.1. Objects flagged as `num` will be ignored for commutation and wick average operations. They can also be combined into a new object if the rest of the term is the same. This is how the code identifies and adds like terms. Multiple objects flagged as `num` in the same term will be multiplied together and reduced to a single object. Objects flagged as `Var` will also be ignored for commutation and wick average operations, can be reordered in any way, and will are be unable to be factored. We do not factor variables, or use any parentheses at all. Objects flagged as `ope` participate in all operations and receive special treatment when they are reordered.

The second enumerated type, `VarName`, contains possible object names as shown in Table B.2. The enumeration is used to sort the objects so that objects with low enumeration appear at the beginning of `Term`s and objects with high enumeration are moved to the end. The exact values of the enumeration

are not relevant but their order is. Not all of these are used in a single computation but they are all retained for flexibility.

VarName		
element	enumeration	purpose
c	-20	a constant integer
p	-19	mean field value
q	-18	anomalous mean field value
sum	-15	summation symbol
g	-14	related to the Bogoliubov transform
gs	-13	related to the Bogoliubov transform
h	-12	related to the Bogoliubov transform
Ep	-10	imaginary exponential of a positive energy
Em	-9	imaginary exponential of a negative energy
Velem	-8	matrix element of the interaction
u	-6	Bogoliubov transform
v	-5	Bogoliubov transform
uu	-4	product of two u's
uv	-3	product of u and v
vv	-2	product of two v's
delta	-1	Kronecker delta
n	5	particle occupation number
m	6	anomalous particle occupation
f	7	one plus particle occupation
nt	8	bogolon occupation number
ft	9	one plus bogolon occupation number
adagger	10	particle creation operator
a	11	particle annihilation operator
bdagger	12	bogolon creation operator
b	12	bogolon annihilation operator
BigF	15	four particle modified U-U term
BigN	16	four particle U-U term

Table B.2: The elements of the enumerated data type, VarName.

B.4 Example Computations

The following examples are designed to exhibit the basic flow of a computation and outline the essential steps. In any computation, we must follow these generic steps:

- generate basic `Exprs` and `Terms`
- manipulate basic `Exprs` and `Terms` to get desired `Exprs`

- perform commutations and reorder operators
- perform wick averages
- simplify
- combine like terms
- output

The first two examples only use some of these steps, while the final example employs them all.

In this example, we generate two `Expr`s, multiply them, and output the result to the console and to a file.

```
Dim E1 As New Expr(1)    'Define Exprs
Dim E2 As New Expr(1)
Dim E As New Expr(1)
E1 = gBFromA(True, 1)    'Generate E1
E2 = gBFromA(False, 2)   'Generate E2
E = Mult(E1, E2)         'Multiply E1 and E2 and store in E
E.DisplaySplit()         'Display E on the console
E.DumpToText("E.txt")    'Save E to a file
EndProgram()
```

The result from this example is

```
u_1*B_1*u_2*b_2 +
u_1*B_1*-1*v_2*B_-2 +
-1*v_1*b_-1*u_2*b_2 +
-1*v_1*b_-1*-1*v_2*B_-2
```

Notice that the user does not need to predict the size of an `Expr`. This is because the routines that return an `Expr` figure out how big the `Expr` needs to be to hold their result and set the size themselves.

In the next example, we use the code to compute the commutator of two simple terms. The result is put into normal order before displaying it. While this sort of computation would be intermediate in some programs, it can also be useful simply for evaluating long commutators for other problems.

```
Dim T1 As Term
Dim T2 As Term
Dim E As New Expr(1)
T1 = gSecondA(True, 1, False, 2)
T2 = gSecondA(True, 3, False, 4)
E = Commute(T1, T2)
E = OrderOperators(E)
E = OrderVarPart(E)
CombineLikeTerms(E)
E.DisplayInline()
EndProgram()
```

The output of this code is

```
-1*d_{1,4}*A_3*a_2 + d_{2,3}*A_1*a_4
```

Which one can check and find as correct. Note that in this case we chose to use `DisplayInline` instead of `DisplaySplit` as the result was rather short. The interpretation of this result is $-\delta_{1,4}\hat{a}_4^\dagger\hat{a}_2+\delta_{2,3}\hat{a}_1^\dagger\hat{a}_4$

In our third example, we perform a Wick average on a simple term.

```
Dim T As Term
Dim E As New Expr(1)
T = gFourthA(True, 1, False, 2, True, 3, False, 4)
E = OrderOperators(TermToExpr(T))
E = Wick(E)
E = OrderVarPart(E)
CombineLikeTerms(E)
E.DisplaySplit()
E.DumpToTeX("E.tex")
EndProgram()
```

Note that we put the term in normal order before Wick averaging. This requires us to use `TermToExpr` to upgrade the `Term T` to an `Expr`. The console output of this code is

```
d_{-1,3}*d_{2,-4}*m_1*m_2 +
d_{1,2}*d_{3,4}*n_1*n_3 +
d_{1,4}*d_{3,2}*n_1*n_3 +
d_{1,4}*d_{2,3}*n_1
```

We chose to output to a file, but in TEXformat. This can be compiled directly or copied into another document. If we copy it here, we see that it is

$$\begin{aligned}
&\delta_{-1,3}\delta_{2,-4}m_1m_2+\\
&\delta_{1,2}\delta_{3,4}n_1n_3+\\
&\delta_{1,4}\delta_{3,2}n_1n_3+\\
&\delta_{1,4}\delta_{2,3}n_1
\end{aligned} \tag{B.13}$$

In our final example, we attempt to use the code to derive the collision term for the Uehling-Uhlenbeck equation. The evolution of $\langle \hat{a}_1^\dagger \hat{a}_1 \rangle$ depends upon

$$\sum_{2,3,4}\sum_{5,6,7,8} V_{1,2,3,4}V_{5,6,7,8}e^{i(\epsilon_1+\epsilon_2-\epsilon_3-\epsilon_4)s/\hbar}\langle\Big[[\hat{a}_1^\dagger(s)\hat{a}_2^\dagger(s)\hat{a}_3(s)\hat{a}_4(s),\hat{a}_9^\dagger\hat{a}_9],\hat{a}_5^\dagger\hat{a}_6^\dagger\hat{a}_7\hat{a}_8\Big]\rangle \tag{B.14}$$

Where $\hat{a}_1^\dagger(s) = e^{i\epsilon_1 s/\hbar}\hat{a}_1^\dagger$, for example. This example contains several new methods in the simplification step. Without these, the result ends up hopelessly long. Correct application of simplification routines is an acquired skill.

```
Dim A As New Term
Dim V1234 As Var = gVar(VarName.Velem, VarType.var, 4, 1, 2, 3, 4)
Dim S234 As Var = gVar(VarName.sum, VarType.var, 3, 2, 3, 4, 0)
Dim E1234 As Term = Mult(Mult(gVar(VarName.Em, VarType.var, 1, 4, \\
    0, 0, 0), gVar(VarName.Em, VarType.var, 1, 3, 0, 0, 0)), \\
    Mult(gVar(VarName.Ep, VarType.var, 1, 2, 0, 0, 0), gVar(VarName.Ep, \\
    VarType.var, 1, 1, 0, 0, 0)))
A = Mult(Mult(S234, V1234), Mult(E1234, gFourthA(True, 4, True, 3, \\
    False, 2, False, 1)))
Dim H1 As New Term
Dim V5678 As Var = gVar(VarName.Velem, VarType.var, 4, 5, 6, 7, 8)
Dim S5678 As Var = gVar(VarName.sum, VarType.var, 4, 5, 6, 7, 8)
H1 = Mult(Mult(S5678, V5678), gFourthA(True, 5, True, 6, False, 7, False, 8))

Dim E As New Expr(1)
E = Commute(H1, A)
E = OrderOperators(E)
E = Wick(E)
ReplaceAllVars(E, VarName.m, gVar(VarName.c, VarType.num, 1, 0, 0, 0, 0))
DoAllDeltas(E, 1, 8)
VelemToDeltas(E)
DoAllDeltas(E, 1, 8)
```

```
CombineSummations(E)
RenameSummationIndicesByOrder(E, 2)
PermuteVIndices(E)

SimplifyNums(E)
E = OrderVarPart(E)
CombineLikeTerms(E)
SimplifyNums(E)
E.DisplaySplit()
EndProgram()
```

The result of this computation is

```
 4*S[2,3,4]*E[+1]*E[+2]*E[-3]*E[-4]*V[1,2,3,4]*V[1,2,3,4]*n_1*n_2*n_3 +
 4*S[2,3,4]*E[+1]*E[+2]*E[-3]*E[-4]*V[1,2,3,4]*V[1,2,3,4]*n_1*n_2 +
-4*S[2,3,4]*E[+1]*E[+2]*E[-3]*E[-4]*V[1,2,3,4]*V[1,2,3,4]*n_1*n_3*n_4 +
 4*S[2,3,4]*E[+1]*E[+2]*E[-3]*E[-4]*V[1,2,3,4]*V[1,2,3,4]*n_1*n_2*n_4 +
-4*S[2,3,4]*E[+1]*E[+2]*E[-3]*E[-4]*V[1,2,3,4]*V[1,2,3,4]*n_2*n_3*n_4 +
-4*S[2,3,4]*E[+1]*E[+2]*E[-3]*E[-4]*V[1,2,3,4]*V[1,2,3,4]*n_3*n_4
```

Which can be interpreted as

$$4\sum_{2,3,4}(\delta_{1,2,3,4})^2 e^{i(\epsilon_1+\epsilon_2-\epsilon_3-\epsilon_4)s/\hbar}\left[n_1n_2+n_1n_2n_3+n_1n_2n_4-n_3n_4-n_1n_3n_4-n_2n_3n_4\right]. \tag{B.15}$$

This is none other that the Uehling-Uhlenbeck collision term.

Bibliography

[1] C. S. Wang Chang and G. E. Uhlenbeck, University of Michigan, Ann Arbor, Project No. M999, 1952. See *Studies in Statistical Mechanics*, edited by J. de Boer and G. E. Uhlenbeck (North-Holland, Amsterdam, 1970), Vol V, Ch. III.

[2] Z. Alterman, K. Frankowski and C. L. Pekeris, Astrophysical Journal **7**, 69 (1962).

[3] O. O. Jenssen, Phys. Norv. **6**, 179 (1972).

[4] B. Shizgal, Can. J. Phys. **62**, 97 (1984).

[5] K. E. Gibble and A. Gallagher, Phys. Rev. A **43**, 1366 (1991).

[6] J. E. M. Haverkort and J. P. Woerdman, Phys. Rev. A **36**, 5251 (1987).

[7] P. R. Berman, J. E. M. Haverkort and J. P. Woerdman, Phys. Rev. A **34**, 4647 (1986).

[8] S. Kryszewski and G. Nienhuis, J. Phys. B **22**, 3435 (1989).

[9] S. Kryszewski and J. Gondek, Phys. Rev. A **56**, 3923 (1997).

[10] R. F. Snider, Phys. Rev. A **33**, 178 (1986).

[11] C. Cercignani, *Theory and Application of the Boltzmann Equation* (Elsevier, New York, 1975), pp. 180-186.

[12] I. Kuščer and N. Corngold, Phys. Rev. **139**, A981 (1965).

[13] R. E. Robson and K. F. Ness, Phys. Rev. A **33**, 3 (1986).

[14] C. S. Shapiro and N. Corngold, Phys. Rev. **137**, A1686 (1965).

[15] I. Kuščer and M. M. R. Williams, Phys. Fluids **10**, 1922 (1967).

[16] A. V. Bobylev, C. Cercignani and I. M. Gamba, Commun. Math. Phys. **291**, 599 (2009).

[17] A. V. Bobylev and E. Mossberg, Kinetic and Related Models **1**, 521 (2008); **3**, 35 (2010).

[18] C. Mouhot and R. M. Strain, J. Math Pures Appl. **87**, 515 (2007).

[19] R. M. Strain and Y. Guo, Arch. Rational Mech. Anal. **187**, 287 (2008).

[20] Y. Guo, Arch. Rational Mech. Anal. **197**, 713 (2010).

[21] S. Peletminskii and A. Yatsenko, Soviet Physics JETP **26** 773 (1968).

[22] A. I. Akhiezer and S. V. Peletminskii, *Methods of Statistical Physics* (Pergamon, Oxford, England, 1981).

[23] V.P. Galaiko, Soviet Physics JETP **34** 203 (1972).

[24] V. S. Shumeiko, Soviet Physics JETP **36** 330 (1973).

[25] L.E. Reichl, J. Stat. Phys. **23** 83 (1980); **23** 111 (1980).

[26] T. R. Kirkpatrick and J. R. Dorfman, J. Low Temp. Phys. **58** 301 (1985); **58** 399 (1985); **59** 1 (1985).

[27] R. Walser, J. Williams, J. Cooper and M. Holland, Phys. Rev. A **59** 3878 (1999).

[28] N. N. Bogoliubov in *Studies in Statistical Mechanics, Vol. 3*, Edited by J. de Boer and G. R. Uhlenbeck (North-Holland, Amsterdam, 1962).

[29] E. A. Uehling and G. E. Uhlenbeck, Phys. Rev. **43**, 552 (1933).

[30] S. Kikuchi and L. Nordheim, Zeits. f. Physik **60**, 652 (1930).

[31] S. T. Beliaev, Soviet Phys. JETP **7**, 289 (1959).

[32] N. M. Hugenholtz and D. Pines, Phys. Rev **116**, 489 (1959).

[33] D. V. Semikoz and I. I. Tkachev, Phys. Rev. Lett. **74**, 3093 (1995).

[34] E. Zaremba, T. Nikuni, and A. Griffin, J. Low Temp. Phys. **116**, 277 (1999).

[35] C. W. Gardiner and P. Zoller, Phys. Rev. A **55**, 2902 (1997).

[36] A. Griffin, T. Nikuni, E. Zaremba, *Bose-Condensed Gases at Finite Temperatures* (Cambridge University Press, Cambridge, 2009).

[37] M. J. Bijlsma, E. Zaremba and H. T. C. Stoof, Phys. Rev. A **62** 063609 (2000).

[38] H. T. C. Stoof, J. Low Temp. Phys. **114**, 11 (1999).

[39] D. Jaksch, C. W. Gardiner and P. Zoller, Phys. Rev. A **56**, 575 (1997).

[40] E. D. Gust and L. E. Reichl, Phys. Rev. E **79**, 031202 (2009).

[41] E. D. Gust and L. E. Reichl, Phys. Rev. E **81**, 061202 (2010).

[42] F. Reif, *Fundamentals of Statistical and Thermal Physics* (McGraw-Hill, 1965), p. 545.

[43] L. E. Reichl, *A Modern Course in Statistical Physics* (John Wiley & Sons, 1998), pp. 704-710.

[44] S. Chapman and T. G. Cowling, *Mathematical Theory of Non-Uniform Gases* (Cambridge University Press, Cambridge, 1970).

[45] James A. McLennan, *Introduction to Non-Equilibrium Statistcal Mechanics* (Prentice Hall, 1989).

[46] J. Kondo, *Integral Equations* (Clarendon Press, Oxford, 1991), Ch. 6.

[47] D. Hilbert, *Grundzüge einer allgemeinen Theorie der linearen Integralgleichungen* (Chelsea Pub. Co., New York, 1953).

[48] P. L. Bhatnagar, E. P. Gross and M. Krook, Phys. Rev. **94**, 511 (1954).

[49] B. J. Alder and T. E. Wainwright, Phys. Rev. Lett. **18**, 988 (1967).

[50] C. J. Pethick and H. Smith, *Bose-Einstein Condensation in Dilute Gases* (Cambridge Univesity Press, Cambridge, 2002), pp. 142-145.

[51] M. S. Child, *Molecular Collision Theory* (Academic Press, New York, 1974), pp. 21-39.

[52] K. B. Davis *et al*, Phys. Rev. Lett. **75**, 3969 (1995).

[53] N. R. Newbury, C. J. Myatt and C. E. Wieman, Phys. Rev. A **51**, R2680 (1995).

[54] D. Kahaner, C. Moler and S. Nash, *Numerical Methods and Software* (Prentice-Hall, Englewood Cliffs, 1989), pp. 153-157.

[55] A. L. Fetter and J. D. Walecka, *Quantum Theory of Many-Particle Systems* (Dover, Mineola, New York, 2003), pp. 314-319.

[56] A. L. Fetter in *Bose-Einstein Condensation in Atomic Gases*, Edited by M. Inguscio, S. Stringari and C. E. Wieman (IOS Press, Washington DC, 1999), pp. 201-215.

[57] C. J. Pethick and H. Smith, *Bose-Einstein Condensation in Dilute Gases* (Cambridge University Press, Cambridge, 2002), Chap. 8.

[58] T. D. Lee and C. N. Yang, Phys. Rev. **105**, 1119 (1957); **106**, 1135 (1957).

[59] K. Burnett in *Bose-Einstein Condensation in Atomic Gases*, Edited by M. Inguscio, S. Stringari and C. E. Wieman (IOS Press, Washington DC, 1999), pp. 273-283.

[60] M. H. Anderson *et al*, Science **269**, 198 (1995).

[61] D. J. Heinzen in *Bose-Einstein Condensation in Atomic Gases*, Edited by M. Inguscio, S. Stringari and C. E. Wieman (IOS Press, Washington DC, 1999), pg. 385.

[62] H. S. Wilf, *Generatingfunctionology* (A K Peters, Natick, Massachusetts, 2006).